

## Reply to Report #1 (Referee #3)

**Manuscript ID:** essd-2018-150

**Title:** WHU-SGCC: A novel approach for blending daily satellite (CHIRP) and precipitation observations over the Jinsha River Basin

**Journal:** Earth System Science Data

**Type:** Article

Dear Reviewer,

Thank you for your insight comments and suggestions. We have modified the manuscript accordingly. We trust that all of your comments have been addressed accordingly in the revised manuscript. If you have further suggestions for changes, please let us know. The detailed corrections are listed below point by point:

All changes in the manuscript are marked with **red color**.

### Major comments

This is my second review of the manuscript. Compared to the first version the authors have substantially improved the manuscript. They extended the data base and performed a more sophisticated analyses to obtain statistically robust results. They have taken all my suggestions into account. Therefore, I recommend publishing the manuscript after addressing a few minor issues:

### Minor comments

1. L.49-50: Use the plural form of the verbs in this sentence.

**Answer:** Thanks. Done. We have changed the introduction and deleted the GOES-R.

2. L.199-210: Please provide a bit more detail about the random forest regression and the bootstrapping used in the study!

**Answer:** Thanks. Done. We have added a bit more detail about forest regression and the bootstrapping.

**Change:** changed

“RFR is a machine-learning algorithm for a predictive model with a large set of regression trees in which each tree in the ensemble is grown from a bootstrap (Johnson, 1998) sample drawn with replacement from the training set. The final prediction is obtained by combining the results of the prediction methods applied to each bootstrap sample (Genuer et al., 2017). The predicted value is calculated by the mean of all trees.

$$Y_o = f_{RFR}(Y_s) \quad (1)$$

where  $Y_o$  denotes each gauge historical observations and  $Y_s$  denotes the corresponding CHIRP grid cell values at C1 pixels,  $f_{RFR}$  is constructed from the time series  $Y_o$  (dependent variable) and  $Y_s$  (independent variable) by means of RFR. The

number of decision trees was set to 500, which was determined by out-of-bag (OOB) error (Appendix B). The OOB error reached the minimum value when the number of decision trees was less than 500.”

to

“RFR is a machine-learning algorithm for a predictive model with a large set of regression trees in which each tree in the ensemble is grown from a bootstrap sample (Johnson, 1998) drawn with a replacement from the training set. **In the process of establishing regression trees, a subset of variables for each node is selected to avoid overfitting.** The final prediction is obtained by combining the results of the prediction methods applied to each bootstrap sample (Genuer et al., 2017). The predicted value is calculated by the **average of the values from all of the decision trees. Each tree can be expressed as**

$$Tree_k = f_{RFR}(Y_o, \Theta_{Y_k}), k=1 \dots n \quad (1)$$

where  $Y_o$  denotes the historical observations at each gauge at the C1 pixels,  $\Theta_{Y_k}$  is a randomly selected vector from  $Y_s$ ,  $Y_s$  denotes the corresponding CHIRP grid cell values at the C1 pixels,  $n$  is the number of trees, and  $f_{RFR}$  is constructed from the time series  $Y_o$  (dependent variable) and  $Y_s$  (independent variable) by means of RFR. The bootstrap sample will be the training set used for growing the tree. **The error rate (out-of-bag, OOB) left out of one-third of the training data is also monitored to determine the number of decision trees. In this study, the minimum OOB error rate was reached when the number of decision trees  $n$  was less than 500 (Appendix C).**”

3. L.357-364: This part is difficult to understand. Please perform a language check and rephrase this part.

**Answer:** Thanks. Done. We have modified the grammar.

**Change:** changed

“Although, the absolute value of BIAS of WHU-SGCC was no significant improvement than CHIRP and slightly higher than CHIRPS, all of the values were approximately to 0. This results of BIAS indicates that all the three kinds of data were much the same on the performance of relative bias. Nevertheless, the NSE of the WHU-SGCC reached -0.0137, an increase of 93.33% and 98.32% compared to CHIRP and CHIRPS, respectively. The NSE of WHU-SGCC was still negative, but it was improved to be zero that indicates the adjusted results are close to the average level of the rain gauge observations, while the NSEs of CHIRP and CHIRPS were much worse. It is noted that the POD of WHU-SGCC was approximate to 1, better than CHIRP and CHIRPS, and the FAR of WHU-SGCC was 0.11, lower than CHIRP and CHIRPS, which represents the better ability on precipitation event predictions of the WHU-SGCC.”

To

“Although the absolute value of the BIAS of the WHU-SGCC in fall are not significantly better than those of CHIRP and CHIRPS, **all of the values are approximately 0. The NSEs of the WHU-SGCC reached 0.2836, 0.2944 and 0.1853 in**

the spring, fall and winter, respectively, which are substantially better than the negative or zero values of CHIRP and CHIRPS. In the summer, the NSE of the WHU-SGCC is still negative, but it is improved to be nearly zero, which indicates that the adjusted results are similar to the average level of the rain gauge observations. It is worth noting that in the spring, summer and fall, the POD values of the WHU-SGCC are in the range of 0.95 to 1, better than CHIRP and CHIRPS, and the FAR values of the WHU-SGCC are approximately 0.3, lower than CHIRP and CHIRPS; these results represent the better ability of the WHU-SGCC method to predict precipitation events. The rainfall detection ability is the worst in the winter compared to the other seasons. This can be explained by the seasonal distribution of precipitation in the Jinsha River Basin, in which the most rainfall occurs in the summer, followed by the fall, spring and winter. The worst errors of forecasting performance in the summer may be attributed to the highest precipitation. The limited precipitation event detection in the winter could also be explained by the lowest precipitation (Xu et al., 2019).”

4. L401: shown → showed

**Answer:** Thanks. Done.

**Change:** changed “shown” to “provides”.

5. Figure 5: The labelling (a,b,c,...) is missing in the subfigures.

**Answer:** Thanks. Done.

**Change:** We have added the labelling (a,b,...,h) into Figure 5.

6. L.417: It should be Table 6 here, not Table 5.

**Answer:** Thanks. Done.

**Change:** changed Table 6 to Table 5 here.

7. L.453: I guess, it is supposed to be “elevation” instead of “evaluation”?

**Answer:** Thanks. Done.

**Change:** changed “evaluations” to “elevation”.

8. L.561: ...by approximately by... ..by approximately...

**Answer:** Thanks. This mistake may on L.461.

**Change:** “reduced by approximately by” to “reduced by approximately”.

9. What is the typical daily rainfall amount in during the monsoon season? Considering, that the proposed method doesn’t perform very well in case of heavy precipitation, it might not be the appropriate tool for monitoring monsoon precipitation.

**Answer:** Thanks. We added all four seasons for WHU-SGCC

The multi-year (1990-2014) average seasonal precipitation over the Jinsha River Basin increases from north to south (Fig. 2). The dynamic and uneven distribution of precipitation is influenced distinctly by the seasonal climate. Most of the precipitation falls in the summer, with the average seasonal precipitation ranging from less than 250 mm to more than 600 mm, while the average seasonal precipitation during the winter

is no more than 50 mm. The average seasonal precipitation and spatial distribution in the spring are similar with those in the fall, with values concentrated in the range of 50 mm to 200 mm.

**Change:** “This approach is a promising tool to monitor monsoon precipitation over the Jinsha River Basin” to “This approach is a promising tool to monitor **daily** precipitation over the Jinsha River Basin”.

## Reply to Report #2 (Referee #4)

Dear Reviewer,

Thank you for your insight comments and suggestions. We have modified the manuscript accordingly. We trust that all of your comments have been addressed accordingly in the revised manuscript. If you have further suggestions for changes, please let us know. The detailed corrections are listed below point by point:

All changes in the manuscript are marked with **red color**.

The manuscript “WHU-SGCC:A novel approach for blending daily satellite (CHIRP) and precipitation observations over Jinsha River Basin” by Shen et al. describes an approach to blend and homogenize daily satellite (CHIRP) and precipitation surface observations over Jinsha River Basin. The approach is named WHU-SGCC.

The manuscript “WHU-SGCC: A novel approach for blending daily satellite (CHIRP) and precipitation observations over Jinsha River Basin” by Shen et al. describes an approach to blend and homogenize daily satellite (CHIRP) and precipitation surface observations over Jinsha River Basin. The approach is named WHU-SGCC.

The manuscript is quite well written though sometimes it is too schematic and should be instead, to my opinion, more discursive. The manuscript is in the scope of ESSD. However, I suggest below a few potential major revisions of the manuscript along with specific line-by-line suggestions or corrections.

### General comments

1. The introduction of the dataset underlines the central role of the observations used as the “reference dataset” to build up the homogenized dataset with the needed bias adjustment. Nevertheless, surface rain gauge observations at present have a very low level of metrologic and uncertainty characterization, therefore the manuscript can benefit from a more accurate description of the real and potential limitations due to the use of rain gauge observations as the reference for the homogenization of other rain gauge data.

**Answer:** Thanks. The gauge stations were provided by the National Climate Centre (NCC) of the China Meteorological Administration (CMA) ([http://data.cma.cn/data/cdcdetail/dataCode/SURF\\_CLI\\_CHN\\_MUL\\_DAY\\_V3.0.html](http://data.cma.cn/data/cdcdetail/dataCode/SURF_CLI_CHN_MUL_DAY_V3.0.html), last access: 10 December, 2018), which imposes strict quality control at the station, provincial and state levels. Therefore, the gauge stations can be regarded as the reference data due to their lower errors and uncertainties.

2. Table 6 and 7 allows the reader to quantify the better performances WHU-SGCC dataset compared to CHIRP and CHIRPS for rain event included in the class 0-10 mm, the moderate improvement for the in 10-25 mm class, while, as the authors themselves

discussed in the manuscript, performances are negative for rain events larger than 25 mm. Though this class of rain events contains a minor number of events, the authors should discuss in the manuscript if this might indicate that extreme rain events in the Jinsha River Basin are attenuated in their intensity by the adopted homogenization approach.

**Answer:** Thanks.

**Change:** We added the discussion about the homogenization.

“the average daily precipitation within the basin less than 10 mm over the study period, which results in numerous rain gauge station data with values lower than 10 mm, which had a significant impact on the establishment of statistical relationships for the WHU-SGCC. The estimates of extreme rain events might also be attenuated during the process of WHU-SGCC adjustment.”

3. The authors should comment more on the effect of and the reason why the pixel spatial autocorrelation (and the temporal autocorrelation only within **the same season of the same year**) is not considered and how its study can help to improve the quality of their results.

**Answer:** Thanks.

**Change:**

Added “**Due to the significant seasonal difference of precipitation, the WHU-SGCC method was applied in the different seasons**”.

In addition, it is reasonable to assume that some pixels are statistically similar to the historical precipitation characteristics (temporal autocorrelation) of the C1 pixels within a certain area. The spatial area in which pixels may have highly similar characteristics is established. Several studies indicate that the geographical location, elevation and other terrain information influence the spatial distribution of rainfall, especially in mountainous areas with complex topography. The size of the spatial range is an important parameter to distinguish the spatial similarity and heterogeneity. So it can be assumed that the pixels are spatial correlation in these certain area.

4. Table 6 shows that most of the data belongs to C4 pixel category (55-60% of the total dataset), given that these data are homogenized using the IDW technique based on the neighboring observations, **the authors should clarify if the application of this technique on the majority of the dataset can smooth out extreme events** (very low or very amount) due to the smoothing introduced at the C4 pixels. Moreover, **it could be helpful to the highlight the position of C1-C3 pixels in Figure 4** to allow the reader to check the position of that part of the dataset where data homogenization is likely more robust.

**Answer:** Thanks.

**Change:**

We added “**Due to the significant seasonal difference of precipitation, the WHU-SGCC method was applied in the different seasons**”.

“In addition, the spatial distribution of C2 and C3 pixels also significantly impact the overall accuracy in different seasons that the most uniform in the fall, while the sparsest

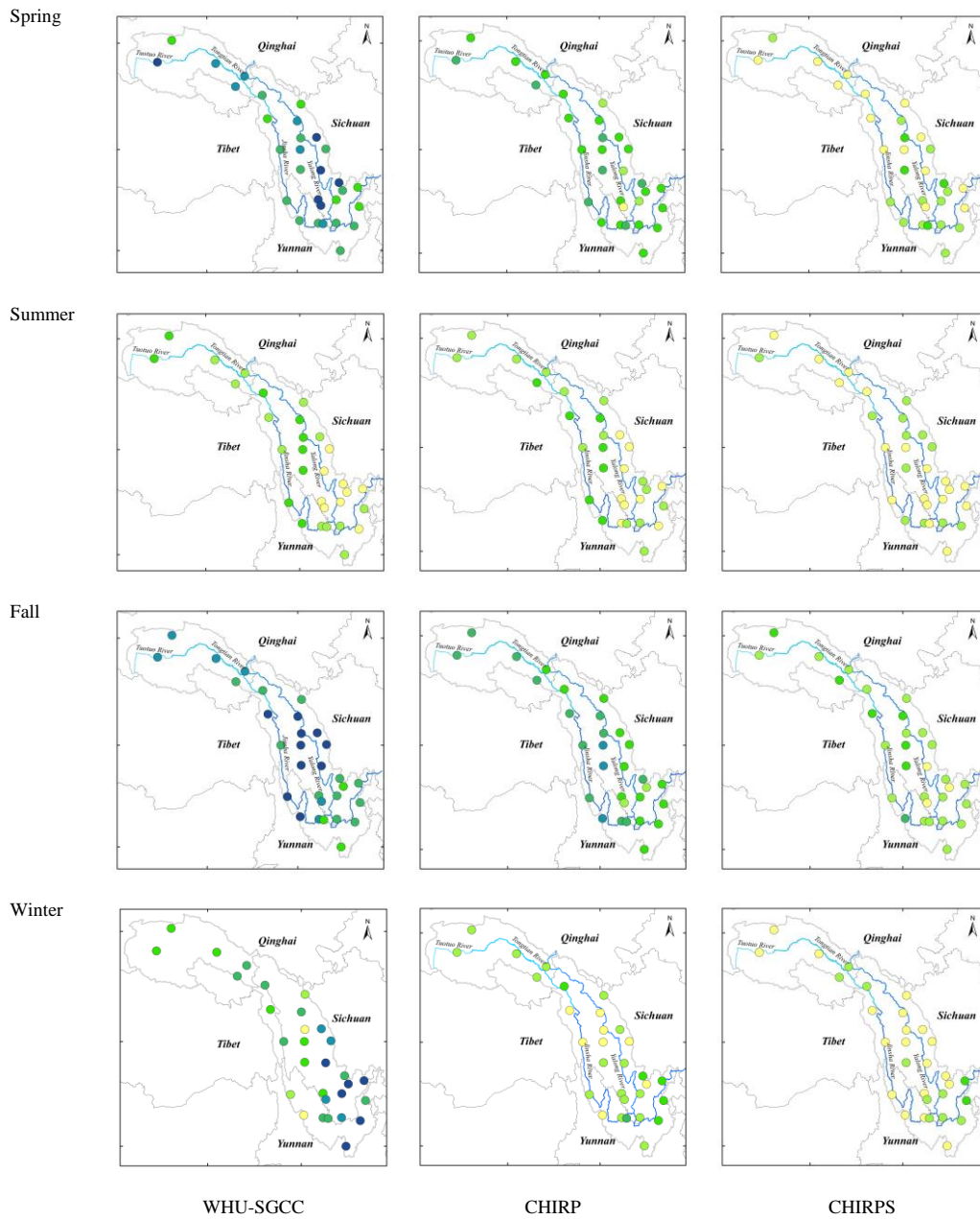
in the winter.”

We also added the spatial distribution of C1-C3 pixels in Appendix D

5. In Figure 4, the spatial distribution of those statistical indicators used to study the WHU-SGCC performances is shown. It would be interesting to compare the results in **Figure 4 with a similar figure showing the statistics for CHIRP**. Though it is true that several table already summarizes the results of the statistics for WHU-SGCC, CHIRP and CHIRPS, a comparison of the reported statistics at the spatial level is missing.

**Answer:** Thanks.

**Change:** We added the comparison with CHIRP and CHIRPS for PCC and RMSE.



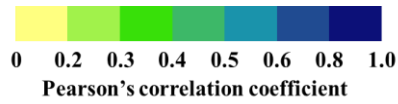
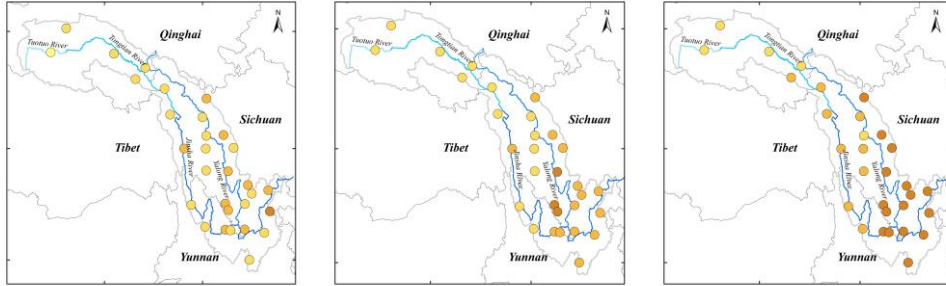
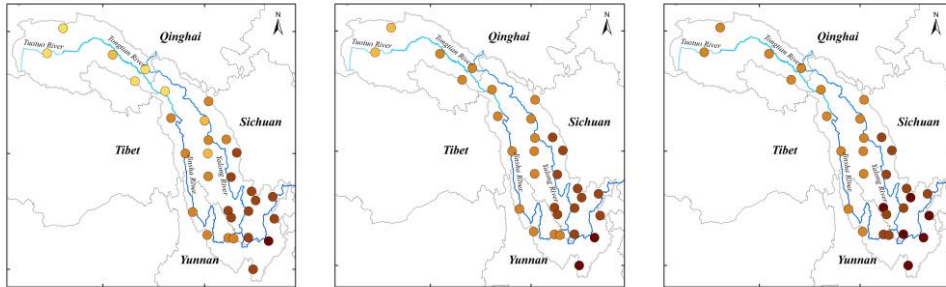


**Figure 4** Spatial distribution of the Pearson's correlation coefficient of the overall agreement between observations and the WHU-SGCC, CHIRP and CHIRPS estimations in the four seasons from 1990 to 2014.

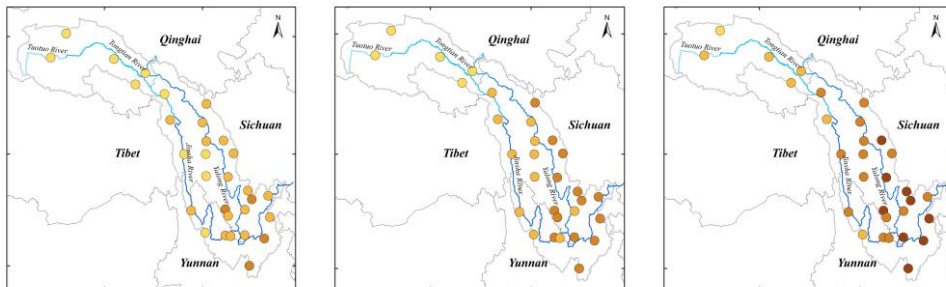
Spring



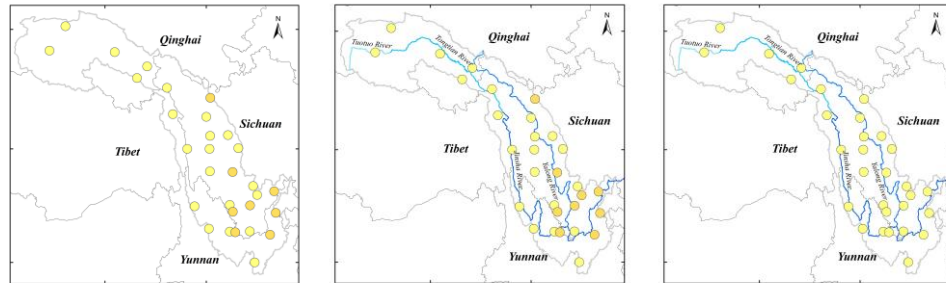
Summer



Fall



Winter



WHU-SGCC

CHIRP

CHIRPS

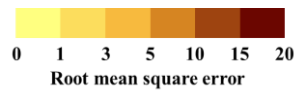


**Figure 5** Spatial distribution of the root mean square errors of the overall agreement between observations and the WHU-SGCC, CHIRP and CHIRPS estimations in the four seasons from 1990 to 2014.

6. The statistical analysis shows that CHIRPS is worse than CHIRP in terms of variability but similar in terms of bias: **the authors should clarify what is the role of the representativeness uncertainty in the merging of gridded and in-situ point observations as happens in CHIRPS.**

**Answer:**

The CHIRPS was derived from blending in-situ precipitation observations and the CHIRP data, with a modified inverse-distance weighting algorithm at a quasi-global area (land only, 50° S-50° N). The blended data (CHIRPS) has an effective performance on a large scale region according to existing studies, such as at the national scale, but there are still large discrepancies with ground observations at the sub-regional level, especially at the river basin scale. The performance and applicability of CHIRPS at the sub-regional level still need to be validated. What's more, the interpolation performance from the limited and sparse rain gauge stations will be affected by more errors which was evaluated with rain gauge stations shown in Table 4.

As such, due to the poor performance of CHIRPS data at the sub-regional scale and the shortcomings of the modified inverse-distance weighting algorithm, the aim of this article is to offer a novel blending approach to improve the precipitation estimated accuracy at the river basin scale.

The Jinsha River Basin is a typically study area, with the complex and varied terrains that the range of elevation is from 263 to 6575 m above sea level, which results in significant temporal and spatial weather variation within the basin. What's more, the multi-year (1990-2014) average annual precipitation increases from north to south and the spatial distribution of precipitation is uneven, with an average annual precipitation ranging from less than 250 mm to more than 600 mm during the summer seasons over the Jinsha River Basin. However, the number of rain gauges stations is limited inside the river basin which cause precipitation estimations bias a lot.

In the previous experiment, the rain gauge stations and gridded points were used as the reference precipitation data. From that data, the training samples represented 70% of total gauged stations and gridded points, and the remaining data were used to verify the model performance. And the WHU-SGCC approach was evaluated for the Jinsha River Basin for JJA 2016.

However, the gridded precipitation used here was from China Meteorological Data Service, interpolated from 2472 rain gauge stations, which was less accurate than the rain gauge stations observations, for example, daily precipitation was more than 1000 mm at one interpolated grid point. So **only the 30 rain gauge stations were used in the new WHU-SGCC experiments.** In the new experiment, selecting 30% of the stations for validation was not an appropriate validation method, while **the leave-one-out cross validation step** was a better instead for using all the stations in WHU-SGCC correction algorithm. What's more, in order to evaluate the model performance more reasonably, the study period was changed from summer of 2016, JJA to a longer study period **in the**

four seasons from 1990 to 2014.

In the results, The average percentage of each class of rain events at the validation gauge station during the four seasons from 1990 to 2014 are shown in Table 5 in the paper and the following figure. The major rain events within the Jinsha River Basin were light rain (0.1-10 mm), which accounted for more than 80% of the total days (the average percentage of rain event days of the total days at each gauge station), while the number of days with daily precipitation greater than the 50 mm was the smallest (no more than 1% of the total days) and fewer than 10% of the days had daily precipitation in the range of 25 mm to 50 mm. In the spring, fall and summer, significantly more no-rain days occurred than rainy days, and approximately 5% of the days had daily precipitation of 10-50 mm. The seasonal distribution of rainfall was concentrated in the summer, and 54.76%, 14.01% and 3.62% of the days had daily precipitation of 0.1-10, 10-25, and 25-50 mm, respectively. The results indicated that the average daily precipitation was less than 10 mm throughout the years of the study.

The WHU-SGCC approach blended daily precipitation gauge data and the CHIRP satellite-derived precipitation, considering the spatial correlation and the historical precipitation characteristics. Therefore, the applicability of the WHU-SGCC method over the complicated mountainous terrain with sparse rain gauge data could be confirmed by the multi-year validation.

### Specific comments

1. Line 11: please here and throughout the manuscript you cannot state that random errors are “removed”. I also encourage to have a consistent use of the terms “error” and “uncertainty”.

**Answer:** Thanks. Done.

**Change:** changed “random errors” to “errors”.

2. Line 21: replace “the” with “a”.

**Answer:** Thanks. Done.

**Change:** changed “This study indicates that the WHU-SGCC approach is a promising tool to monitor monsoon precipitation over the Jinsha River Basin, a complicated mountainous terrain with sparse rain gauge data, considering the spatial correlation and the historical precipitation characteristics.” to “In spite of the correction, the uncertainties in the seasonal precipitation forecasts in the summer and winter are still large, which may due to the homogenization attenuating the simulation of extreme rain event. However, the WHU-SGCC approach may serve as a promising tool to monitor daily precipitation over the Jinsha River Basin, which contains complicated mountainous terrain with sparse rain gauge data, based on the spatial correlation and the historical precipitation characteristics.”

3. Line 62: it looks clear that the Jinsha River Basin is a region of interest for monitoring precipitation, not only for the authors; however, in order to justify the relevance of the dataset presented in the manuscript, it could be appropriate for the authors to say something more general about Jinsha River Basin and the interest to focus on this region

as a special place to monitor monsoon precipitations.

**Answer:** The Jinsha River Basin is a typically study area, with the complex and varied terrains that the range of elevation is from 263 to 6575 m above sea level, which results in significant temporal and spatial weather variation within the basin. What's more, the multi-year (1990-2014) average annual precipitation increases from north to south and the spatial distribution of precipitation is uneven, with an average annual precipitation ranging from less than 250 mm to more than 600 mm during the summer seasons over the Jinsha River Basin. However, the number of rain gauges stations is limited inside the river basin which cause precipitation estimations bias a lot. So the precipitation over Jinsha River Basin is poor at high accuracy precipitation monitoring. What's more, the climate of the Jinsha River Basin has more precipitation during the summer season (June-July-August, JJA), which is affected by oceanic southwest and southeast monsoons. Therefore, the blending of satellite estimations with gauged observations during the JJA is the main focus of this research.

**Change:** We added the sentence “**The Jinsha River Basin is a typical study area with complex and varied terrain, an uneven spatial distribution of precipitation, and a sparse spatial distribution of rain gauges, which limit high accuracy precipitation monitoring.**”

4. Line 71: gauge-satellite fusing means “combined gauge-satellite products”?

**Answer:** Thanks. Gauge-satellite fusing means “blending gauge observations and satellite estimates to produce a new dataset”.

5. Line 76: please check the style to report citation in the text.

**Answer:** Thanks. Done.

**Changed:** changed “Bai et al., 2018” to “**Bai et al. (2018)**” and changed “Trejo et al., 2016” to “**Trejo et al. (2016)**”.

6. Line 102: please add “weather and climate variations” instead of only climate.

**Answer:** Thanks. Done.

**Change:** We changed “which results in significant temporal and spatial climate variation within the basin” to “which results in significant temporal and spatial **climate and weather** variations within the basin.”

7. Line 117-118: Discuss in more detailed the limitation of your “reference” dataset, here in the text.

**Answer:** Thanks. We discuss in more detailed the limitation.

**Change:** We added the sentence “**However, the sparseness of gauges, their uneven spatial distribution, and high proportion of missing data may limit the high accuracy estimation in rainfall monitoring.**”

8. Line 131: what does it indicates the word “strict” here? Please be more specific because this is critical to learn more about the data quality used as “reference” in your approach.

**Answer:** Daily rain gauge observations at 30 national standard rain stations inside the

Jinsha River Basin during the JJA from 1990 to 2014 were provided by the National Climate Centre (NCC) of the China Meteorological Administration (CMA) ([http://data.cma.cn/data/cdcdetail/dataCode/SURF\\_CLI\\_CHN\\_MUL\\_DAY\\_V3.0.html](http://data.cma.cn/data/cdcdetail/dataCode/SURF_CLI_CHN_MUL_DAY_V3.0.html), last access: 10 December, 2018), which imposes a strict quality control at station-provincial-state levels. The process of quality control is as follows:

- (1) Climate threshold or allowable value check;
- (2) Extreme values at gauge stations check;
- (3) Internal consistency check between fixed value, daily average value and daily extreme value;
- (4) Time consistency check;
- (5) Manual verification and correction;

This quality control approach is provided by the official document from CMA. So the daily rain gauge observations were used as the “reference dataset”.

9. Line 159: “longer length” instead of “longer-term”

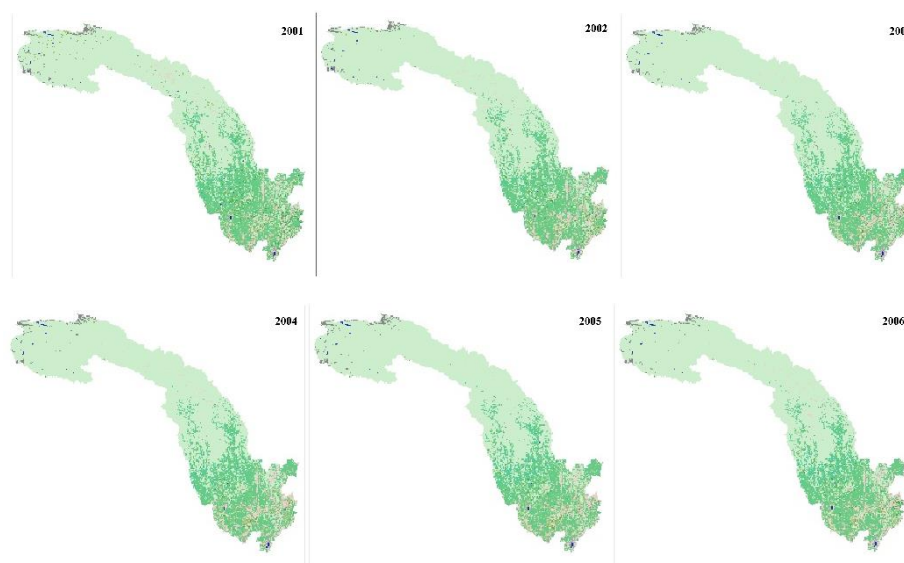
**Answer:** Thanks. Done.

**Change:** changed “longer-term” instead of “longer length”.

10. Line 195: This sentence should be supported by metadata, a reference, maps, or photos.

**Answer:** Thanks. Done.

**Change:** The multi-year land cover types in the Jinsha River Basin from 2001 to 2013 are shown in Fig. B1. All of the land cover type maps were derived from the MODIS/Terra+Aqua Land Cover Type Yearly L3 Global 500 m SIN Grid V051 data set, which is available online at [https://search.earthdata.nasa.gov/search/granules?p=C200106111-LPDAAC\\_ECS&q=MCD12&ok=MCD12](https://search.earthdata.nasa.gov/search/granules?p=C200106111-LPDAAC_ECS&q=MCD12&ok=MCD12) (last access: 23 July 2019). Fig. B1 shows that the land use had no obvious changes over the study period. In addition, the upstream area of the Jinsha River is an untraversed region that has not been affected significantly by human activities. Thus, the land use in the study area has hardly changed.



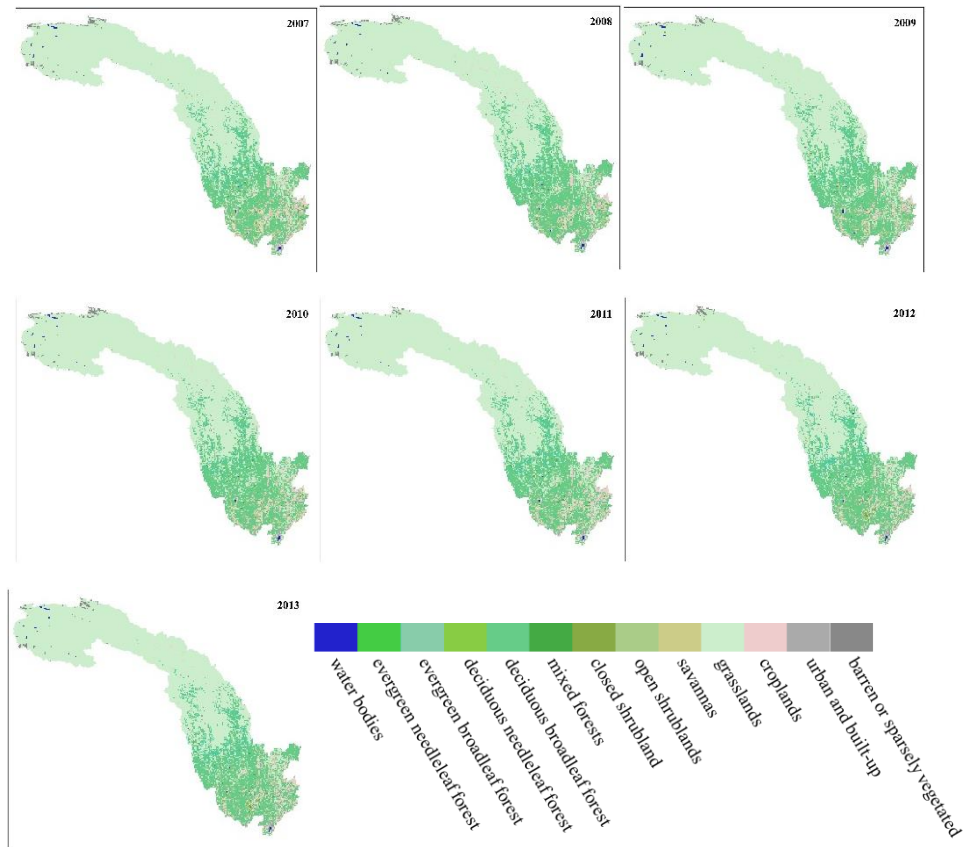


**Figure B1 Land cover types over the Jinsha River Basin from 2001 to 2013.**

11. Line 196: Are you assuming that there are no outliers? Please explain more.

**Answer:** Yes. Thanks. We explained more.

**Change:** changed “Spearman’s Correlation Coefficient (SCC) can indicate the similarity of rainfall characteristics among pixels over a seasonal scale.” to “**There are no long-held outliers at one pixel of the CHIRP dataset, so Pearson’s Correlation Coefficient (PCC) can represent the statistical similarity of rainfall characteristics among pixels over a seasonal scale.**”

12. Line 219-220: these seems to be a repetition of previous text, please check.

**Answer:** Thanks. This sentence mainly explains the terrain factors influencing the spatial distribution of rainfall. And the previous text in introduction discusses various factors affecting precipitation monitor inside mountainous areas, including topography, seasonality, climate impact and sparseness of rain gauges: “The existing research indicates that estimations over mountainous areas with complex topography often have large uncertainties and errors due to the topography, seasonality, climate impact and sparseness of rain gauges (Derin et al., 2016;Maggioni and Massari, 2018;Zambrano-Bigiarini et al., 2017).”

13. Line 246: can the authors validate their cluster analysis with a GIS map, for example, showing the **terrain features**?

**Answer:** The results of spatial clustering derived from the FCM method were shown in Appendix E.

14. Line 295-296: “Excluding the C1, C2 and C3 pixels, the number of remaining pixels, called C4 pixels which are adjusted by Inverse Distance Weighted (IDW)” there is something in this sentence.

**Answer:**

**Change:** changed “Excluding the C1, C2 and C3 pixels, the number of remaining pixels, called C4 pixels which are adjusted by Inverse Distance Weighted (IDW)” to “**The pixels other than the C1, C2 and C3 pixels are called C4 pixels and they are adjusted by inverse distance weighting (IDW).**”

15. Line 321-322: the word strength here is incorrect. SCC measures if a process is linear or not, you cannot infer more than this.

**Answer:** Thanks. In the new experiment, we changed the statistical metric of SCC to Pearson’s correlation coefficient (PCC) because PCC measures the linear correlation between two series better than SCC to evaluate the adjusted precipitation accuracy.

**Change:**

“The performance of the WHU-SGCC adjusted precipitation estimates was evaluated by eight mathematic metrics: the Pearson’s correlation coefficient (PCC), root mean square error (RMSE), mean absolute error (MAE), relative bias (BIAS), Nash-Sutcliffe efficiency coefficient (NSE), probability of detection (POD), false alarm ratio (FAR) and critical success index (CSI). **The results of accuracy assessment are the average values validated by the leave-one-out cross method. Each validated pixel will probably be a C2, C3 or C4 pixel in the process of the WHU-SGCC algorithm.** The PCC, RMSE, MAE and BIAS were used to evaluate how well the WHU-SGCC method adjusted the satellite estimation bias, while POD, FAR and CSI were used to evaluate the performance of precipitation forecasting (Su et al., 2011). **The PCC measures the strength of the correlation relationship between the satellite estimations and observations.**”

16. Line 350: To perform the accuracy evaluation, did you use the 30% of in-situ observation mentioned at the beginning? From this section, this is not clear and how this fraction of observation was selected, is it nor clear as well.

**Answer:** Thanks. Selecting 30% of the stations for validation was not an appropriate validation method, while the leave-one-out cross validation step was a better instead.

**Change:** The validation method was changed from “selecting 30% of the stations for validation” to “**leave-one-out cross validation for using all the rain gauge stations**”;

“**The leave-one-out cross validation step was applied to computing the out-of-sample adjusted error with gauge stations.**”; “**The WHU-SGCC algorithm was repeated 30**

times, each time leaving one station as the validation station.”

”

## Reply to Report #3 (Referee #5)

**Manuscript ID:** essd-2018-150

**Title:** WHU-SGCC: A novel approach for blending daily satellite (CHIRP) and precipitation observations over the Jinsha River Basin

**Journal:** Earth System Science Data

**Type:** Article

Dear Reviewer,

Thank you for your insight comments and suggestions. We have modified the manuscript accordingly. We trust that all of your comments have been addressed accordingly in the revised manuscript. If you have further suggestions for changes, please let us know. The detailed corrections are listed below point by point:

All changes in the manuscript are marked with **red color**.

### General comments

**(1) Phase1:** The manuscript describes a method of merging daily gauge measurements with satellite precipitation product (CHIRP) in the mountainous region of Jinsha River Basin in China. The methodology seems to be quite rigorous in statistical sense. The algorithm is not perfect as it does not take into account the skewed nature of precipitation distribution and the improvements are mostly shown on light rain events but not the heavy rain events. But overall it is a commendable effort and worth publishing.

**(2) Phase2:** One major question is the choice of CHIRP data instead of CHIRPS to start with. Perhaps because CHIRPS with all additional gauge and model data actually performs worse than CHIRP in this particular area as the statistics later in the paper shows. If this is the reason, the authors should mention it in the beginning. It is expected that the new data will perform better than CHIRPS because WHU-SGCC incorporates more surface gauge measurements. The question is then the improvement is due to more gauge stations or better merging and correction methodology? If the WHU-SGCC method only takes the station data used by CHIRPS, will the results be better than CHIRPS?

(1)

**Answer:** Thanks. We chose CHIRP data instead of CHIRPS for gauge-satellite fusing due to the poor performance of CHIRPS data at the sub-regional scale and the shortcomings of the existing blending algorithms.

**Change:**

We mention the reason for the choice of CHIRP data in the introduction. Changed “As such, due to the poor performance of CHIRPS data at the sub-regional scale and the shortcomings of the existing blending algorithms, the aim of this article is to offer a

novel approach for blending daily liquid precipitation gauge data and the Climate Hazards Group Infrared Precipitation (CHIRP) satellite-derived precipitation estimates developed by the UC Santa Barbara, over the Jinsha River Basin.” to “As such, due to the poor performance at the sub-regional scale, **the gauge-satellite fusing algorithms can be assumed to limit high accuracy estimations in the process of CHIRPS data production.** Therefore, the aim of this article is to present a novel approach for reblending daily liquid precipitation gauge data and the Climate Hazards Group Infrared Precipitation (CHIRP) satellite-derived precipitation estimates developed by UC Santa Barbara, over the Jinsha River Basin.”

(2)

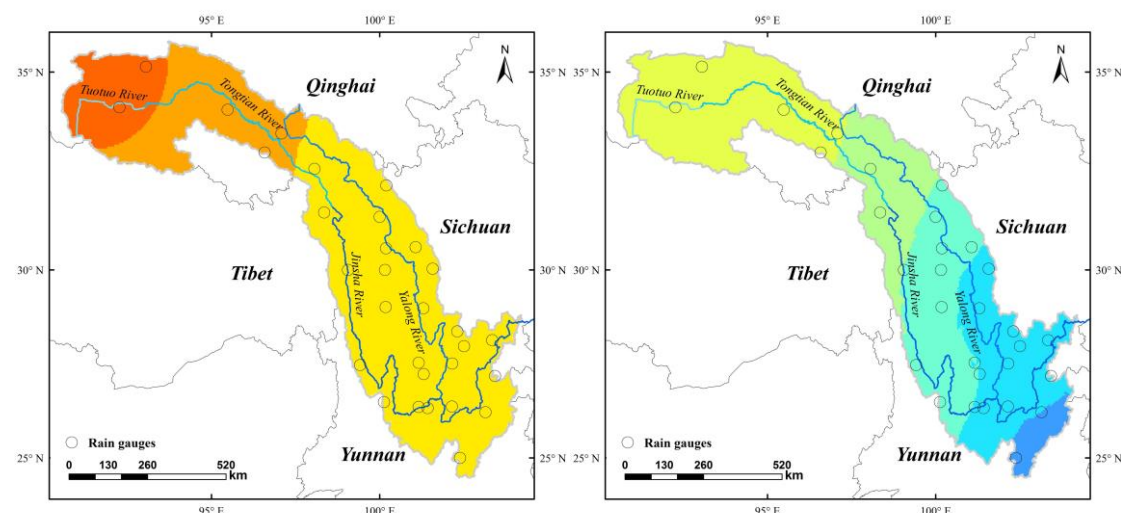
**Answer:**

The CHIRPS station processing stream incorporates data from five public data streams and several private archives. The public data streams are the GHCN monthly, GHCN daily, Global Summary of the Day (GSOD), GTS and Southern African Science Service Centre for Climate Change and Adaptive Land Management (SASSCAL, [www.sasscalweathernet.org](http://www.sasscalweathernet.org)). GTS data are collected daily; GHCN, GSOD and SASSCAL data are updated monthly.

However, the stations for daily CHIRPS data have a different spatial distribution than those downloaded from the CMA, and the precipitation values used for CHIRPS production are the monthly values available online ([ftp://ftp.chg.ucsb.edu/pub/org/chg/products/CHIRPS-2.0/diagnostics/monthly\\_station\\_data/](ftp://ftp.chg.ucsb.edu/pub/org/chg/products/CHIRPS-2.0/diagnostics/monthly_station_data/)).

**For the daily precipitation adjustments over the Jinsha River Basin, the daily gauge observations from the CMA are blended with the daily CHIRP data due to the unknown spatial distribution and precipitation values of gauge stations used in the process of daily CHIRPS merging.**

**Change:** We reconfirmed the gauge stations used for CHIRPS merging at the official website and redrawn the map of daily gauge stations (Figure 2).



(a) Spring

(b) Summer

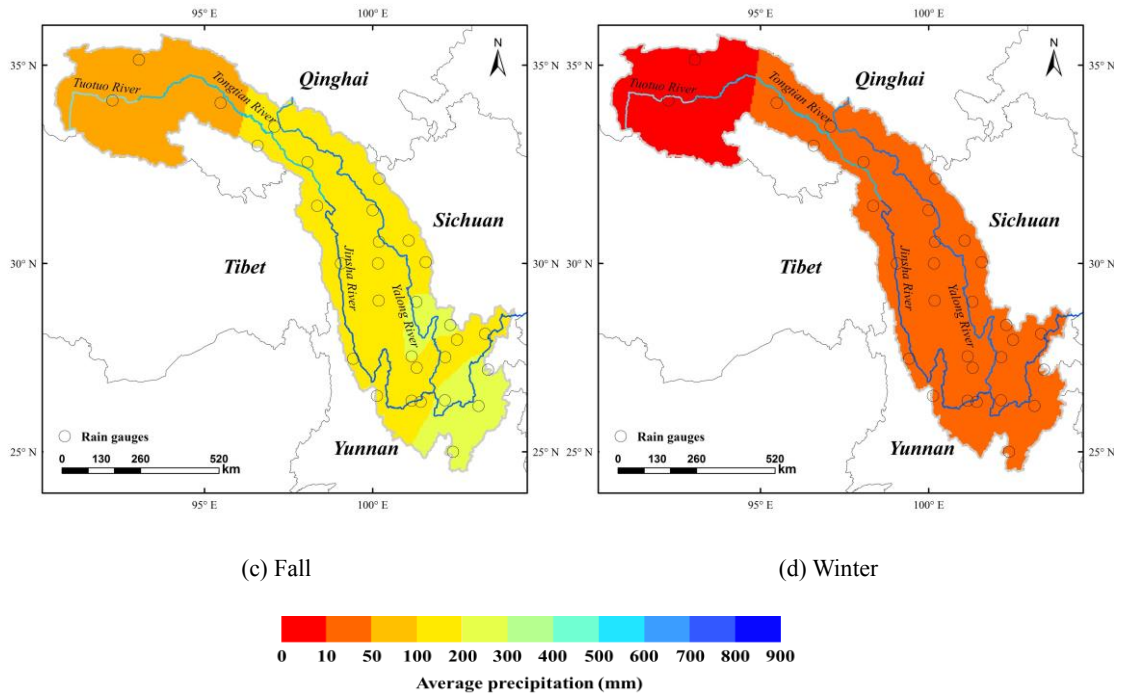


**Figure 2** The multi-year (1990-2014) average seasonal precipitation over the Jinsha River Basin interpolated from 30 rain gauges downloaded from the China Meteorological Administration stations.

The following figure shows the daily gauge stations from CMA and monthly gauge stations in the process of CHIRPS merging which includes the unknown spatial distribution and precipitation values of daily stations

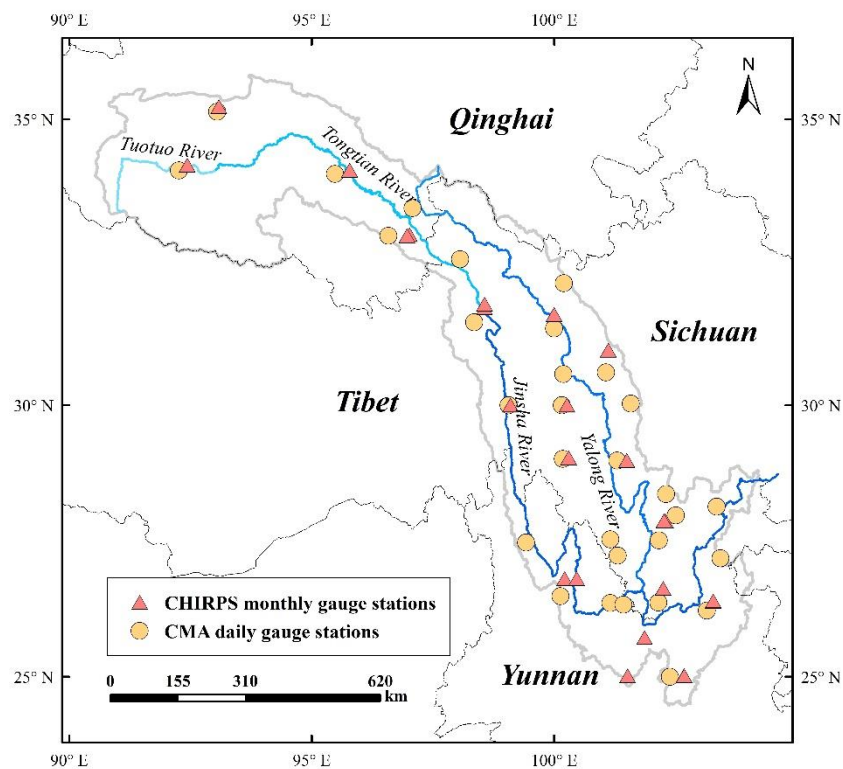


**Figure** The daily gauge stations from CMA and monthly gauge stations in the process of CHIRPS merging

**(3) Phase3:** Besides this, the methodology and validation seem to be reasonable. The authors should emphasize that the validation is against the gauge measurements (from using leave-one-out) and not against CHIRP and CHIRPS. Only the error statistics of CHIRP and CHIRPS data are used for comparison purpose. There are still quite a lot of English usage problems. More careful proofreading is needed.

**Answer:** Thanks. The rainfall from CHIRP, CHIRPS, and the adjusted rainfall from WHU-SGCC are all evaluated with gauge observations so that we can know how the performance of WHU-SGCC on daily precipitation monitoring over the mountainous area before and after correction, and the limitations of CHIRPS data.

**Change:** We corrected English usage problems.

**Minor comments:**

1. Line 46, 49: Use Huffman et al. (2018) reference for IMERG data and Huffman et al (2010) for TMPA data. These are official IMERG and TMPA references.

Huffman, G. J, D. T. Bolvin, D. Braithwaite, K. Hsu, R. Joyce, P. Xie (2018). NASA Global Precipitation Measurement Integrated Multi-satellitE Retrievals for GPM (IMERG), NASA Algorithm theoretical basis document (ATBD) version 5.2., 35 pp. [https://pmm.nasa.gov/sites/default/files/document\\_files/IMERG\\_ATBD\\_V5.2.pdf](https://pmm.nasa.gov/sites/default/files/document_files/IMERG_ATBD_V5.2.pdf)

Huffman, G.J., R.F. Adler, D.T. Bolvin, and E. Nelkin (2010). The TRMM Multi-satellite Precipitation Analysis (TMPA). In F. Hossain and M. Gebremichael (Ed.), Satellite Rainfall Applications for Surface Hydrology. (3-22). Springer Verlag. ISBN: 978-90-481-2914-0

**Answer:** Thanks. Done;

**Change:** We have added these two references.

2. Line 41-62: These satellite precipitation data or merged data seem to be introduced in random order.

**Answer:** Thanks. We have introduced the multi-satellite precipitation products in order.

**Change:** changed from

“Accordingly, there are many kinds of precipitation estimates combining multiple sources datasets. Since 1997, the Tropical Rainfall Measurement Mission (TRMM) has improved satellite-based rainfall retrievals over tropical regions (Kummerow et al., 1998; Simpson et al., 1988), and then applies a stepwise method for blending daily TRMM Multisatellite Precipitation Analysis (TMPA) output with rain gauges in South America (Vila et al., 2009). The Global Precipitation Measurement (GPM) satellite was launched after the success of the TRMM satellite by the cooperation of National Aeronautics and Space Administration (NASA) and Japan Aerospace Exploration Agency (JAXA) on February 27, 2014 (Mahmoud et al., 2018; Ning et al., 2016). The main core observatory satellite (GPM) cooperates with the ten other satellites (partners) to offer the high spatiotemporal resolution products ( $0.1^\circ \times 0.1^\circ$ - half- hourly) of the global real-time precipitation estimates (Mahmoud et al., 2019). The Geostationary Operational Environmental Satellite (GOES)-R Series is the geostationary weather satellites, which significantly improves the detection and observation of environmental

phenomena. The Advanced Baseline Imager (ABI) onboard the GOES-R platform will provide images in 16 spectral bands, spatial resolution of 0.5 to 2 km (2 km in the infrared and 1-0.5 km in the visible), and full-disk scanning every 5 minutes over the continental United States. The GOES-R Series will offer the enhanced capabilities for satellite-based rainfall estimation and nowcasting (Behrangi et al., 2009; Schmit et al., 2005). The Global Precipitation Climatology Project (GPCP) is one of the successful projects for blending rain gauge analysis and multiple satellite-based precipitation estimates, and constructed a relatively coarse-resolution (monthly,  $2.5^\circ \times 2.5^\circ$ ) global precipitation dataset (Adler et al., 2003; Huffman et al., 1997). To improve the resolution of this satellite-based dataset, the GPCP network data was incorporated into remote sensing information with Artificial Neural Networks (PERSIANN) rainfall estimates, which provides finer temporal and spatial resolutions (daily,  $0.25^\circ \times 0.25^\circ$ ) (Ashouri et al., 2015). The CPC Merged Analysis of Precipitation (CMAP) product is a data blending and fusion analysis of gauge data and satellite-based precipitation estimates (Xie and Arkin, 1996). CMAP has a long-term dataset series from 1979, while the resolution is relatively coarse. Although the aforementioned products are widely used and have performed well, the data resolution cannot achieve high accuracy in precipitation monitoring over the Jinsha River Basin, China.”

to

“Accordingly, many kinds of precipitation estimates combining multiple sources and datasets are available. Table 1 shows the temporal and spatial resolution of current major satellite-based precipitation datasets. Since 1997, the Tropical Rainfall Measurement Mission (TRMM) has improved satellite-based rainfall retrievals over tropical regions (Kummerow et al., 1998; Simpson et al., 1988). High spatial and temporal resolution multi-satellite precipitation products have been developed continuously during the TRMM era (Maggioni et al., 2016), including: (1) the TRMM Multisatellite Precipitation Analysis (TMPA) products, which are derived from gauge-satellite fusing (Huffman et al., 2010; Vila et al., 2009); (2) the Climate Prediction Center (CPC) morphing technique (Joyce et al., 2004; Joyce and Xie, 2011; Xie et al., 2017), which integrates geosynchronous infrared (GEO IR) and polar-orbiting microwave (PMW) sensor data and is available three-hourly on a grid with a spacing of  $0.25^\circ$ ; (3) the Precipitation Estimation from Remotely Sensed Information using Artificial Neural Networks - Climate Data Record (PERSIANN-CDR) produced by the PERSIANN algorithm, which has daily temporal and  $0.25^\circ \times 0.25^\circ$  spatial resolutions (Ashouri et al., 2015); and (4) the Global Satellite Mapping of Precipitation (GSMaP) project, which produces global rainfall estimates in near-real time and applies the motion vector Kalman filter based on physical models (GSMaP-NRT and GSMaP-MVK, respectively) (Aonashi et al., 2009; Ushio et al., 2009; Ushio and Kachi, 2010). In 2014, the Global Precipitation Measurement (GPM) satellite was launched after the success of the TRMM satellite by a cooperation between the National Aeronautics and Space Administration (NASA) and Japan Aerospace Exploration Agency (JAXA) (Mahmoud et al., 2018; Ning et al., 2016). The main core observatory satellite (GPM) integrates advanced radar and radiometer systems to obtain the precipitation physics and takes advantages of TMPA, the Climate Prediction Center morphing technique

(CMORPH), and PERSIANN algorithms to offer high spatiotemporal resolution products ( $0.1^\circ \times 0.1^\circ$ , half-hourly) of global real-time precipitation estimates (Huffman et al., 2018; Skofronick-Jackson et al., 2017; Hou et al., 2014). Nevertheless, the major aforementioned products have only been available since 1998, which limits long-term climatological studies. Only the PERSIANN-CDR data set has temporal coverage since 1983. However, the spatial resolution of PERSIANN-CDR is relatively coarse, and the data resolution must be degraded to achieve high accuracy in precipitation monitoring. To fill the gap in high resolution and long-term global multi-satellite precipitation monitoring, the Multi-Source Weighted-Ensemble Precipitation (MSWEP) product (Beck et al., 2017; Beck et al., 2019), and the Climate Hazards Group Infrared Precipitation with Station data (CHIRPS) product from UC Santa Barbara (Funk et al., 2015 a) were developed. MSWEP is a precipitation data set with global coverage available at  $0.1^\circ$  spatial resolution and at three-hourly, daily, and monthly temporal resolutions. MSWEP is multi-source data that take advantage of the complementary strengths of gauge-, satellite-, and reanalysis-based data. However, to provide precipitation estimates at a higher spatial resolution, the CHIRPS data set is used in this study.”

**Table 1** Coverage and spatiotemporal resolutions of major satellite precipitation datasets.

Product	Temporal resolution	Spatial resolution	Period	Coverage
TRMM 3B42-RT	3 hourly	$0.25^\circ$	1998-present	$50^\circ\text{S}-50^\circ\text{N}$
CMORPH	30 min	8 km	1998-	$60^\circ\text{S}-60^\circ\text{N}$
PERSIANN-CDR	Daily	$0.25^\circ$	1983-(delayed) present	$60^\circ\text{S}-60^\circ\text{N}$
GsMaP-NRT	hourly	$0.01^\circ$	2007	$60^\circ\text{S}-60^\circ\text{N}$
GsMaP-MVK	hourly	$0.01^\circ$	2000	$60^\circ\text{S}-60^\circ\text{N}$
	30 min/Hourly/			$60^\circ\text{S}-60^\circ\text{N}$
GPM	3 hourly/Daily/3Day/7 Day/Monthly	$0.1^\circ/0.25^\circ/0.05^\circ/5^\circ$	2014-present	$70^\circ\text{N}-70^\circ\text{S}$ $90^\circ\text{N}-90^\circ\text{S}$
MSWEP	3 hourly/Daily/Monthly	$0.1^\circ$	1979-2017	$90^\circ\text{N}-90^\circ\text{S}$
CHIRPS	Annual/Monthly/ Dekad/Pentad/Daily	$0.05^\circ/0.25^\circ$	1981- present	$50^\circ\text{S}-50^\circ\text{N}$

3. Line 65: The sentence “Table 1 shows ...” should appear in the beginning of previous paragraph before introducing different data set.

**Answer:** Thanks. Done.

**Change:** The sentence “Table 1 shows ...” was **changed** to appear in the beginning of previous paragraph before introducing different data set.

4. Line 69: Temporal resolution?

**Answer:** Thanks. The CHIRPS data has the different temporal resolutions, such as annual, monthly, daily and so on.

5. Table 1: GPCP has a daily product

CMAP has pentad product?

CHIRPS: what is Dekad/Pentad? The temporal resolution does not match 3-day and 6-

day resolution described in Line 151.

**Answer:** Thanks. We changed Table 1.

**Change:** We deleted the CMAP product, which is not very relevant to this study.

(1) 6 pentads = 1 calendar month. Each of first 5 pentads in a month have 5 days. The last pentad contains all the days from the 26th to the end of the month.

(2) A dekad = sum of 2 pentads. There are 3 dekads in a calendar month.

So we changed “It covers a quasi-global area (land only, 50° S-50° N) with several temporal scales (daily, pentad, dekad or monthly time steps)” to “It covers a quasi-global area (land only, 50° S-50° N) with several temporal scales (**daily, pentad, dekad or monthly temporal resolutions**)”

**Table 1** Coverage and spatiotemporal resolutions of major satellite precipitation datasets.

Product	Temporal resolution	Spatial resolution	Period	Coverage
TRMM 3B42-RT	3 hourly	0.25°	1998-present	50°S-50°N
CMORPH	30 min	8 km	1998-	60°S-60°N
PERSIANN-CDR	Daily	0.25°	1983-(delayed) present	60°S-60°N
GsMaP-NRT	hourly	0.01°	2007	60°S-60°N
GsMaP-MVK	hourly	0.01°	2000	60°S-60°N
	30 min/Hourly/			60°S-60°N
GPM	3 hourly/Daily/3Day/7 Day/Monthly	0.1°/0.25°/0.05°/5°	2014-present	70°N-70°S
				90°N-90°S
MSWEP	3 hourly/Daily/Monthly	0.1°	1979-2017	90°N-90°S
	Annual/Monthly/			
CHIRPS	Dekad/Pentad/Daily	0.05°/0.25°	1981- present	50°S-50°N

6. Line 137 and Figure 2 caption: annual precipitation during JJA is not correct usage. Should remove “annual”.

**Answer:** Thanks. We changed the study period from summer season to the four seasons.

**Change:** changed “**Figure 2** The multi-year (1990-2014) average annual precipitation during JJA over the Jinsha River Basin. 30 rain stations were provided by the China Meteorological Administration stations, the other 18 CHIRPS fusion stations were provided by the Climate Hazards Group UC Santa Barbara online at [ftp://ftp.chg.ucsb.edu/pub/org/chg/products/CHIRPS-](ftp://ftp.chg.ucsb.edu/pub/org/chg/products/CHIRPS-2.0/diagnostics/global_monthly_station_density/tifs/p05/)

2.0/diagnostics/global\_monthly\_station\_density/tifs/p05/ (last access: 10 December, 2018).” to “**Figure 2** The multi-year (1990-2014) average seasonal precipitation over the Jinsha River Basin interpolated from 30 rain gauges downloaded from the China Meteorological Administration stations. ”

7. Line 157: TRMM 3B42 is itself a merged product including both geostationary IR and microwave measurements from polar orbiting satellites and some gauge data.

**Answer:** Thanks. There are some errors with CHIRPS data introduction.

**Change:** changed

“This dataset contains a wide variety of satellite-based rainfall products derived from multiple data sources and incorporates four data types: monthly precipitation from

CHPClim v.1.0 (Climate Hazards Group's Precipitation Climatology version 1) derived from the combination of the satellite fields, gridded physiographic indicators, and in situ climate normal with the geospatial modelling approach based on moving window regressions and inverse distance weighting interpolation (Funk et al., 2015 b), quasi-global geostationary thermal infrared satellite observations (TRMM 3B42 version 7), atmospheric model rainfall fields CFS (Climate Forecast System) from NOAA, and surface based precipitation observations from various sources including national or regional meteorological services. The differences from other frequently used precipitation products are the higher resolution of 0.05°, wider coverage and the longer-term data series from 1981 to the present (Funk et al., 2015 a).”

to

“This dataset contains a wide variety of satellite-based rainfall products derived from multiple data sources and incorporates **five** data types: (1) the montxinhly precipitation from CHPClim v.1.0 (Climate Hazards Group's Precipitation Climatology version 1) derived from the combination of the satellite fields, gridded physiographic indicators, and in situ climate normal with the geospatial modelling approach based on moving window regressions and inverse distance weighting interpolation (Funk et al., 2015 b); (2) quasi-global geostationary thermal infrared (IR) satellite observations; (3)**TRMM 3B42 product (Huffman et al., 2007)**; (4) atmospheric model rainfall fields CFS (Climate Forecast System, version 2) from NOAA; (5) and surface based precipitation observations from various sources including national and regional meteorological services. The differences from other frequently used precipitation products are the higher resolution of 0.05°, wider coverage and the longer-term data series from 1981 to the near-real time (Funk et al., 2015 a). ”

8. Line 161: Are you sure that the IR rainfall estimates have pentad resolution?

**Answer:** Yes. Thanks.

“CHIRPS is the product of a two part process. First, IR Precipitation (IRP) pentad rainfall estimates are created from satellite data by calculating the percentage of time during the pentad that the IR observations indicate cold cloud tops (<235° K), and converting that value into millimeters of precipitation by means of previously determined local regression with TRMM 3B42 precipitation pentads.” (Funk et al., 2014)

Funk, C. C., Peterson, P. J., Landsfeld, M. F., Pedreros, D. H., Verdin, J. P., Rowland, J. D., Romero, B. E., Husak, G. J., Michaelsen, J. C., and Verdin, A. P.: A quasi-global precipitation time series for drought monitoring, US Geological Survey Data Series, 832, 1-12, 2014.

9. Line 167-168: Don't understand why CHIRPS is used as validation data. The new data is supposed to perform better because more surface station is available?

**Answer:** Thanks.

(1) The rainfall from CHIRP, CHIRPS, and the adjusted rainfall from WHU-SGCC are all evaluated with gauge observations so that we can know how the performance of WHU-SGCC on daily precipitation monitoring over the mountainous area before and

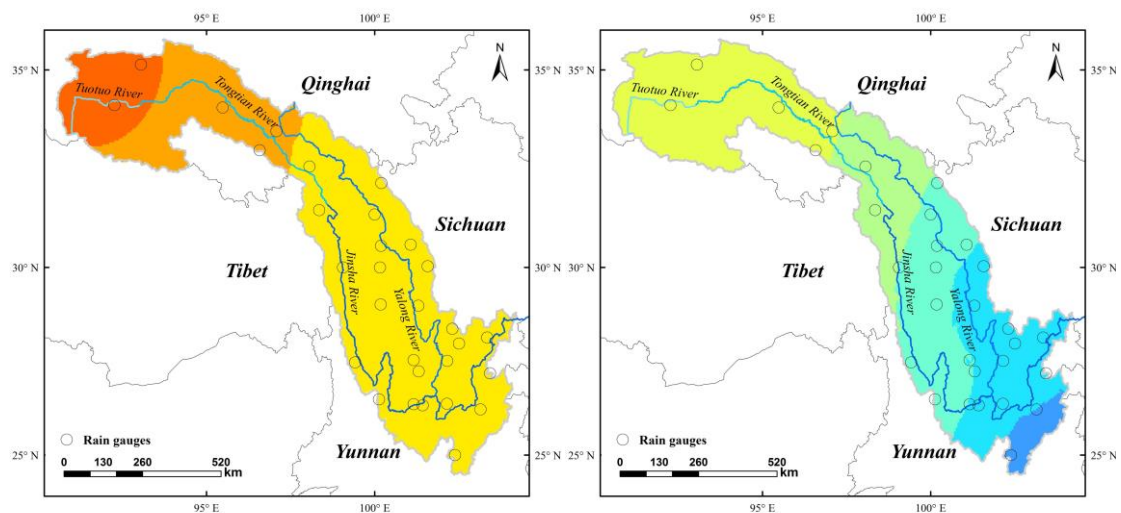
after correction, and the limitations of CHIRPS data.

(2) The WHU-SGCC approach is a promising tool to monitor the summer precipitation over the Jinsha River Basin, considering the spatial correlation and historical precipitation characteristics which is different from the process of CHIRPS merging.

And then, the CHIRPS station processing stream incorporates data from five public data streams and several private archives. The public data streams are the GHCN monthly, GHCN daily, Global Summary of the Day (GSOD), GTS and Southern African Science Service Centre for Climate Change and Adaptive Land Management (SASSCAL, [www.sasscalweathernet.org](http://www.sasscalweathernet.org)). GTS data are collected daily; GHCN, GSOD and SASSCAL data are updated monthly. However, the stations for daily CHIRPS are different from those download from CMA in the spatial distribution, and the precipitation values used for CHIRPS production are only monthly values available online:

[ftp://ftp.chg.ucsb.edu/pub/org/chg/products/CHIRPS-2.0/diagnostics/monthly\\_station\\_data/](ftp://ftp.chg.ucsb.edu/pub/org/chg/products/CHIRPS-2.0/diagnostics/monthly_station_data/)). **With the aim of daily precipitation adjustment over the Jinsha River Basin, the daily gauge observations from CMA are considered into the study to reblend with daily CHIRP data, due to the unknown spatial distribution and precipitation values of gauge stations in the process of daily CHIRPS merging.**

**Change:** We reconfirmed the gauge stations used for CHIRPS merging at the official website and redrawn the map of daily gauge stations (Figure 2).



(a) Spring

(b) Summer

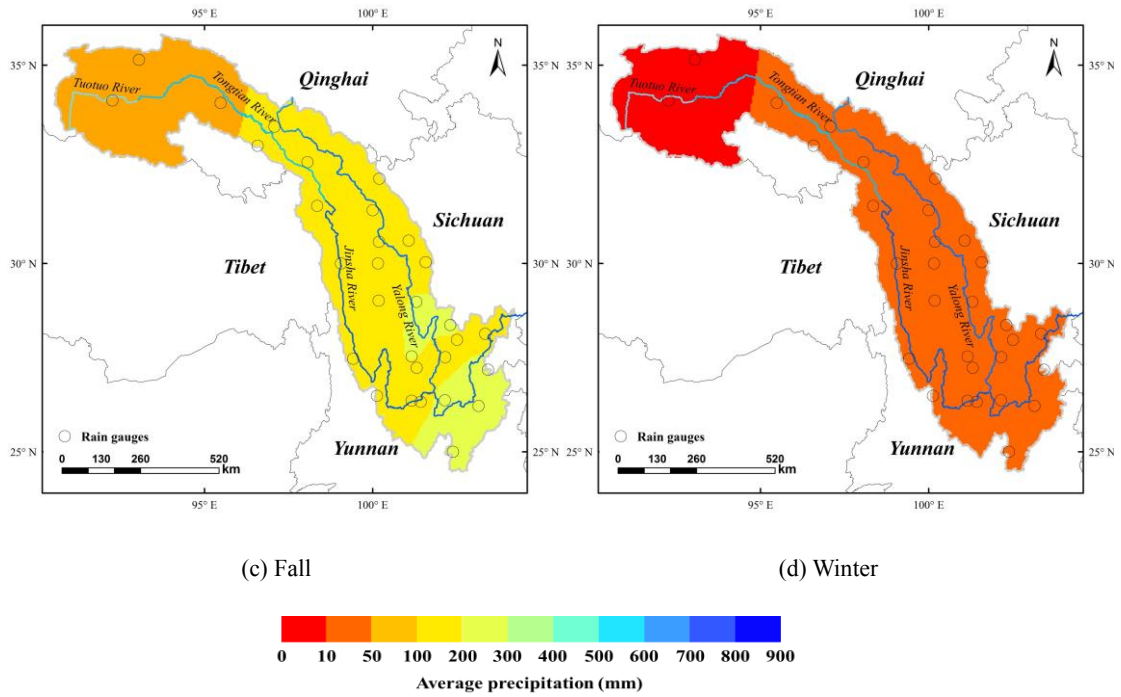


**Figure 2** The multi-year (1990-2014) average seasonal precipitation over the Jinsha River Basin interpolated from 30 rain gauges downloaded from the China Meteorological Administration stations.

The following figure shows the daily gauge stations from CMA and monthly gauge stations in the process of CHIRPS merging which includes the unknown spatial distribution and precipitation values of daily stations

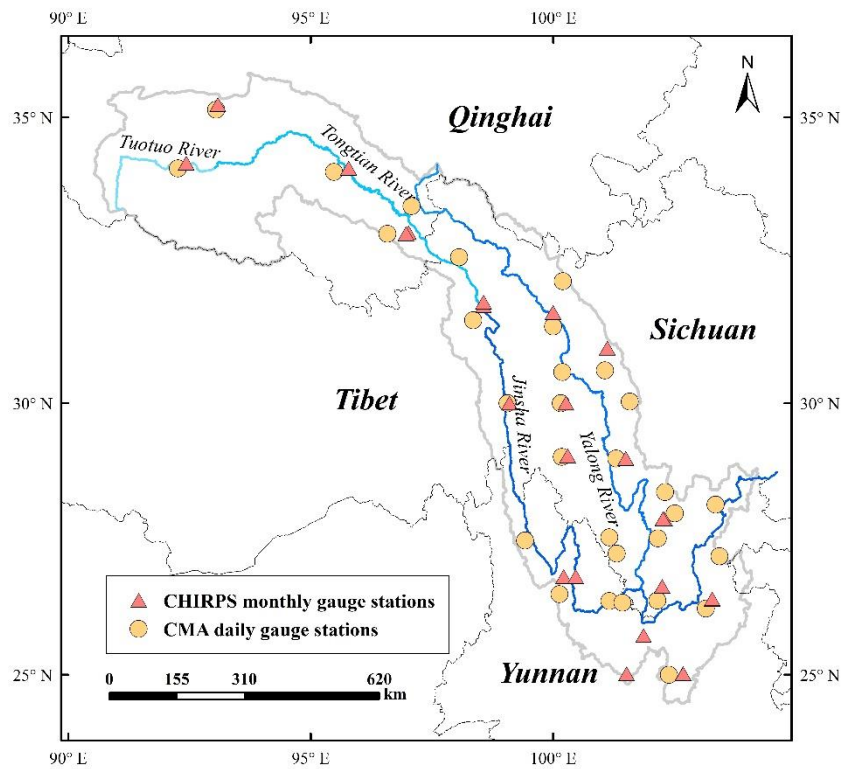


**Figure** The daily gauge stations from CMA and monthly gauge stations in the process of CHIRPS merging

10. Line 187: Analyze

**Answer:** Thanks. Done.

**Change:** changed “Analyse the relationships” to “**Analyze** the relationships”

11. Line 196: replace “statistically” with “statistical”

**Answer:** Thanks. Done.

**Change:** changed “Pearson’s Correlation Coefficient (PCC) can indicate the statistically similarity of rainfall characteristics among pixels over a seasonal scale.” to “Pearson’s Correlation Coefficient (PCC) can represent the **statistical** similarity of the rainfall characteristics among the pixels in a certain spatial area at a seasonal scale..”

12. Line 231: “molecular” should be numerator Rule 2 generates clusters of precipitation areas for the JinSha River region. Can you plot the cluster map?

**Answer:** Thanks. Done.

**Change:** changed “molecular” to “**numerator**” and the cluster map is in **Appendix E**.

13. Line 291: Equation (12): It seems that you choose to adjust C3 precipitation based on one C2 pixel that provides maximum precipitation value. What is the rational here?

**Answer:** Thanks. Equation (12) is to avoid precipitation estimates adjusted by Rule 3 below 0 and the negative values is set to 0.

14. Don’t understand this sentence. Aren’t C4 pixels adjusted in Rule 4? How are C1 pixels adjusted in the end?

**Answer:** Thanks.

Rule 1 is only to establish a regression model between each gauge historical observations and the corresponding CHIRP grid cell values, so the C1 pixels are not adjusted in this process. Then after Rule 1, Rule 2 and Rule 3, the unknown spatial precipitation data include both C1 and C4 pixels. Finally, all the remaining unknown pixels are adjusted by Rule 4.

15. Line 430: “In hence”, there is no such usage. Use “Therefore” instead.

**Answer:** Thanks. Done.

**Change:** changed “In hence” to “**Therefore**”.

16. Line 470: Should be “multi-model”

**Answer:** Thanks. Done.

**Change:** changed “mulit-model” to “**multi-model**”.

17. Table 5: Why CHIRPS has much worse performance than CHIRP?

**Answer:**

The CHIRPS was derived from blending in-suit precipitation observations and the CHIRP data, with a modified inverse-distance weighting algorithm at a quasi-global area (land only, 50° S-50° N). The blended data (CHIRPS) has an effective performance

on a large scale region, such as at the national scale, but there are still large discrepancies with ground observations at the sub-regional level, especially at the river basin scale. The performance and applicability of CHIRPS at the sub-regional level still need to be validated. What's more, the interpolation performance from the limited and sparse rain gauge stations will be affected by more errors which was evaluated with rain gauge stations shown in Table 5.

As such, due to the poor performance at the sub-regional scale, the gauge-satellite fusing algorithms can be assumed to limit high accuracy estimations in the process of CHIRPS data production. Therefore, the aim of this article is to present a novel approach for reblending daily liquid precipitation gauge data and the Climate Hazards Group Infrared Precipitation (CHIRP) satellite-derived precipitation estimates developed by UC Santa Barbara to improve the precipitation estimated accuracy at the river basin scale.

## Reply to Report #4 (Referee #6)

**Manuscript ID:** essd-2018-150

**Title:** WHU-SGCC: A novel approach for blending daily satellite (CHIRP) and precipitation observations over the Jinsha River Basin

**Journal:** Earth System Science Data

**Type:** Article

Dear Reviewer,

Thank you for your insight comments and suggestions. We have modified the manuscript accordingly. We trust that all of your comments have been addressed accordingly in the revised manuscript. If you have further suggestions for changes, please let us know. The detailed corrections are listed below point by point:

All changes in the manuscript are marked with **red color**.

In this manuscript, authors have proposed a new method to combine satellite and rain gauge precipitation estimates at fine spatial resolution over a river basin. The merged precipitation product is also compared with CHIRPS dataset.

### Specific comments

My specific comments are given below.

1. L43-44: TMPA uses monthly rain gauge analysis over the tropical land, not only over the South America. For the production of TMPA product, reference of Huffman et al. (2008, JHM/2010, Book chapter) must be there.

**Answer:** Thanks. Done.

**Change:** changed “and then applies a stepwise method for blending daily TRMM Multisatellite Precipitation Analysis (TMPA) output with rain gauges in South America (Vila et al., 2009).” to “**the TRMM Multisatellite Precipitation Analysis (TMPA) products, which are derived from gauge-satellite fusing** (Huffman et al., 2010; Vila et al., 2009);”

Huffman, G. J., Adler, R. F., Bolvin, D. T., and Nelkin, E. J.: The TRMM Multi-Satellite Precipitation Analysis (TMPA), in: Satellite Rainfall Applications for Surface Hydrology, edited by: Gebremichael, M., and Hossain, F., Springer Netherlands, Dordrecht, 3-22, 2010.

2. L46-49: These references for GPM are not relevant here. It must be replaced by Hou et al. (2014, BAMS) and Skofronick-Jackson et al. (2017, BAMS).

**Answer:** Thanks.

**Change:** changed. We replaced the references.

Changed from “The Global Precipitation Measurement (GPM) satellite was launched after the success of the TRMM satellite by the cooperation of National Aeronautics and

Space Administration (NASA) and Japan Aerospace Exploration Agency (JAXA) on February 27, 2014 (Mahmoud et al., 2018; Ning et al., 2016). The main core observatory satellite (GPM) cooperates with the ten other satellites (partners) to offer the high spatiotemporal resolution products ( $0.1^\circ \times 0.1^\circ$ - half- hourly) of the global real-time precipitation estimates (Mahmoud et al., 2019; Huffman et al., 2018).”

To

“In 2014, the Global Precipitation Measurement (GPM) satellite was launched after the success of the TRMM satellite by a cooperation between the National Aeronautics and Space Administration (NASA) and Japan Aerospace Exploration Agency (JAXA) (Mahmoud et al., 2018; Ning et al., 2016). The main core observatory satellite (GPM) integrates advanced radar and radiometer systems to obtain the precipitation physics and takes advantages of TMPA, the Climate Prediction Center morphing technique (CMORPH), and PERSIANN algorithms to offer high spatiotemporal resolution products ( $0.1^\circ \times 0.1^\circ$ , half-hourly) of global real-time precipitation estimates (Huffman et al., 2018; Skofronick-Jackson et al., 2017; Hou et al., 2014).”

Hou, A. Y., Kakar, R. K., Neeck, S., Azarbarzin, A. A., Kummerow, C. D., Kojima, M., Oki, R., Nakamura, K., and Iguchi, T.: The Global Precipitation Measurement Mission, *Bulletin of the American Meteorological Society*, 95, 701-722, 10.1175/bams-d-13-00164.1, 2014.

Skofronick-Jackson, G., Petersen, W. A., Berg, W., Kidd, C., Stocker, E. F., Kirschbaum, D. B., Kakar, R., Braun, S. A., Huffman, G. J., Iguchi, T., Kirstetter, P. E., Kummerow, C., Meneghini, R., Oki, R., Olson, W. S., Takayabu, Y. N., Furukawa, K., and Wilheit, T.: The Global Precipitation Measurement (GPM) Mission for Science and Society, *Bulletin of the American Meteorological Society*, 98, 1679-1695, 10.1175/bams-d-15-00306.1, 2017.

3. L49-53: Why authors introduced GOES-R here? It is suggested to maintain a hierarchy such as infrared-only, MW-only followed by multi-satellite precipitation products. Actually, this whole paragraph does not read good to me.

**Answer:** Thanks. We deleted the introduction of GOES-R and modified the explanation

**Change:** changed from

“Accordingly, there are many kinds of precipitation estimates combining multiple sources datasets. Since 1997, the Tropical Rainfall Measurement Mission (TRMM) has improved satellite-based rainfall retrievals over tropical regions (Kummerow et al., 1998; Simpson et al., 1988), and then applies a stepwise method for blending daily TRMM Multisatellite Precipitation Analysis (TMPA) output with rain gauges in South America (Vila et al., 2009). The Global Precipitation Measurement (GPM) satellite was launched after the success of the TRMM satellite by the cooperation of National Aeronautics and Space Administration (NASA) and Japan Aerospace Exploration Agency (JAXA) on February 27, 2014 (Mahmoud et al., 2018; Ning et al., 2016). The main core observatory satellite (GPM) cooperates with the ten other satellites (partners) to offer the high spatiotemporal resolution products ( $0.1^\circ \times 0.1^\circ$ - half- hourly) of the global real-time precipitation estimates (Mahmoud et al., 2019). The Geostationary Operational Environmental Satellite (GOES)-R Series is the geostationary weather satellites, which significantly improves the detection and observation of environmental phenomena. The Advanced Baseline Imager (ABI) onboard the GOES-R platform will

provide images in 16 spectral bands, spatial resolution of 0.5 to 2 km (2 km in the infrared and 1-0.5 km in the visible), and full-disk scanning every 5 minutes over the continental United States. The GOES-R Series will offer the enhanced capabilities for satellite-based rainfall estimation and nowcasting (Behrangi et al., 2009;Schmit et al., 2005). The Global Precipitation Climatology Project (GPCP) is one of the successful projects for blending rain gauge analysis and multiple satellite-based precipitation estimates, and constructed a relatively coarse-resolution (monthly,  $2.5^{\circ} \times 2.5^{\circ}$ ) global precipitation dataset (Adler et al., 2003;Huffman et al., 1997). To improve the resolution of this satellite-based dataset, the GPCP network data was incorporated into remote sensing information with Artificial Neural Networks (PERSIANN) rainfall estimates, which provides finer temporal and spatial resolutions (daily,  $0.25^{\circ} \times 0.25^{\circ}$ ) (Ashouri et al., 2015). The CPC Merged Analysis of Precipitation (CMAP) product is a data blending and fusion analysis of gauge data and satellite-based precipitation estimates (Xie and Arkin, 1996). CMAP has a long-term dataset series from 1979, while the resolution is relatively coarse. Although the aforementioned products are widely used and have performed well, the data resolution cannot achieve high accuracy in precipitation monitoring over the Jinsha River Basin, China.”

to

“Accordingly, many kinds of precipitation estimates combining multiple sources and datasets are available. Table 1 shows the temporal and spatial resolution of current major satellite-based precipitation datasets. Since 1997, the Tropical Rainfall Measurement Mission (TRMM) has improved satellite-based rainfall retrievals over tropical regions (Kummerow et al., 1998;Simpson et al., 1988). High spatial and temporal resolution multi-satellite precipitation products have been developed continuously during the TRMM era (Maggioni et al., 2016), including: (1) the TRMM Multisatellite Precipitation Analysis (TMPA) products, which are derived from gauge-satellite fusing (Huffman et al., 2010;Vila et al., 2009); (2) the Climate Prediction Center (CPC) morphing technique (Joyce et al., 2004;Joyce and Xie, 2011;Xie et al., 2017), which integrates geosynchronous infrared (GEO IR) and polar-orbiting microwave (PMW) sensor data and is available three-hourly on a grid with a spacing of  $0.25^{\circ}$ ; (3) the Precipitation Estimation from Remotely Sensed Information using Artificial Neural Networks - Climate Data Record (PERSIANN-CDR) produced by the PERSIANN algorithm, which has daily temporal and  $0.25^{\circ} \times 0.25^{\circ}$  spatial resolutions (Ashouri et al., 2015); and (4) the Global Satellite Mapping of Precipitation (GSMaP) project, which produces global rainfall estimates in near-real time and applies the motion vector Kalman filter based on physical models (GSMaP-NRT and GSMaP-MVK, respectively) (Aonashi et al., 2009;Ushio et al., 2009;Ushio and Kachi, 2010). In 2014, the Global Precipitation Measurement (GPM) satellite was launched after the success of the TRMM satellite by a cooperation between the National Aeronautics and Space Administration (NASA) and Japan Aerospace Exploration Agency (JAXA) (Mahmoud et al., 2018;Ning et al., 2016). The main core observatory satellite (GPM) integrates advanced radar and radiometer systems to obtain the precipitation physics and takes advantages of TMPA, the Climate Prediction Center morphing technique (CMORPH), and PERSIANN algorithms to offer high spatiotemporal resolution

products ( $0.1^\circ \times 0.1^\circ$ , half-hourly) of global real-time precipitation estimates (Huffman et al., 2018; Skofronick-Jackson et al., 2017; Hou et al., 2014). Nevertheless, the major aforementioned products have only been available since 1998, which limits long-term climatological studies. Only the PERSIANN-CDR data set has temporal coverage since 1983. However, the spatial resolution of PERSIANN-CDR is relatively coarse, and the data resolution must be degraded to achieve high accuracy in precipitation monitoring. To fill the gap in high resolution and long-term global multi-satellite precipitation monitoring, the Multi-Source Weighted-Ensemble Precipitation (MSWEP) product (Beck et al., 2017; Beck et al., 2019), and the Climate Hazards Group Infrared Precipitation with Station data (CHIRPS) product from UC Santa Barbara (Funk et al., 2015 a) were developed. MSWEP is a precipitation data set with global coverage available at  $0.1^\circ$  spatial resolution and at three-hourly, daily, and monthly temporal resolutions. MSWEP is multi-source data that take advantage of the complementary strengths of gauge-, satellite-, and reanalysis-based data. However, to provide precipitation estimates at a higher spatial resolution, the CHIRPS data set is used in this study.”

**Table 1** Coverage and spatiotemporal resolutions of major satellite precipitation datasets.

Product	Temporal resolution	Spatial resolution	Period	Coverage
TRMM 3B42-RT	3 hourly	$0.25^\circ$	1998-present	$50^\circ\text{S}-50^\circ\text{N}$
CMORPH	30 min	8 km	1998-	$60^\circ\text{S}-60^\circ\text{N}$
PERSIANN-CDR	Daily	$0.25^\circ$	1983-(delayed) present	$60^\circ\text{S}-60^\circ\text{N}$
GsMaP-NRT	hourly	$0.01^\circ$	2007	$60^\circ\text{S}-60^\circ\text{N}$
GsMaP-MVK	hourly	$0.01^\circ$	2000	$60^\circ\text{S}-60^\circ\text{N}$
	30 min/Hourly/			$60^\circ\text{S}-60^\circ\text{N}$
GPM	3 hourly/Daily/3Day/7 Day/Monthly	$0.1^\circ/0.25^\circ/0.05^\circ/5^\circ$	2014-present	$70^\circ\text{N}-70^\circ\text{S}$ $90^\circ\text{N}-90^\circ\text{S}$
MSWEP	3 hourly/Daily/Monthly	$0.1^\circ$	1979-2017	$90^\circ\text{N}-90^\circ\text{S}$
CHIRPS	Annual/Monthly/ Dekad/Pentad/Daily	$0.05^\circ/0.25^\circ$	1981- present	$50^\circ\text{S}-50^\circ\text{N}$

4. L69: Recent study (<https://doi.org/10.1016/j.jhydrol.2019.01.036>) needs to be included.

**Answer:** Thanks. Done.

**Change:** Added the reference.

“The CHIRPS precipitation dataset with several temporal and spatial scales has been evaluated in Brazil (Nogueira et al., 2018;Paredes-Trejo et al., 2017), Chile (Yang et al., 2016;Zambrano-Bigiarini et al., 2017), China (Bai et al., 2018), Cyprus (Katsanos et al., 2016a;Katsanos et al., 2016b), India (Ali and Mishra, 2017) and Italy (Duan et al., 2016).” to

“The CHIRPS precipitation dataset with several temporal and spatial scales has been evaluated in Brazil (Nogueira et al., 2018;Paredes-Trejo et al., 2017), Chile (Yang et al., 2016;Zambrano-Bigiarini et al., 2017), China (Bai et al., 2018), Cyprus (Katsanos et al., 2016a;Katsanos et al., 2016b), India (Ali and Mishra, 2017; Prakash, 2019) and Italy (Duan et al., 2016).”

Prakash, S.: Performance assessment of CHIRPS, MSWEP, SM2RAIN-CCI, and TMPA precipitation products across India, Journal of Hydrology, 571, 50-59, 10.1016/j.jhydrol.2019.01.036, 2019.

5. Table 2 should be kept as “Supplementary Material”.

**Answer:** Thanks. Done.

**Change:** changed Table 2 to Appendix A.

6. Fig. 2: Symbols are not clearly visible. The mean precipitation is derived from 30 rain gauges or from CHIRPS?

**Answer:** Thanks. Done. The mean precipitation is derived from 30 rain gauges.

**Change:** We redrawn the Fig. 2 in the four seasons.

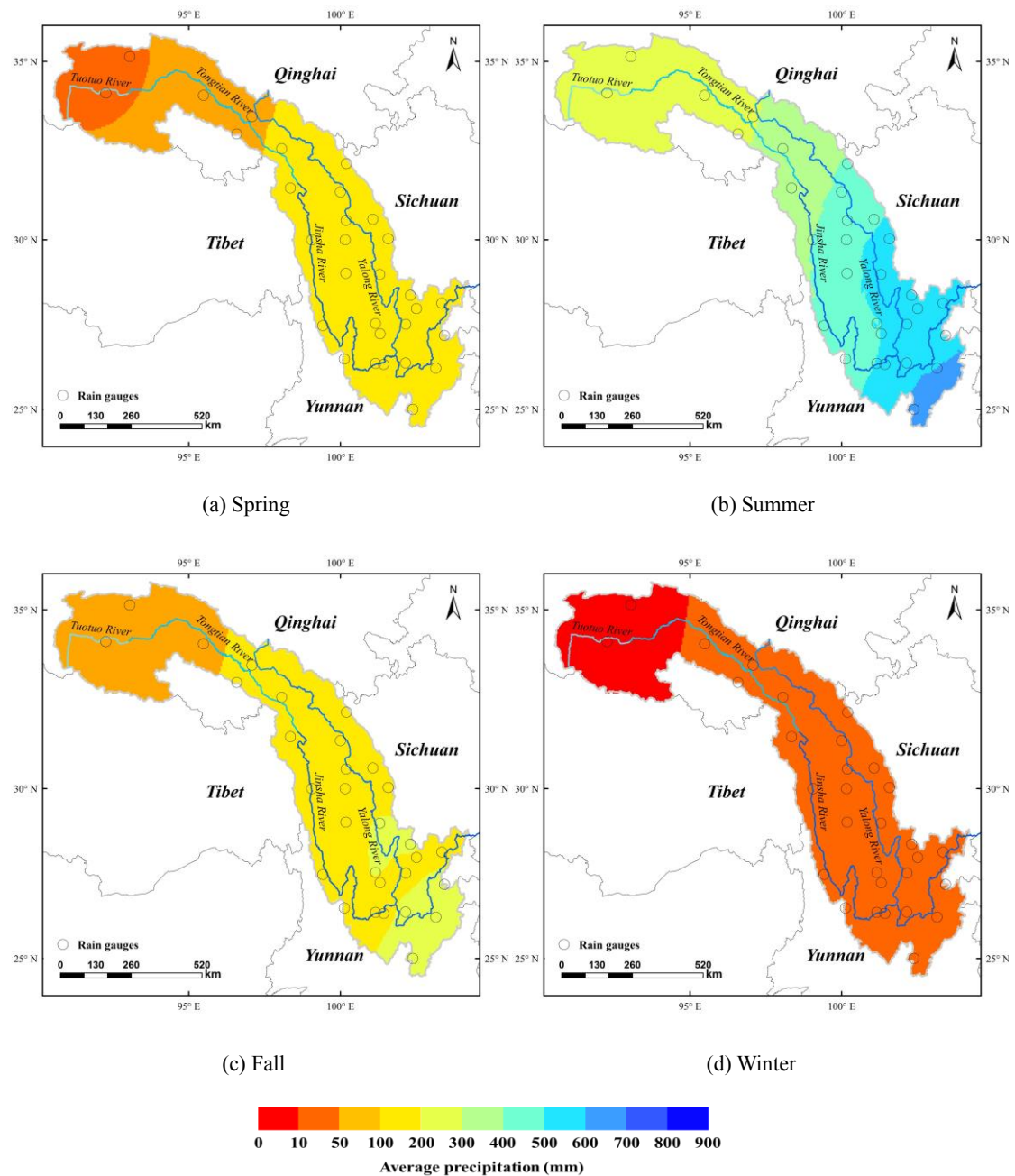


**Figure 2** The multi-year (1990-2014) average seasonal precipitation over the Jinsha River Basin interpolated from 30 rain gauges downloaded from the China Meteorological Administration stations.

7. L172-173: Whether 18 gauges of CHIRPS are subset of 30 gauges of CMA? It needs to be elaborated.

**Answer:**

The CHIRPS station processing stream incorporates data from five public data streams and several private archives. The public data streams are the GHCN monthly, GHCN daily, Global Summary of the Day (GSOD), GTS and Southern African Science Service Centre for Climate Change and Adaptive Land Management (SASSCAL, [www.sasscalweathernet.org](http://www.sasscalweathernet.org)). GTS data are collected daily; GHCN, GSOD and SASSCAL data are updated monthly.

However, the stations for daily CHIRPS data have a different spatial distribution than those downloaded from the CMA, and the precipitation values used for CHIRPS production are the monthly values available online ([ftp://ftp.chg.ucsb.edu/pub/org/chg/products/CHIRPS-2.0/diagnostics/monthly\\_station\\_data/](ftp://ftp.chg.ucsb.edu/pub/org/chg/products/CHIRPS-2.0/diagnostics/monthly_station_data/)). For the daily precipitation adjustments over the Jinsha River Basin, the daily gauge observations from the CMA are blended with the daily CHIRP data due to the unknown spatial distribution and precipitation values of gauge stations used in the process of daily CHIRPS merging.

**Change:** We reconfirmed the gauge stations used for CHIRPS merging at the official website and redrawn the map of daily gauge stations (Figure 2).

The following figure shows the daily gauge stations from CMA and monthly gauge stations in the process of CHIRPS merging which includes the unknown spatial distribution and precipitation values of daily stations

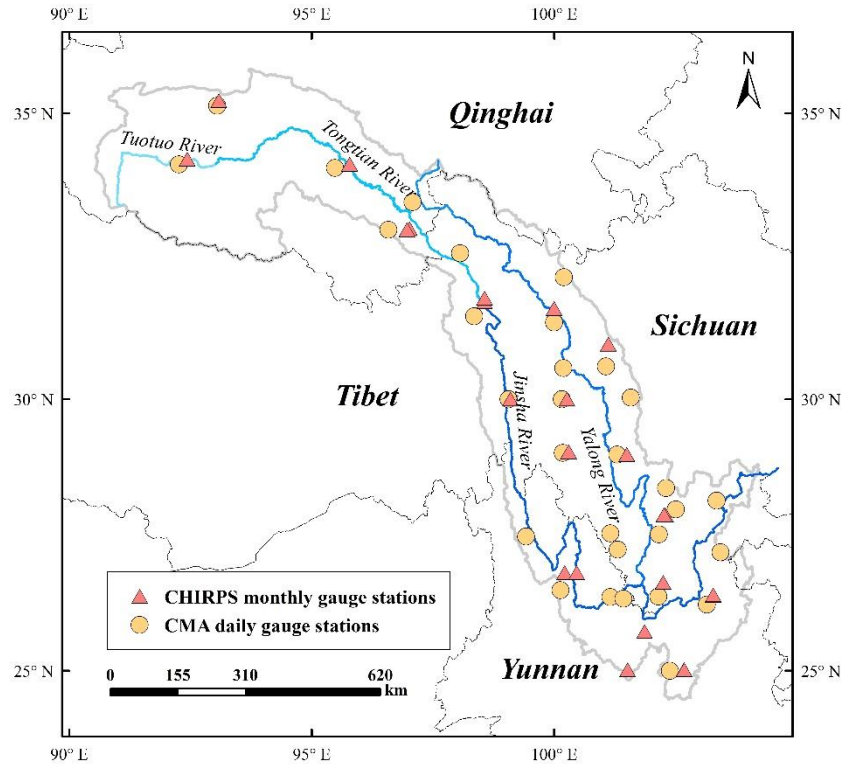


**Figure** The daily gauge stations from CMA and monthly gauge stations in the process of CHIRPS merging

8. This study proposes a new method to merge satellite and rain gauge observations. However, it is still not clear that the proposed method is better than any existing merging technique. I would suggest to compare your technique with few operational techniques and present the improvement in accuracy of precipitation estimation by the proposed method.

**Answer:** Thank you for your valuable comments.

As such, due to the poor performance at the sub-regional scale, the gauge-satellite fusing algorithms can be assumed to limit high accuracy estimations in the process of CHIRPS data production. Therefore, the aim of this article is to present a novel approach (WHU-SGCC) for reblending daily liquid precipitation gauge data and CHIRP satellite-derived precipitation estimates developed by UC Santa Barbara, over the Jinsha River Basin. The results adjusted by WHU-SGCC were compared with those of CHIRP and CHIRPS at the overall, daily and rain events evaluations. According to the performance of the WHU-SGCC, we can see that the precipitation adjusted by the WHU-SGCC method can achieve greater accuracy compared with CHIRP and CHIRPS, with average improvements of Pearson's correlation coefficient (PCC) of 0.01-0.23 and 0.06-0.32, respectively. The PCCs were improved to more than 0.5 in the spring and fall and to approximately 0.5 in the winter, and they were the worst in the summer, which may be attributed to the greater precipitation in the summer and lower precipitation in the winter. In addition, the NSE of the WHU-SGCC provides substantial improvements over CHIRP and CHIRPS, which reached 0.2836, 0.2944 and

0.1853 in the spring, fall and winter, respectively. In the summer, the NSE of the WHU-SGCC is still negative, but it is improved to be nearly zero, which indicates that the adjusted results are similar to the average level of the rain gauge observations. All of the measured errors were reduced except for the BIAS, which showed no significant improvement in the summer but was approximately 0. The results indicate that the WHU-SGCC has the best ability to reduce precipitation errors for daily accuracy evaluations, with average reductions of 15% and 34% compared to CHIRP and CHIRPS, respectively. Overall, the WHU-SGCC approach achieves good performance in error correction of CHIRP and CHIRPS.

In the future, we will further investigate the performance of the WHU-SGCC method when time is sufficient by comparing with more methods, such as Quantile Mapping and Bayesian methods.

9. I would suggest to use **normalized parameters** for error/bias computation for better assessment.

**Answer:** Thanks. The BIAS used in this study is the **normalized bias**.

$$\text{BIAS} = \frac{\sum_{i=1}^n (C_i - Y_{oi})}{\sum_{i=1}^n Y_{oi}}$$

## Reply to Report #5 (Referee #7)

**Manuscript ID:** essd-2018-150

**Title:** WHU-SGCC: A novel approach for blending daily satellite (CHIRP) and precipitation observations over the Jinsha River Basin

**Journal:** Earth System Science Data

**Type:** Article

Dear Reviewer,

Thank you for your insight comments and suggestions. We have modified the manuscript accordingly. We trust that all of your comments have been addressed accordingly in the revised manuscript. If you have further suggestions for changes, please let us know. The detailed corrections are listed below point by point:

All changes in the manuscript are marked with **red color**.

1. L11: The authors mention that the existing blending algorithms are very bad at removing random errors at the daily scale. However, in the introduction, the authors only mention three articles related to blending techniques. The authors must present a better literature review. I do not agree that all the algorithms are very bad at removing random errors at the daily scale; see MSWEP as an example. MSWEP is a merged precipitation product (using rain gauges, reanalysis, and satellite-based precipitation products) which has good performance in many areas.

**Answer:** Thanks. We changed the description of the shortcomings of existing methods in abstract.

**Changed:** changed “and the existing data blending algorithms are very bad at removing the day-by-day random errors.” to “and **most of** the existing data blending algorithms **are not good** at removing the day-by-day errors”

2. L70: The authors mention that the articles presented between L67-69 evaluated the products mainly at monthly and seasonal scales lacking the evaluation of daily precipitation. In the case of Chile, **Zambrano-Bigiarini et al., (2017) include a daily evaluation and Yang et al., (2016)** is a study of bias correction and its also at daily scale.

**Answer:** Thanks. The evaluations of CHIRPS at daily scale are indeed conducted in Chile, however, the bias correction is still limited.

**Change:** changed from “Nevertheless, the temporal resolutions of the aforementioned applications were mainly at seasonal and monthly scales, lacking the evaluation of daily precipitation.” to “However, the temporal resolutions of these applications were mainly at seasonal and monthly scales, lacking the **evaluation and correction** of daily precipitation.”

3. Table 1: I think that MSWEP should be included in the study because is a state-of-the-art merged product, it can be compared to the product obtained applying this method.  
**Answer:** Thanks. We changed the introduction.

**Changed:**

“To fill the gap in high resolution and long-term global multi-satellite precipitation monitoring, the Multi-Source Weighted-Ensemble Precipitation (MSWEP) product (Beck et al., 2017; Beck et al., 2019), and the Climate Hazards Group Infrared Precipitation with Station data (CHIRPS) product from UC Santa Barbara (Funk et al., 2015 a) were developed. MSWEP is a precipitation data set with global coverage available at 0.1° spatial resolution and at three-hourly, daily, and monthly temporal resolutions. MSWEP is multi-source data that takes advantage of the complementary strengths of gauge-, satellite-, and reanalysis-based data. However, to provide precipitation estimates at a higher spatial resolution, the CHIRPS data set is used in this study.”

**Table 1** Coverage and spatiotemporal resolutions of major satellite precipitation datasets.

Product	Temporal resolution	Spatial resolution	Period	Coverage
TRMM 3B42-RT	3 hourly	0.25°	1998-present	50°S-50°N
CMORPH	30 min	8 km	1998-	60°S-60°N
PERSIANN-CDR	Daily	0.25°	1983-(delayed) present	60°S-60°N
GsMaP-NRT	hourly	0.01°	2007	60°S-60°N
GsMaP-MVK	hourly	0.01°	2000	60°S-60°N
	30 min/Hourly/			60°S-60°N
GPM	3 hourly/Daily/3Day/7 Day/Monthly	0.1°/0.25°/0.05°/5°	2014-present	70°N-70°S 90°N-90°S
MSWEP	3 hourly/Daily/Monthly	0.1°	1979-2017	90°N-90°S
CHIRPS	Annual/Monthly/ Dekad/Pentad/Daily	0.05°/0.25°	1981- present	50°S-50°N

4. L122: Here the authors mention that: 'because of the Jinsha River Basin has more precipitation during the summer season the blending of satellite estimations with gauged observations during JJA is the main focus of the research'. I completely disagree with this... If the authors are presenting a novel approach for blending ground-based measurements with a satellite product it has to be evaluated throughout the year and not only for one season.

**Answer:** Thanks.

**Change:** We demonstrated the WHU-SGCC method by applying it to daily precipitation over the Jinsha River Basin in the different seasons from 1990 to 2014.

5. L196: Assumption number three states that the correlation coefficient can indicate the statistical similarity of rainfall characteristics among pixels. What would happen if two different areas show similar correlation values but different precipitation amounts?

**Answer:** Thanks. We assumed that there are no long-held outliers at one pixel of the CHIRP dataset, so Pearson’s Correlation Coefficient (PCC) can represent the statistical similarity of rainfall characteristics among pixels over a seasonal scale. Here, PCC are

calculated between raster pixels from long-term CHIRP data set at a certain spatial scope, which will have the same precipitation over a seasonal scale.

**Change:** changed “Pearson’s Correlation Coefficient (PCC) can indicate the statistically similarity of rainfall characteristics among pixels over a seasonal scale.” to “**There are no long-held outliers at one pixel in the CHIRP dataset**, so Pearson’s Correlation Coefficient (PCC) can represent the statistical similarity of the rainfall characteristics among the pixels **in a certain spatial area** at a seasonal scale.”

6. The authors present four classes of pixels: C1 (pixels with at least 1 station); C2 (pixels statistically similar to C1); C3 (similar to C2); and C4 (the rest of the pixels): How does the total precipitation amount is considered when the authors apply the RF models to the C2 pixels?

**Answer:** Thanks. The historical precipitation features between CHIRP pixels at C1 and C2 pixels are the main consideration of this study, but not the total precipitation amount. It is reasonable to assume that there are some pixels that are statistically similar to the **historical precipitation characteristics** of C1 pixels in a certain spatial scope. Therefore, it is feasible to adjust the satellite estimation bias of C2 pixels by referring to the appropriate regression relationships at corresponding C1 pixels based on Rule 1. The determination of C2 pixels is as the following procedure:

With exception of the C1 pixels, the remaining pixels in each cluster represent potential C2 pixels called R pixels. Pearson’s correlation coefficient (PCC) and p-values between the satellite estimations (**multi-year daily CHIRP grid cell values** during the summer seasons from 1990 to 2014) at R pixels and the C1 pixels are the criteria for final determination of C2 pixels. **The critical values for PCC and p-value are 0.5 and 0.05, so the selected C2 pixels can then be considered statistically similar to the precipitation characteristics of the corresponding C1 pixels in their defined spatial scope.**

7. The authors mention that the development of methods for high-accuracy precipitation estimates over complex terrain is of vital importance, how is this considered in the

**Answer:** In Rule 2, the terrain factors were considered to divide rainfall area.

Some studies indicate that geographical location, elevation and other terrain information influences the spatial distribution of rainfall, especially in mountainous areas with complex topography (Anders et al., 2006; Long and Singh, 2013). Therefore, it is reasonable to assume that there are some pixels statistically similar to historical precipitation characteristics in a certain spatial scope. In Rule 2, the approach of fuzzy c-means (FCM) clustering was explored to determine the spatial range considered as each pixel’s terrain factors including longitude, latitude, elevation, slope, aspect and curvature. The pixels with statistically similar precipitation characteristics are determined at a physically similar area (the region with similar terrain features) in WHU-SGCC algorithm, which can contribute to improve the accuracy of precipitation estimates.

8. The amount of C4 pixels is around 60%, and for these pixels the authors apply an IDW interpolation, how do the authors justify that some pixels are blended with machine learning and others are simply interpolated? Which are the expected errors of this methodology for each type of pixels (C1-4)? What happen with the small scale convective events (which are present in summer) neover the C4 pixels?

**Answer:** Thanks.

The WHU-SGCC process shown that the adjustment method for C2 pixels was derived from C1 pixels, the adjustment method for C3 pixels was derived from C2 pixels, and the adjusted values for C1 and C4 pixels were interpolated by IDW with C2 and C3 pixels. There were statistically relationship among C1, C2, C3 and C4 pixels. Thus, the performance of WHU-SGCC method would be evaluated on the overall accuracy, not on a certain class of pixels.

In addition, we added the spatial distribution of C1-C3 pixels in Appendix D. The C4 pixels can be interpolated by the IDW based on the C2 and C3 pixels due to the amount and spatial distribution of the C2 and C3 pixels.

We also added the pixel type in Appendix D. Each validation gauge station could be identified as either C2, C3 or C4 pixels to evaluate the performances of all the rules in the WHU-SGCC method.

Validation gauge station	Pixel type			
	Spring	Summer	Fall	Winter
52908	C4	C4	C4	C4
56004	C4	C4	C4	C4
56021	C2	C2	C2	C3
56029	C2	C3	C2	C3
56034	C2	C3	C2	C3
56038	C4	C4	C4	C4
56144	C4	C4	C4	C4
56146	C4	C4	C4	C4
56152	C2	C3	C3	C4
56167	C4	C2	C2	C4
56247	C4	C4	C4	C4
56251	C2	C2	C3	C3
56257	C4	C4	C4	C4
56357	C4	C4	C4	C4
56374	C4	C4	C3	C4
56459	C4	C4	C4	C4
56462	C4	C4	C4	C4
56475	C4	C3	C3	C3
56479	C4	C4	C4	C4
56485	C3	C2	C2	C3
56543	C3	C3	C4	C4

56565	C2	C2	C3	C3
56571	C2	C4	C4	C4
56586	C2	C3	C2	C3
56651	C3	C2	C2	C3
56664	C4	C4	C4	C4
56666	C3	C3	C3	C3
56671	C3	C2	C2	C3
56684	C2	C2	C2	C4
56778	C4	C3	C3	C4

9. The authors should present a map with the mean annual precipitation for the study area using CHIRP and the blended product. This would be interesting because it would help the reader to see if the transition of precipitation between the different classes of pixels is smooth.

**Answer:** Thanks. We added the maps with the average seasonal precipitation for the study area in Fig. 4.

**Changed:** The multi-year (1990-2014) average seasonal precipitation over the Jinsha River Basin interpolated from WHU-SGCC, CHIRP and CHIRPS is shown in Fig. 4. There exist some differences in the spatial pattern of precipitation estimates. Overall, the WHU-SGCC method exhibits the similar spatial distribution of precipitation to the CHIRP and CHIRPS, while the WHU-SGCC method attenuated the intense rain in the central area. The statistical accuracy evaluations are needed to further analyze the performance of the WHU-SGCC method.

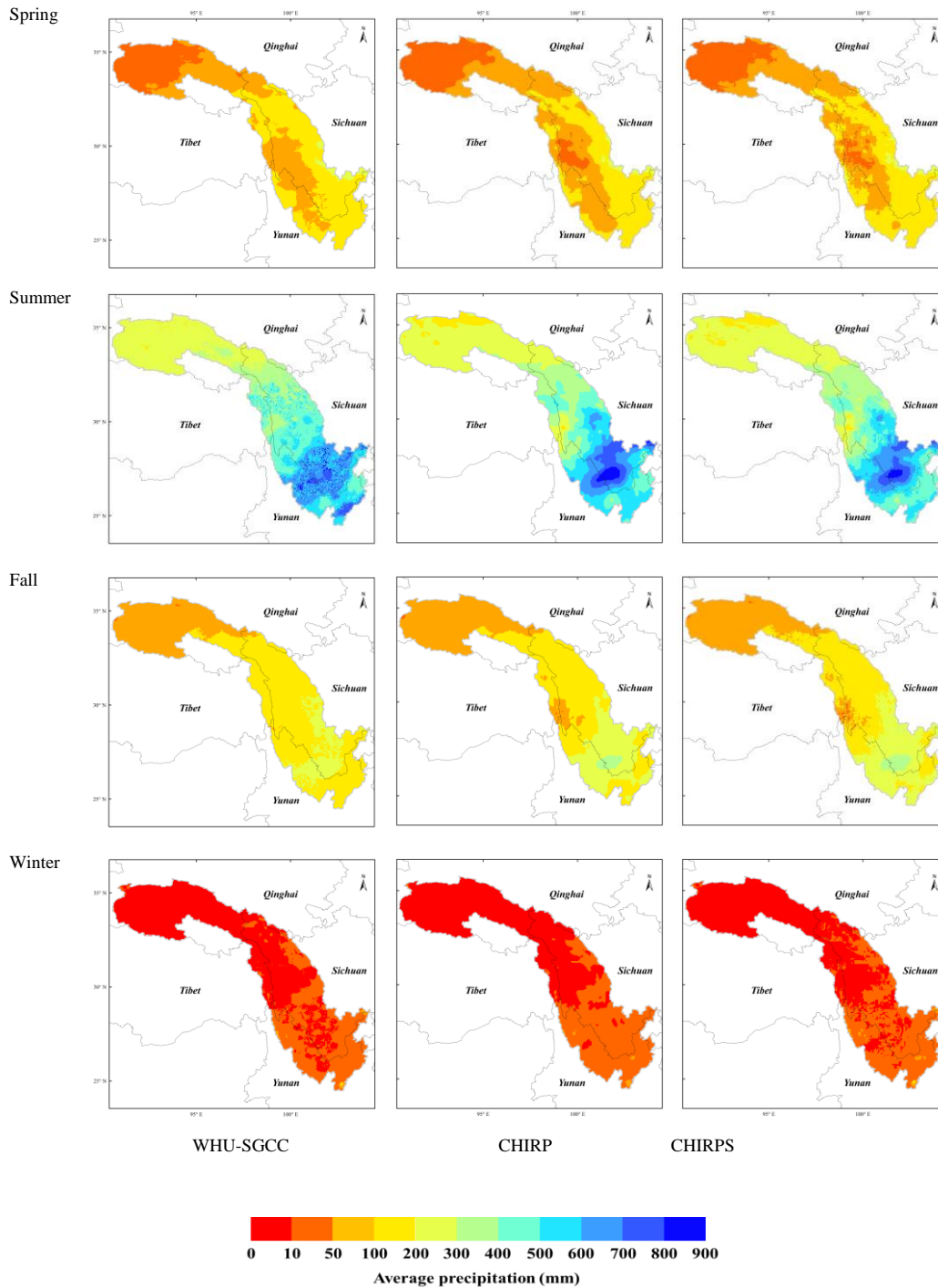


**Figure 4** The multi-year (1990-2014) average seasonal precipitation over the Jinsha River Basin interpolated from WHU-SGCC, CHIRP and CHIRPS.

10. Table 5: which values are represented here? mean, median?

**Answer:** These are mean values of the results validated by leave-one-out cross methods.

11. L360: The authors mention an increase of NSE of 93% which sounds very good, however, this value is still negative. The authors should present the values and not the percentage of improvement as it is relative to the performance of the product and it can

be misleading.

**Answer:** Thanks. Done.

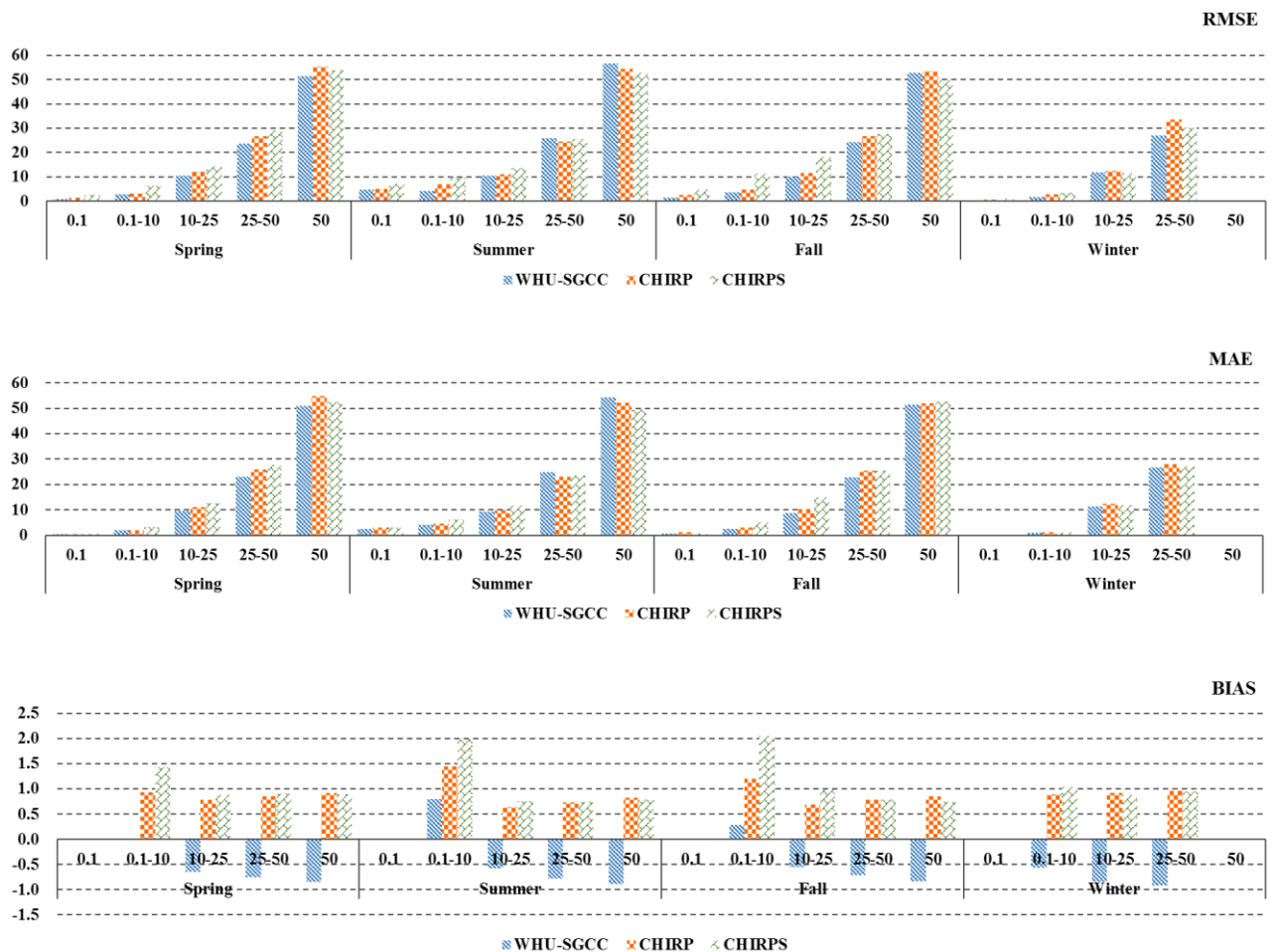
**Change:** changed “Nevertheless, the NSE of the WHU-SGCC reached -0.0137, an increase of 93.33% and 98.32% compared to CHIRP and CHIRPS, respectively.” to “In addition, the NSE of the WHU-SGCC provides substantial improvements over CHIRP and CHIRPS, which reached 0.2941, 0.3087 and 0.1853 in the spring, fall and winter, respectively. In the summer, the NSE of the WHU-SGCC is still negative, but it is improved to be nearly zero, which indicates that the adjusted results are similar to the average level of the rain gauge observations.”

12. Table 5: There is some improvement in POD, however, the PCC and the BIAS are almost similar. The categorical indices (POD, FAR, and CSI) can be decomposed to different precipitation intensities in order to see if the method improves the detection of medium and high intensities or only the no-rain events which are higher in number.

**Answer:** Thanks. We added the POD and CSI for rain events assessment in Fig. 8. The POD and CSI are improved at the different rain events, especially with the total rainfall less than 25 mm.

However, the FAR for different rain events cannot be conducted due to the values of 0 for the number of false alarms at the gauge stations.

**Change:**



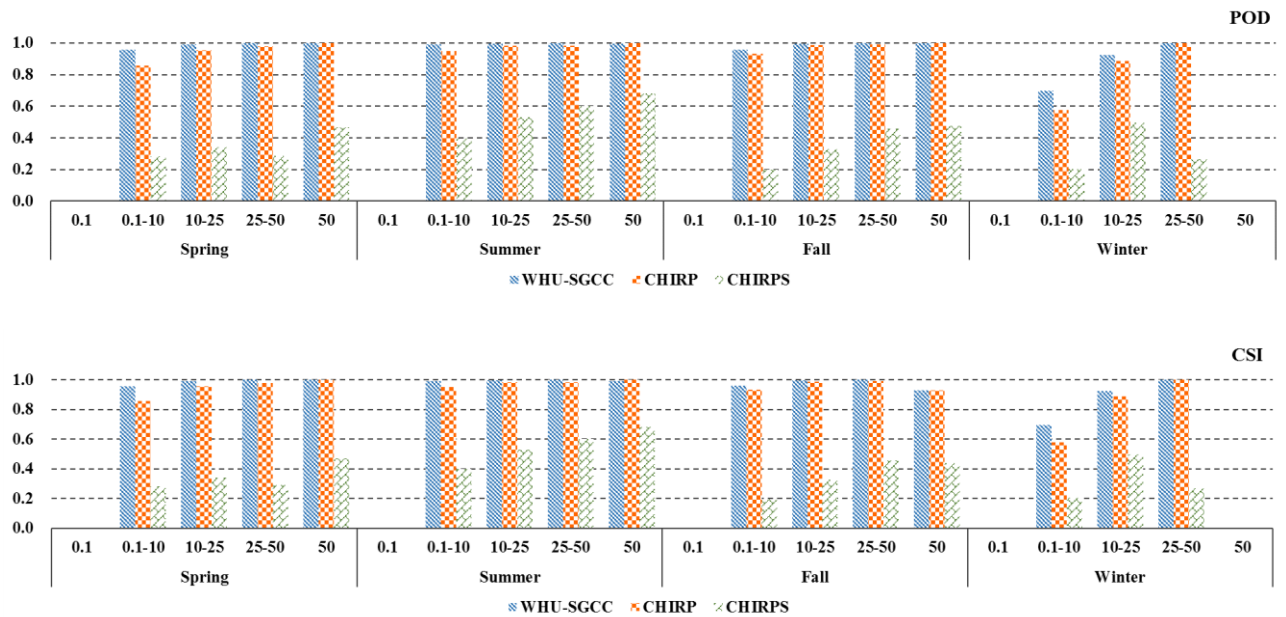


**Figure 8** Accuracy assessment of liquid precipitation events from 1990 to 2014.

13. L381: The authors mention that the presented approach is still effective in adjusting the satellite biases. However, in L357 it is mentioned that the bias showed no significant improvement (which is in agreement with Table 5).

**Answer: Thanks.** We added the spring, fall and winter and changed the discussion.

**Change:** changed from “Although, the absolute value of BIAS of WHU-SGCC was no significant improvement than CHIRP 357 and slightly higher than CHIRPS, all of the values were approximately to 0.” to “The absolute values of the BIAS of the WHU-SGCC are substantial improved in the spring, followed by the summer, winter and fall. Although the absolute value of the BIAS of the WHU-SGCC in fall are not significantly better than those of CHIRP and CHIRPS, all of the values are approximately 0.”

14. Figure 4a and 4d: The legend should be improved. The correlation (PCC) goes from 0.1-0.2; 0.2-0.3 and then just >0.3. If 1.0 is the maximum and 0.3 is still low correlation why not showing the complete ranges?

**Change:** Thanks. We redraw the maps about the spatial distribution of the Pearson’s correlation coefficient with the complete ranges.

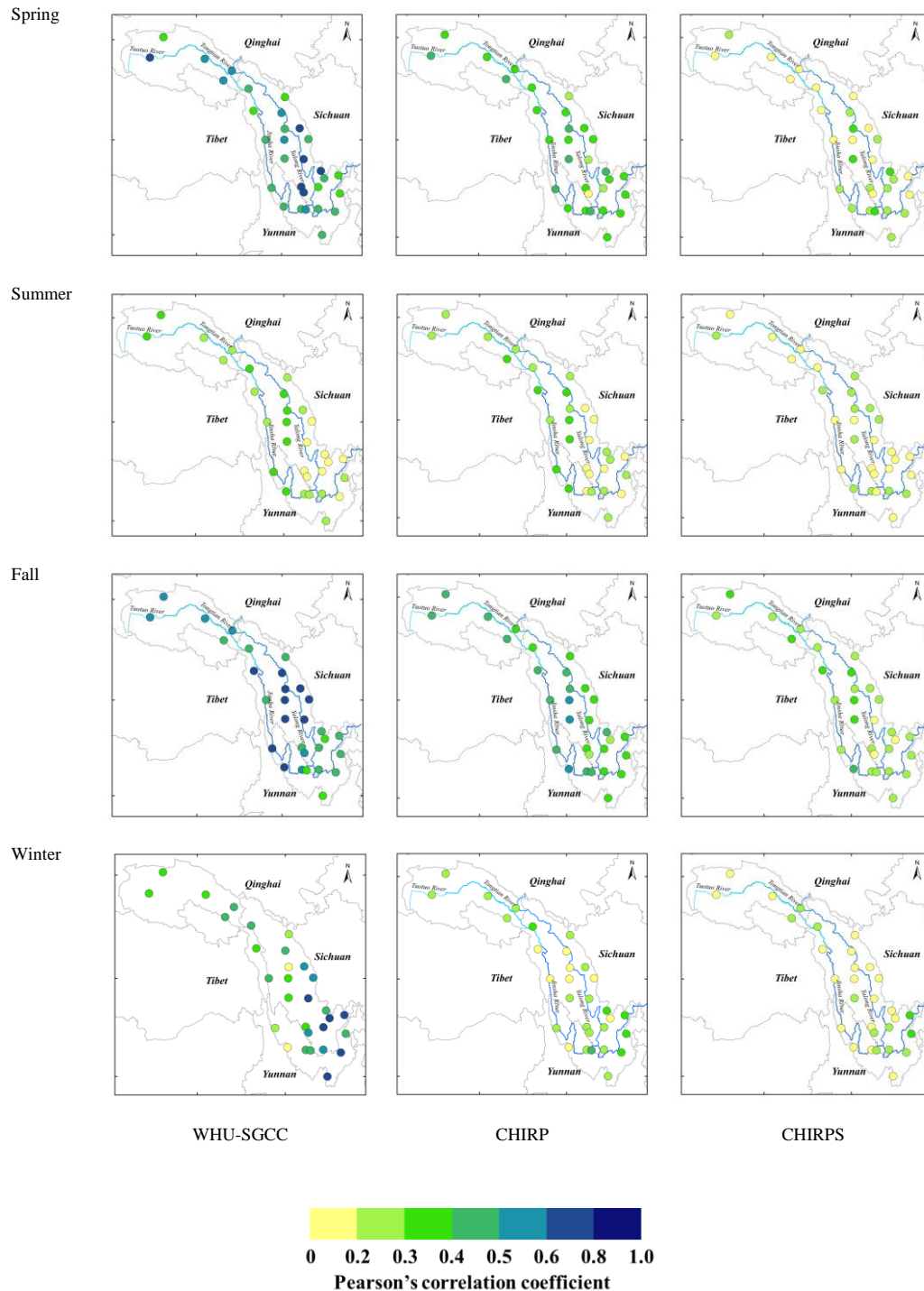


**Figure 5** Spatial distribution of the Pearson's correlation coefficient of the overall agreement between observations and the WHU-SGCC, CHIRP and CHIRPS estimations in the four seasons from 1990 to 2014.

15. L393: If PCCs of WHU-SGCC, CHIRP and CHIRPS are roughly the same, then there was no improvement in the daily correction of events. Can the authors discuss this?

**Answer:** Figure 7 shows the evaluation of daily accuracy.

The evaluation of the daily accuracy indicates that the PCCs of the WHU-SGCC were slightly better than those of CHIRP and CHIRPS in the spring, fall and winter but were not as good in the summer and winter. The WHU-SGCC had lower RMSEs and MAEs than CHIRP and CHIRPS, especially compared to CHIRPS. The daily RMSE and MAE in the summer are the highest, although the WHU-SGCC still corrects the errors. Figure 7 indicates that there is a slight increase in the PCC, with average improvements of 0.02-0.04 and 0.04-0.14, respectively; however, the PCC is a relative metric of the magnitude of the association between paired variables, and a relative consistency may not indicate absolute proximity. Thus, the absolute measure indicated by the RMSE may be more reasonable. In this study, the RMSE and MAE derived from the WHU-SGCC are reduced by approximately 15% and 34% on average compared to CHIRP and CHIRPS, respectively.

Overall, the WHU-SGCC approach can be regarded as an effective tool for daily precipitation adjustments.

16. L403: The authors mention that the WHU-SGCC method seems to be more promising in detecting precipitation compared to CHIRP and CHIRPS although it performs poorly when evaluated with the FAR. However the objective is to provide high quality precipitation estimates.

**Answer:** Thanks.

Although, the FAR of WHU-SGCC is lower than CHIRP and CHIRPS in some days, the overall assessment of FAR is the best.

In terms of the POD, FAR and CSI, except for the results in winter, the WHU-SGCC method appears to be better at detecting precipitation than CHIRP and CHIRPS; the results of POD and CSI are closest to 1, although FAR is worse than CHIRPS on some days. However, the overall result of FAR is the best in the WHU-SGCC. The POD and FAR results are the worst in the winter, and the CSI is slightly higher, which may be attributed to the overestimation of no-rain events and the inherent uncertainty in the CHIRP.

Overall, the WHU-SGCC approach can be regarded as an effective tool for daily precipitation adjustments.

17. Figure 5: There are not labels in each boxplot.

**Answer:** Thanks. Done.

**Change:** We have added the labelling (a,b,...,h) into Fig. 7.

18. Table 7: Please include POD, FAR, and CSI to see the categorical performance over different rainfall intensities.

**Answer:** We added the POD and CSI for rain events assessment in Fig. 8. The FAR for different rain events cannot be conducted due to the values of 0 for the number of false alarms at the gauge stations.

**Change:**



Figure 8 Accuracy assessment of liquid precipitation events from 1990 to 2014.

## Reply to Interactive comment

1. <[authors should] explain more clearly how they did the leave-one-out validation as this important information is not emphasized in the paper. By leaving-one-out if I understand correctly, they will have to repeat the algorithm 30 more times with each time leaving one station as validation station. The pixel that has that station therefore could be identified as either C2, C3 or even C4 pixels. If this is the case, this validation will allow them to validate corrections for all types of pixels. I would then highly recommend that they add (C2, C3, C4 pixel type) near the station number in Table 4. If however, all the station shows as C2 pixels (can't be C1), then the validation is indeed not complete.>

**Answer:** Thanks. We explain more clearly about the leave-one-out validation.

### Change:

(1) Added the following sentence into the first paragraph of section 3.1:

“The leave-one-out cross validation step was applied to computing the out-of-sample adjusted error with gauge stations. **The WHU-SGCC algorithm was repeated 30 times with each time leaving one station as validation station. Each validated pixel will probably be C2, C3 or C4 pixel in the process of WHU-SGCC algorithm.**”

Added the following sentence into the first paragraph of section 3.2: “**The results of accuracy assessment are the average values validated by the leave-one-out cross method.**”

(2) Added the pixel type in Appendix D. Each validation gauge station could be identified as either C2, C3 or C4 pixels to evaluate the performances of all the rules in the WHU-SGCC method.

Validation gauge station	Pixel type			
	Spring	Summer	Fall	Winter
52908	C4	C4	C4	C4
56004	C4	C4	C4	C4
56021	C2	C2	C2	C3
56029	C2	C3	C2	C3
56034	C2	C3	C2	C3
56038	C4	C4	C4	C4
56144	C4	C4	C4	C4
56146	C4	C4	C4	C4
56152	C2	C3	C3	C4
56167	C4	C2	C2	C4
56247	C4	C4	C4	C4
56251	C2	C2	C3	C3
56257	C4	C4	C4	C4

56357	C4	C4	C4	C4
56374	C4	C4	C3	C4
56459	C4	C4	C4	C4
56462	C4	C4	C4	C4
56475	C4	C3	C3	C3
56479	C4	C4	C4	C4
56485	C3	C2	C2	C3
56543	C3	C3	C4	C4
56565	C2	C2	C3	C3
56571	C2	C4	C4	C4
56586	C2	C3	C2	C3
56651	C3	C2	C2	C3
56664	C4	C4	C4	C4
56666	C3	C3	C3	C3
56671	C3	C2	C2	C3
56684	C2	C2	C2	C4
56778	C4	C3	C3	C4

---

# WHU-SGCC: A novel approach for blending daily satellite (CHIRP) and precipitation observations over the Jinsha River Basin

Gaoyun Shen<sup>1</sup>, Nengcheng Chen<sup>1,2</sup>, Wei Wang<sup>1,2</sup>, Zeqiang Chen<sup>1,2</sup>

<sup>1</sup> State Key Laboratory of Information Engineering in Surveying, Mapping and Remote Sensing, Wuhan University, 129 Luoyu Road, Wuhan 430079, China

<sup>2</sup> Collaborative Innovation Center of Geospatial Technology, Wuhan 430079, China

Correspondence to: ZeqiangChen@whu.edu.cn; Tel.: +86 13871025965; Fax: +86 27 68778229.

**Abstract.** Accurate and consistent satellite-based precipitation estimates blended with rain gauge data are important for regional precipitation monitoring and hydrological applications, especially in regions with limited rain gauges. However, the existing fusion precipitation estimates often have large uncertainties over mountainous areas with complex topography and sparse rain gauges, and most of the existing data blending algorithms are not good at removing the day-by-day random errors. Therefore, the development of effective methods for high-accuracy precipitation estimates over complex terrain and on a daily scale is of vital importance for mountainous hydrological applications. This study aims to offer a novel approach for blending daily precipitation gauge data and the Climate Hazards Group Infrared Precipitation (CHIRP; daily, 0.05°) satellite-derived precipitation developed by the UC Santa Barbara over the Jinsha River Basin for the period of June–July–August from 1994 to 2014. This method is named the Wuhan University Satellite and Gauge precipitation Collaborated Correction (WHU-SGCC). The results show that the WHU-SGCC method is effective in liquid precipitation bias-error adjustments from points to surfaces as evaluated by multiple error statistics and from different perspectives. Compared with CHIRP and CHIRP with station data (CHIRPS), the precipitation adjusted by the WHU-SGCC method has greater accuracy with overall average improvements of the Pearson's correlation coefficient (PCC) by 0.01–0.23 and 0.06–0.32, respectively, and decreases in the root mean square error (RMSE) by 0.06–0.1 mm and 0.2–3 mm, respectively. In addition, the NSE of the WHU-SGCC provides substantial improvements than CHIRP and CHIRPS, which reached 0.2836, 0.2944 and 0.1853 in the spring, fall and winter. Daily accuracy evaluations indicate that the WHU-SGCC method has the best ability to reduce precipitation error, with average reductions of 15% and 34 % compared to CHIRP and CHIRPS, respectively. Moreover, the accuracy of the spatial distribution of the precipitation estimates derived from the WHU-SGCC method is related to the complexity of the topography. The validation also verifies that the proposed approach is effective at detecting the major precipitation events inside the Jinsha River Basin with the daily precipitation less than 25 mm. In spite of the correction, the uncertainties in the seasonal precipitation forecasts in the summer and winter are still large, which may due to the homogenization attenuating the simulation of extreme rain event. However, this study indicates that the WHU-SGCC approach may serve as a promising tool to monitor daily monsoon precipitation over the Jinsha River Basin, the which contains complicated mountainous terrain with sparse rain gauge data, considering based on the spatial correlation and the historical precipitation characteristics. The daily precipitation estimations at the 0.05° resolution over the Jinsha River Basin during the all summer four seasons from 1990 to 2014, derived from WHU-SGCC are available at the PANGAEA Data Publisher for Earth & Environmental Science portal (<https://doi.pangaea.de/10.1594/PANGAEA.900620>).

## 1 Introduction

Accurate and consistent estimates of precipitation are vital for hydrological modelling, flood forecasting and climatological studies in support of better planning and decision making (Agutu et al., 2017; Cattani et al., 2018; Roy et al., 2017). In general, ground-based gauge networks include a substantial number of liquid precipitation observations measured with high accuracy, high temporal resolution, and long historical records. However, the sparse distribution and point measurements limit the

40 accurate estimation of spatially gridded rainfall (Martens et al., 2013).

41 Due to the sparseness of rain gauges and their uneven spatial distribution of rain gauges – and the high proportion of missing  
42 data, satellite-derived precipitation data are an attractive supplement offering the advantage of plentiful information with high  
43 spatio-temporal resolution over widespread regions, particularly over oceans, high elevation mountainous regions, and other  
44 remote regions where gauge networks are difficult to deploy. However, satellite estimates are susceptible to systematic biases  
45 that can influence hydrological modelling and the retrieval algorithms are relatively insensitive to light rainfall events,  
46 especially in complex terrain, resulting in underestimations of the magnitudes of precipitation events (Behrangi et al.,  
47 2014; Thiemeig et al., 2013; Yang et al., 2017). Without adjustments, inaccurate satellite-based precipitation estimates will lead  
48 to unreliable assessments of risk and reliability (AghaKouchak et al., 2011).

49 Accordingly, there are many kinds of precipitation estimates combining multiple sources and datasets are available. Table 1  
50 shows the temporal and spatial resolution of current major satellite-based precipitation datasets. Since 1997, the Tropical  
51 Rainfall Measurement Mission (TRMM) has improved satellite-based rainfall retrievals over tropical regions (Kummerow et  
52 al., 1998; Simpson et al., 1988). High spatial and temporal resolution multi-satellite precipitation products have been developed  
53 continuously during the TRMM era (Maggioni et al., 2016), including: and then applies a stepwise method for blending daily  
54 (1) the TRMM Multisatellite Precipitation Analysis (TMPA) products, which are derived from gauge-satellite fusing output  
55 with rain gauges in South America (Huffman et al., 2010; Vila et al., 2009); (2) the Climate Prediction Center (CPC)  
56 morphing technique (Joyce et al., 2004; Joyce and Xie, 2011; Xie et al., 2017), which integrates geosynchronous infrared (GEO  
57 IR) and polar-orbiting microwave (PMW) sensor data and is available three-hourly on a grid with a spacing of 0.25°; (3)  
58 the Precipitation Estimation from Remotely Sensed Information using Artificial Neural Networks - Climate Data Record  
59 (PERSIANN-CDR) produced by the PERSIANN algorithm, which has daily temporal and 0.25° × 0.25° spatial resolutions  
60 (Ashouri et al., 2015); and (4) the Global Satellite Mapping of Precipitation (GSMaP) project, which produces global  
61 rainfall estimates in near-real time and applies the motion vector Kalman filter based on physical models (GSMaP-NRT  
62 and GSMaP-MVK, respectively) (Aonashi et al., 2009; Ushio et al., 2009; Ushio and Kachi, 2010). In 2014, the  
63 Global Precipitation Measurement (GPM) satellite was launched after the success of the TRMM satellite by the cooperation  
64 between the National Aeronautics and Space Administration (NASA) and Japan Aerospace Exploration Agency (JAXA) on  
65 February 27, 2014 (Mahmoud et al., 2018; Ning et al., 2016). The main core observatory satellite (GPM) integrates cooperates  
66 with the ten other satellites (partners) advanced radar and radiometer systems to obtain the precipitation physics and takes  
67 advantages of TMPA, the Climate Prediction Center morphing technique (CMORPH), and PERSIANN algorithms to offer the  
68 high spatiotemporal resolution products (0.1° × 0.1°- half-hourly) of the global real-time precipitation estimates (Mahmoud  
69 et al., 2019; Huffman et al., 2018; Skofronick-Jackson et al., 2017; Hou et al., 2014). The Geostationary Operational  
70 Environmental Satellite (GOES) R Series is the geostationary weather satellites, which significantly improves the detection  
71 and observation of environmental phenomena. The Advanced Baseline Imager (ABI) onboard the GOES R platform will  
72 provide images in 16 spectral bands, spatial resolution of 0.5 to 2 km (2 km in the infrared and 1-0.5 km in the visible), and  
73 full-disk scanning every 5 minutes over the continental United States. The GOES R Series will offer the enhanced capabilities  
74 for satellite-based rainfall estimation and nowcasting (Behrangi et al., 2009; Schmit et al., 2005). Nevertheless, the major  
75 aforementioned products have only been available since 1998, which limits long-term climatological studies. Only the  
76 PERSIANN-CDR data set has temporal coverage since 1983. However, the spatial resolution of PERSIANN-CDR is relatively  
77 coarse, and the data resolution must be degraded to achieve high accuracy in precipitation monitoring. To fill the gap in high  
78 resolution and long-term global multi-satellite precipitation monitoring, the Multi-Source Weighted-Ensemble Precipitation  
79 (MSWEP) product (Beck et al., 2017; Beck et al., 2019), and the Climate Hazards Group Infrared Precipitation with Station  
80 data (CHIRPS) product from UC Santa Barbara (Funk et al., 2015 a) were developed. MSWEP is a precipitation data set with  
81 global coverage available at 0.1° spatial resolution and at three-hourly, daily, and monthly temporal resolutions. MSWEP is

域代码已更改

域代码已更改

multi-source data that takes advantage of the complementary strengths of gauge-, satellite-, and reanalysis-based data. However, to provide precipitation estimates at a higher spatial resolution, the CHIRPS data set is used in this study.

The Global Precipitation Climatology Project (GPCP) is one of the successful projects for blending rain gauge analysis and multiple satellite-based precipitation estimates, and constructed a relatively coarse-resolution (monthly,  $2.5^\circ \times 2.5^\circ$ ) global precipitation dataset (Adler et al., 2003; Huffman et al., 1997). To improve the resolution of this satellite-based dataset, the GPCP network data was incorporated into remote sensing information with Artificial Neural Networks (PERSIANN) rainfall estimates, which provides finer temporal and spatial resolutions (daily,  $0.25^\circ \times 0.25^\circ$ ) (Ashouri et al., 2015). The CPC Merged Analysis of Precipitation (CMAP) product is a data blending and fusion analysis of gauge data and satellite-based precipitation estimates (Xie and Arkin, 1996). CMAP has a long-term dataset series from 1979, while the resolution is relatively coarse. Although the aforementioned products are widely used and have performed well, the data resolution cannot achieve high accuracy in precipitation monitoring over the Jinsha River Basin, China.

Currently, the Climate Hazards Group Infrared Precipitation with Station data (CHIRPS) developed by the UC Santa Barbara, which has a higher spatial resolution ( $0.05^\circ$ ), can solve the scale problem. CHIRPS is a longer length long-term precipitation data series with a higher spatial resolution ( $0.05^\circ$ ) that, which merges three types of information: global climatology, satellite estimates and in situ observations. Table 1 shows the temporal and spatial resolution of current major satellite-based precipitation datasets. The CHIRPS precipitation dataset with several temporal and spatial scales has been evaluated in Brazil (Nogueira et al., 2018; Paredes-Trejo et al., 2017), Chile (Yang et al., 2016; Zambrano-Bigiarini et al., 2017), China (Bai et al., 2018), Cyprus (Katsanos et al., 2016a; Katsanos et al., 2016b), India (Ali and Mishra, 2017; Prakash, 2019) and Italy (Duan et al., 2016). Nevertheless, however, the temporal resolutions of the aforementioned these applications were mainly at seasonal and monthly scales, lacking the evaluation and correction of daily precipitation. Additionally, despite the great potential of gauge-satellite fusing products for large-scale environmental monitoring, there are still large discrepancies with ground observations at the sub-regional level where these data have been applied. Furthermore, the CHIRPS product's reliability has not been analysed in detail over the Jinsha River Basin, in China, particularly on a daily scale. The Jinsha River Basin is a typical study area with complex and varied terrain, an uneven spatial distribution of precipitation, and a sparse spatial distribution of rain gauges, which limit high accuracy precipitation monitoring. The existing research indicates that estimations over mountainous areas with complex topography often have large uncertainties and systematic errors due to the topography, seasonality, climate impact and sparseness of rain gauges (Derin et al., 2016; Maggioni and Massari, 2018; Zambrano-Bigiarini et al., 2017). Moreover, Bai et al. (2018) evaluates CHIRPS over mainland China and indicates that the performance of CHIRPS is poor over the Sichuan Basin and the Northern China Plain, which have complex terrains with substantial variations in elevation. Additionally, Trejo et al. (2016) shows that CHIRPS overestimates low monthly rainfall and underestimates high monthly rainfall using several numerical metrics, and that the rainfall event frequency is overestimated excluding outside the rainy season.

域代码已更改

域代码已更改

域代码已更改

**Table 1** Coverage and spatiotemporal resolutions of major satellite precipitation datasets.

Product	Temporal resolution	Spatial resolution	Period	Coverage
TRMM 3B42	3hours 30min/Hourly/	$0.25^\circ$	1998-present	$50^\circ\text{S}-50^\circ\text{N}$ $60^\circ\text{S}-60^\circ\text{N}$
GPM	3hours/Daily/3Day/7- Day/Monthly	$0.1^\circ/0.25^\circ/0.05^\circ/5^\circ$	2014-present	$70^\circ\text{N}-70^\circ\text{S}$ $90^\circ\text{N}-90^\circ\text{S}$ the continental United States/ western- hemisphere
GOES-R	5min/15min	$0.5-2\text{ km}$	2016-present	$90^\circ\text{S}-90^\circ\text{N}$ $60^\circ\text{S}-60^\circ\text{N}$ $90^\circ\text{S}-90^\circ\text{N}$
GPCP	Monthly/Pentad	$2.5^\circ$	1979-(delayed)-present	$90^\circ\text{S}-90^\circ\text{N}$
PERSIANN-CDR	Daily	$0.25^\circ$	1983-(delayed)-present	$60^\circ\text{S}-60^\circ\text{N}$
CMAP	Monthly	$2.5^\circ$	1979-present	$90^\circ\text{S}-90^\circ\text{N}$
CHIRPS	Annual/Monthly/ Dekad/Pentad/Daily	$0.05^\circ/0.25^\circ$	1981-present	$50^\circ\text{S}-50^\circ\text{N}$

16 **Table 1** Coverage and spatiotemporal resolutions of major satellite precipitation datasets.

Product	Temporal resolution	Spatial resolution	Period	Coverage
TRMM 3B42-RT	3 hourly	0.25°	1998-present	50°S-50°N
CMORPH	30 min	8 km	1998-	60°S-60°N
PERSIANN-CDR	Daily	0.25°	1983-(delayed) present	60°S-60°N
GsMaP-NRT	hourly	0.01°	2007	60°S-60°N
GsMaP-MVK	hourly	0.01°	2000	60°S-60°N
	30 min/Hourly/			60°S-60°N
GPM	3 hourly/Daily/3Day/7	0.1°/0.25°/0.05°/5°	2014-present	70°N-70°S
	Day/Monthly			90°N-90°S
MSWEP	3 hourly/Daily/Monthly	0.1°	1979-2017	90°N-90°S
	Annual/Monthly/			
CHIRPS	Dekad/Pentad/Daily	0.05°/0.25°	1981- present	50°S-50°N

17 To overcome these limitations, many studies have focused on proposing effective methodologies for blending rain gauge  
18 observations, ~~and~~ satellite-based precipitation estimates, and sometimes radar data to take advantage of each dataset. Many  
19 numerical models ~~have been~~ established ~~among~~ ~~with~~ these datasets for high-accuracy precipitation estimations, such as bias  
20 adjustment by a quantile mapping (QM) approach (Yang et al., 2016), Bayesian kriging (BK) (Verdin et al., 2015) and a  
21 conditional merging technique (Berndt et al., 2014). ~~Among aforementioned methods,~~ ~~†~~The QM approach is a distribution-  
22 based approach, which works with historical data for bias adjustment and is effective ~~in~~ ~~at~~ reducing the systematic bias of  
23 regional climate model precipitation estimates at monthly or seasonal scales (Chen et al., 2013). However, the QM approach  
24 offers very limited improvement in removing day-by-day ~~random~~ errors. The BK approach ~~shows~~ ~~provides~~ very good model  
25 fit with precipitation observations, ~~but~~ ~~Unfortunately~~, the Gaussian assumption of the BK model is invalid for daily scales.  
26 Overall, there is a lack of effective methods for high-accuracy precipitation estimates over complex terrain ~~on~~ ~~at~~ a daily scale.

27 As such, due to the poor performance ~~of CHIRPS data~~ at the sub-regional scale, ~~the gauge-satellite fusing algorithms can~~  
28 ~~be assumed to limit high accuracy estimations in the process of CHIRPS data production, and the shortcomings of the existing~~  
29 ~~blending algorithms;~~ ~~Therefore~~, the aim of this article is to ~~offer~~ ~~present~~ a novel approach for ~~re~~blending daily liquid  
30 precipitation gauge data and the Climate Hazards Group Infrared Precipitation (CHIRP) satellite-derived precipitation  
31 estimates developed by ~~the~~ UC Santa Barbara, over the Jinsha River Basin. ~~Here, we will~~ We use precipitation to ~~name~~ ~~denote~~  
32 liquid precipitation throughout the text. The CHIRP ~~data are~~ ~~is~~ the raw data of CHIRPS before blending ~~with the~~ ~~in~~ rain gauge  
33 data. The objective is to build corresponding precipitation models that consider terrain factors and precipitation characteristics  
34 to produce high-quality precipitation estimates. This novel method is ~~named~~ ~~called~~ the Wuhan University Satellite and Gauge  
35 precipitation Collaborated Correction (WHU-SGCC) method. We demonstrate this method by applying it to daily precipitation  
36 over the Jinsha River Basin ~~during~~ ~~in~~ the ~~different~~ ~~summer~~ seasons from 1990 to 2014. The results support the validity of the  
37 proposed approach for producing refined satellite-gauge precipitation estimates over mountainous areas.

38 The remainder of this paper is organized as follows: Section 2 describes the study region, ~~and~~ rain gauges and CHIRPS  
39 dataset used in this study. Section 3 presents the principle of the WHU-SGCC approach for high-accuracy daily precipitation  
40 estimates. The results and discussion are analysed in Section 4, the data available ~~is~~ ~~are~~ described in Section 5, and ~~the~~  
41 conclusions and future work are presented in Section 6.

## 142 2 Study Region and Data

### 143 2.1 Study Region

144 The Yangtze River, one of the largest and most important rivers in Southeast Asia, originates on the Tibetan Plateau and extends  
145 approximately 6300 km eastward to the East China Sea. The river's catchment covers an area of approximately  $\sim 180 \times 10^4$   
146 km<sup>2</sup> and the average annual precipitation is approximately 1100 mm (Zhang et al., 2019). ~~The~~ Yangtze River is divided into  
147 nine sub-basins, the upper drainage basin is the Jinsha River Basin, which flows through the provinces of Qinghai, Sichuan,  
148 and Yunnan in western China. ~~Inside~~ ~~Within~~ the Jinsha River Basin, the total river length is 3486 km, accounting for 77% of  
149 the length of the upper Yangtze River, and covering a watershed area of  $460 \times 10^3$  km<sup>2</sup>. The location of the Jinsha River Basin

is shown in Fig. 1, and it covers the eastern part of the Tibetan Plateau and the part of the Hengduan Mountains. The southern portion of the river basin is the Northern Yunnan Plateau and the eastern portion includes a wide area of the southwestern margin of the Sichuan basin. Crossing complex and varied terrains, the elevation of the Jinsha River ranges from 263 to 6575 m above sea level, which results in significant temporal and spatial climate and weather variations inside the basin. The average annual precipitation of the Jinsha River Basin is approximately 710 mm, the average annual precipitation of the lower reaches is approximately 900-1300 mm, while the average annual precipitation of the middle and upper reaches is approximately 600-800 mm (Yuan et al., 2018). The Jinsha River Basin has four seasons: spring (March-April-May), summer (June-July-August), fall (September-October-November) and winter (December-January-February). The climate of the Jinsha River Basin has more precipitation during the summer season (June July August, JJA), which is affected by oceanic southwest and southeast monsoons, resulting in more precipitation during the summer. Therefore, the blending of satellite estimations with gauged observations during the different seasons JJA is the main focus of this research.

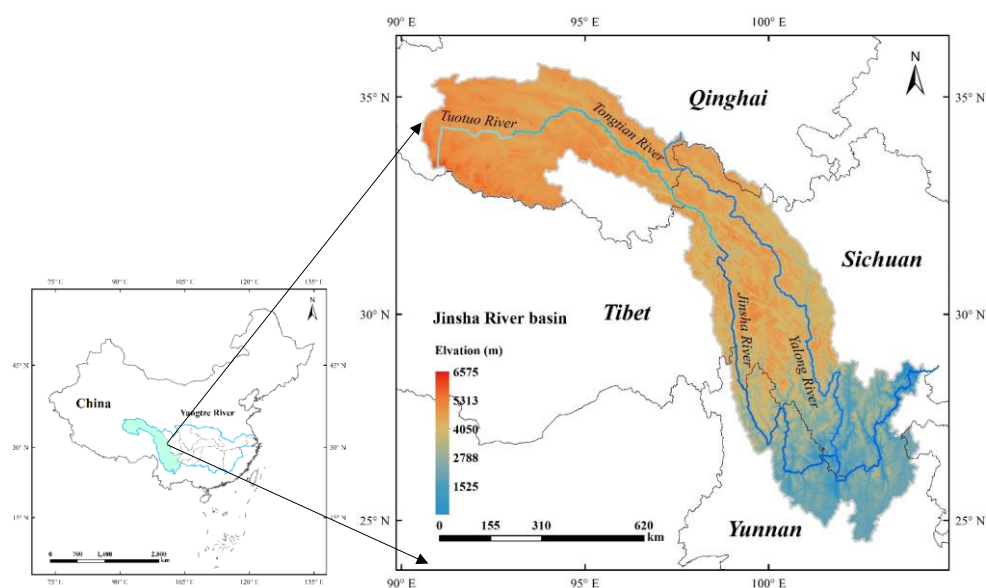


Figure 1 Location of the study area with key topographic features.

## 2.2 Study Data

### 2.2.1 Precipitation gauge observations

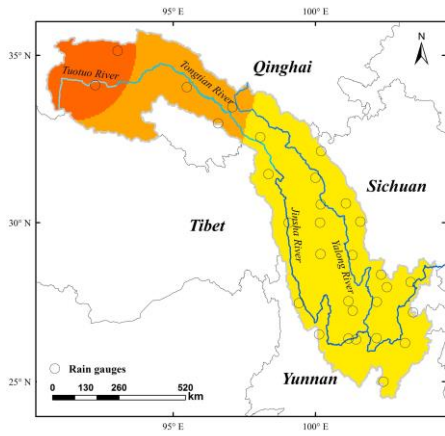
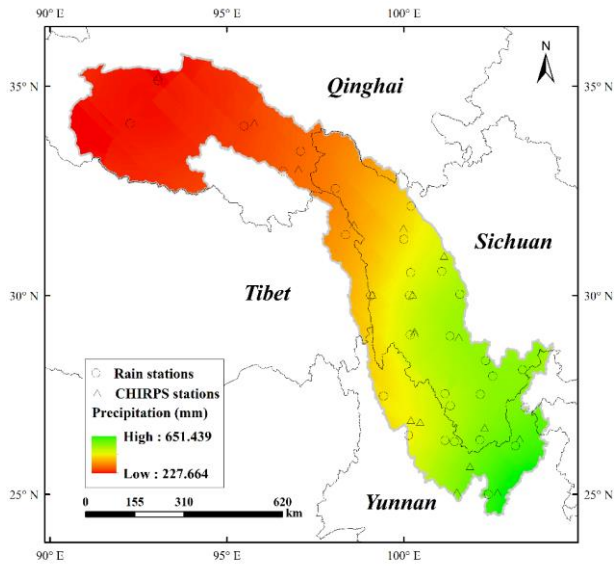
Daily rain gauge observations at 30 national standard rain stations inside within the Jinsha River Basin during the JJA from 1 March 1990 to February 2015 were provided by the National Climate Centre (NCC) of the China Meteorological Administration (CMA) ([http://data.cma.cn/data/cdcdetail/dataCode/SURF\\_CLI\\_CHN\\_MUL\\_DAY\\_V3.0.html](http://data.cma.cn/data/cdcdetail/dataCode/SURF_CLI_CHN_MUL_DAY_V3.0.html), last access: 10 December, 2018), which imposes a strict quality control at the station, provincial, and state levels. The station identification numbers and relevant geographical characteristics are shown in Table Appendix 2A, and their uneven spatial distribution is shown in Fig. 2. The selected rain gauges are located in Qinghai, Tibet, Sichuan and Yunnan Provinces but are mainly scattered in Sichuan Province, and the number of rain gauges in the northern river basin contains fewer rain gauges is less than in the southern river basin. In this study, the gauge observations were used as the reference data in bias for the error adjustment of satellite precipitation estimations.

Table 2 Geographical characteristics of rain stations

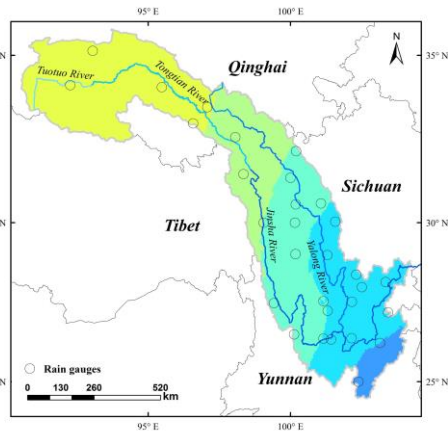
Station number	Province	Lat.(°N)	Lon.(°E)	Elevation (m)
52908	Qinghai	35.13	93.05	4823
56004	Qinghai	34.13	92.26	4744
56021	Qinghai	34.07	95.48	5049
56029	Qinghai	33.00	96.58	4510
56034	Qinghai	33.48	97.08	4503
56144	Tibet	31.48	98.35	4743
56038	Sichuan	32.59	98.06	4285
56146	Sichuan	31.37	100.00	4703
56152	Sichuan	32.17	100.20	4401
56167	Sichuan	30.59	101.07	3374
56247	Sichuan	30.00	99.06	2948
56251	Sichuan	30.56	100.19	4284
56257	Sichuan	30.00	100.16	3971
56257	Sichuan	29.03	100.18	4280
56374	Sichuan	30.03	101.58	3902
56459	Sichuan	27.56	101.16	3002
56462	Sichuan	29.00	101.30	4019
56475	Sichuan	28.39	102.31	1850
56479	Sichuan	28.00	102.51	2470
56485	Sichuan	28.16	103.35	2060
56565	Sichuan	27.26	101.31	2578
56571	Sichuan	27.54	102.16	1503
56666	Sichuan	26.35	101.43	1567
56671	Sichuan	26.39	102.15	1125
56543	Yunnan	27.50	99.42	3216
56586	Yunnan	27.21	103.43	2349
56651	Yunnan	26.51	100.13	2449
56664	Yunnan	26.38	101.16	1540
56684	Yunnan	26.24	103.15	2184
56778	Yunnan	25.00	102.39	1975

175 The multi-year (1990-2014) average ~~annual-seasonal~~ precipitation ~~during the JJA~~ over the Jinsha River Basin increases from  
176 north to south (Fig. 2). ~~The dynamic and uneven distribution of precipitation is influenced distinctly by the seasonal climate.~~  
177 ~~Most of the precipitation falls in the summer~~~~The spatial distribution of precipitation is uneven, with an the average annual~~  
178 ~~seasonal precipitation ranging from less than 250 mm to more than 600 mm, while the average seasonal precipitation during~~  
179 ~~the winter is no more than 50 mm during the summer seasons.~~ The average seasonal precipitation and spatial distribution in  
180 the spring are similar with those in the fall, with values concentrated in the range of 50 mm to 200 mm.

181 Figure 2 also shows the multi-year average daily precipitation during the JJA is no more than 10mm.



(a) Spring



(b) Summer

域代码已更改

域代码已更改

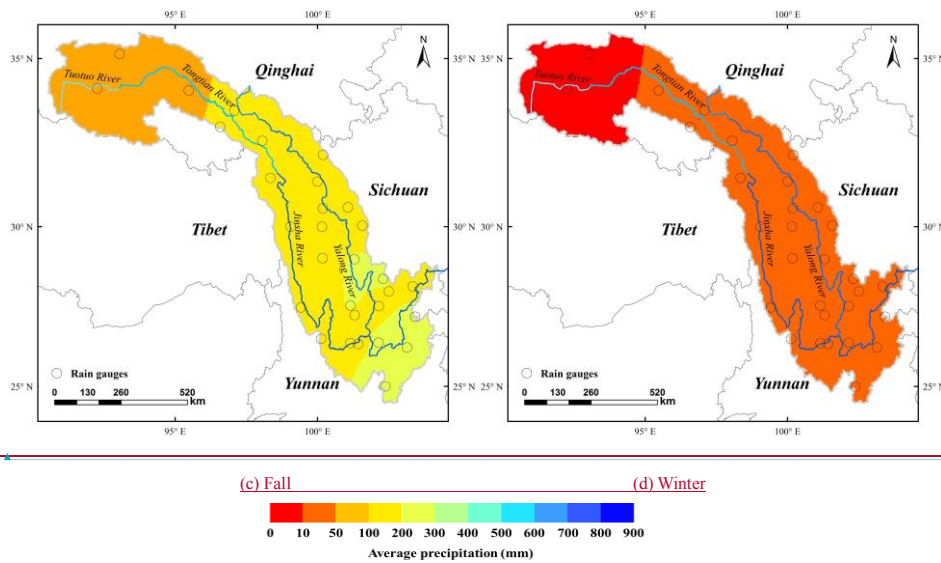


Figure 2 The multi-year (1990–2014) (1990–2014) average annual seasonal precipitation during JJA over the Jinsha River Basin interpolated from 30 rain gauges stations downloaded from were provided by the China Meteorological Administration stations, the other 18 CHIRPS fusion stations were provided by the Climate Hazards Group UC Santa Barbara online at [ftp://ftp.chg.ucsb.edu/pub/org/chg/products/CHIRPS-2.0/diagnostics/global\\_monthly\\_station\\_density/tifs/p05/](ftp://ftp.chg.ucsb.edu/pub/org/chg/products/CHIRPS-2.0/diagnostics/global_monthly_station_density/tifs/p05/) (last access: 10 December, 2018).

### 2.2.2 CHIRPS satellite-gauge fusion precipitation estimates

The CHIRPS v.2 dataset, a satellite-based daily rainfall product, is available online at [ftp://ftp.chg.ucsb.edu/pub/org/chg/products/CHIRPS-2.0/global\\_daily/tifs/p05/](ftp://ftp.chg.ucsb.edu/pub/org/chg/products/CHIRPS-2.0/global_daily/tifs/p05/) (last access: 10 December, 2018). It covers a quasi-global area (land only, 50° S–50° N) with a several temporal scales (daily, 3-day pentad, 6-day dekad, or monthly and annual time steps temporal resolutions) and a high spatial resolution (0.05°) (Rivera et al., 2018). This dataset contains a wide variety of satellite-based rainfall products derived from a multiple data sources and incorporates four-five data types: (1) the monthly precipitation from CHPClim v.1.0 (Climate Hazards Group's Precipitation Climatology version 1) derived from the a combination of the satellite fields, gridded physiographic indicators, and in situ climate normal with the geospatial modelling approach based on moving window regressions and inverse distance weighting interpolation (Funk et al., 2015 b); (2) quasi-global geostationary thermal infrared (IR) satellite observations; (3) the TRMM 3B42 product (Huffman et al., 2007) version 7; (4) the CFS (Climate Forecast System, version 2) atmospheric model rainfall fields CFS (Climate Forecast System) from NOAA; and (5) and surface-based surface-based precipitation observations from various sources including national or and regional meteorological services. The differences from other frequently used precipitation products are the higher resolution of 0.05°, wider coverage and the longer-term longer length data series from 1981 to the near-real time present (Funk et al., 2015 a).

CHIRPS is the blended product of a two-part process. First, IR precipitation (IRP) pentad rainfall estimates are fused with corresponding CHPClim pentad data to produce an unbiased gridded estimate, called the Climate Hazards Group IR Precipitation (CHIRP called CHIRP), which is available online at <ftp://ftp.chg.ucsb.edu/pub/org/chg/products/CHIRP/daily/> (last access: 10 December, 2018). In the second part of the process, the CHIRP data is are blended with in situ precipitation

216 observations obtained from a variety of sources, including national and regional meteorological services by means of a  
217 modified inverse-distance weighting algorithm to create the final blended product, CHIRPS (Funk et al., 2014). The daily  
218 CHIRP satellite-based data over the Jinsha River Basin ~~during the summer seasons~~ from 1990.02 to 2014.02 ~~was were~~  
219 selected as the input for WHU-SGCC blending with rain observations, and the corresponding daily CHIRPS blended data was  
220 used for comparisons of ~~the~~ precipitation accuracy.

221 The blended in situ daily precipitation observations of ~~the~~ CHIRPS data come from a variety of sources, such as: the daily  
222 GHCN archive (Durre et al., 2010), the Global Summary of the Day dataset (GSOD) provided by NOAA's National Climatic  
223 Data Center, the World Meteorological Organization's Global Telecommunication System (GTS) daily archive provided by  
224 NOAA CPC, and ~~over more than~~ a dozen national and regional meteorological services. ~~However, the stations for daily~~  
225 ~~CHIRPS data have a different spatial distribution than those downloaded from the CMA, and the precipitation values used for~~  
226 ~~CHIRPS production are the monthly values available online (ftp://ftp.chg.ucsb.edu/pub/org/chg/products/CHIRPS-~~  
227 ~~2.0/diagnostics/monthly\_station\_data/). For the daily precipitation adjustments over the Jinsha River Basin, the daily gauge~~  
228 ~~observations from the CMA are blended with the daily CHIRP data due to the unknown spatial distribution and precipitation~~  
229 ~~values of gauge stations used in the process of daily CHIRPS merging.~~

230 ~~The number of daily observation stations used for CHIRPS data over the Jinsha River Basin was only 18, compared to the~~  
231 ~~30 rain gauge stations provided by CMA (Fig. 2).~~

### 232 3 Methods

#### 233 3.1 The WHU-SGCC approach

234 In this study, the ~~approach of the~~ WHU-SGCC ~~approach~~ is to estimate the precipitation ~~for at~~ every pixel by blending satellite  
235 estimates and rain gauge observations considering the terrain factors and precipitation characteristics. ~~Due to the significant~~  
236 ~~seasonal difference of precipitation, the WHU-SGCC method was applied in the different seasons. There were four~~ steps  
237 ~~were used~~ to establish the numerical relationship between ~~the~~ gauge stations and the corresponding satellite pixels, and ~~for the~~  
238 interpolation ~~offer~~ the remaining pixels. ~~On this basis,~~ ~~the~~ WHU-SGCC method identifies the geographical locations and  
239 topographical features of each pixel and applies the four classification and blending rules. A flowchart of the WHU-SGCC  
240 method is shown in Fig. 3. The proposed approach was evaluated over the Jinsha River Basin based on 30 gauge stations and  
241 CHIRP satellite-based precipitation estimations ~~in the different during the seasons~~ from 1990 to 2014. The leave-one-out  
242 cross validation step was applied to ~~computing compute~~ the out-of-sample adjusted error with ~~the~~ gauge stations. ~~The WHU-~~  
243 ~~SGCC algorithm was repeated 30 times, each time leaving one station as the validation station.~~

244 The basic description of the WHU-SGCC method is given below, ~~with and the~~ details ~~are~~ illustrated separately in later  
245 sections:

246 (1) Classify all regional pixels into four types: C1 (pixels including one gauge station in ~~its their~~ area), C2 (pixels statistically  
247 similar to C1), C3 (pixels statistically similar to C2) and C4 (remaining pixels).

248 (2) ~~Analyse-Analyze~~ the relationships between ~~the~~ precipitation observations and the C1, C2, and C3 pixel types, and  
249 interpolate for the C4 pixels. These relationships are described by four rules, ~~which are described detailed~~ below as Rules 1  
250 through 4.

251 (3) Establish statistical models and screen ~~the~~ target pixels based on the four ~~aforementioned~~ rules.

252 (4) Correct all ~~of the~~ precipitation pixels in ~~the~~ daily regional precipitation images.

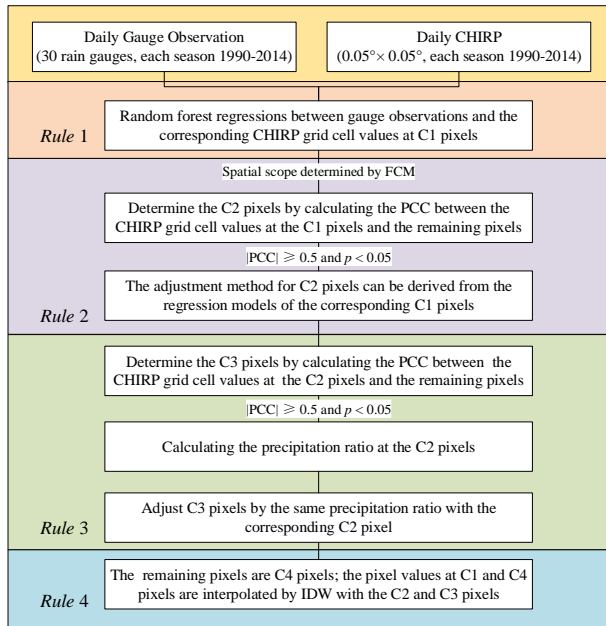


Figure 3 Flowchart of the WHU-SGCC approach with the four rules applied in this study.

### 3.1.1 Assumptions

- (1) Gauge observations are the most accurate, or “true”, values for reference purposes. However, the sparseness of the gauges, their uneven spatial distribution, and the high proportion of missing data may limit high accuracy estimation in rainfall monitoring.
- (2) No major terrain changes occurred during the twenty years (Appendix B).
- (3) There are no long-held outliers at one pixel in the CHIRP dataset, so Pearson’s Correlation Coefficient (PCC) can indicate represent the statistically similarity of the rainfall characteristics among the pixels in a certain spatial area over-at a seasonal scale.

### 3.1.2 Rule 1 of the WHU-SGCC method

In general, the satellite precipitation estimations deviated from the ground-based measurements, which were assumed to be the true values. Rule 1 aims to establish a regression model between each-gauge the historical observations at each gauge and the corresponding CHIRP grid cell values. The regression relationship was derived by random forest regression (RFR) at each gauge station. RFR is a machine-learning algorithm for a predictive model with a large set of regression trees in which each tree in the ensemble is grown from a bootstrap sample (Johnson, 1998) sample-drawn with a replacement from the training set. In the process of establishing regression trees, a subset of variables for each node is selected to avoid overfitting. The final prediction is obtained by combining the results of the prediction methods applied to each bootstrap sample (Genuer et al., 2017). The predicted value is calculated by the mean-average of the values from all of the decision trees. Each tree can be expressed as

$$Tree_k = f_{RFR}(Y_o, \Theta_{Y_k}), k=1 \dots n \quad (1)$$

where  $Y_o$  denotes the historical observations at each gauge at the C1 pixels,  $\Theta_{Y_k}$  is a randomly selected vector from  $Y_s$ .

域代码已更改

带格式的: 缩进: 首行缩进: 0 厘米

域代码已更改

275  $Y_s$  denotes the corresponding CHIRP grid cell values at the C1 pixels,  $n$  is the number of trees, and where  $Y_o$  denotes each  
 276 gauge historical observations and  $Y_s$  denotes the corresponding CHIRP grid cell values at C1 pixels;  $f_{RFR}$  is constructed  
 277 from the time series  $Y_o$  (dependent variable) and  $Y_s$  (independent variable) by means of RFR. The bootstrap sample will  
 278 be the training set used for growing the tree. The error rate (out-of-bag, OOB) left out of one-third of the training data is also  
 279 monitored to determine the The number of decision trees, was set to 500, which was determined by out of bag (OOB) error  
 280 (Appendix A). In this study, The the minimum OOB error rate was reached the minimum value when the number of decision  
 281 trees  $n$  was less than 500 (Appendix C).

282 The Rule 1 builds the statistical relationships between the gauge observations and the corresponding CHIRP grid cell values,  
 283 which is the key idea in correcting the satellite-based precipitation estimations in the whole entire study area. As Because there  
 284 are 30 gauge stations in the study area, 30 regression relationships at the C1 pixels were derived from Rule 1. The values of  
 285 the C1 pixels are not corrected in Rule 1; but are interpolated in Rule 4.

### 286 3.1.3 Rule 2 of the WHU-SGCC method

287 It is reasonable to assume that there are some pixels that are statistically similar to the historical precipitation characteristics  
 288 of the C1 pixels within a certain spatial scope area. Therefore, it is feasible to adjust the satellite estimation bias of the C2 pixels  
 289 by referring to the appropriate regression relationships at the corresponding C1 pixels based on Rule 1.

290 First, the spatial scope area in which pixels may have highly similar characteristics is established. Some Several studies  
 291 indicate that the geographical location, elevation and other terrain information influences the spatial distribution of rainfall,  
 292 especially in mountainous areas with complex topography (Anders et al., 2006; Long and Singh, 2013). The size of the spatial  
 293 range is an important parameter to distinguish the spatial similarity and heterogeneity. In the WHU-SGCC method, the  
 294 approach of fuzzy c-means (FCM) clustering approach was explored used to determine the spatial range considered as for each  
 295 pixel's terrain factors, including longitude, latitude, elevation, slope, aspect and curvature. The FCM method was developed  
 296 by J.C. Dunn in 1973 (Dunn, 1973), and improved in 1983 (Wang, 1983). It is an unsupervised fuzzy clustering method and  
 297 the its steps are as follows (Pessoa et al., 2018):

298 1) Choose the number of clusters  $c$ . The optimum number of clusters was is determined by  $L(c)$ , which was is derived from  
 299 the inter-distance and inner distance of the samples in Eq. (2). It is ensured that the distance between the same similar samples  
 300 is smaller, while the distance between the different samples is larger.

$$301 \quad L(c) = \frac{\sum_{i=1}^c \sum_{j=1}^n w_{ij}^m \|c_i - \bar{x}\|^2 / (c-1)}{\sum_{i=1}^c \sum_{j=1}^n w_{ij}^m \|x_j - c_i\|^2 / (n-c)} \quad (2)$$

302 In Eq. (2), the denominator is the inner distance, and the numerator molecular is the inter-distance. The initial value of  $c$  is  
 303 1 and the maximum value of  $c$  is the number of gauge stations in this the study area. The optimum number of clusters was  
 304 optimized to maximize the  $L(c)$ . For this reason, the value of  $c$  value is conducted varied from in the range of 1 to the number  
 305 of gauge stations with an incremental interval value of 1 in this study.

306 2) Assign coefficients randomly to each data point  $x_i$  for the degree to which it belongs in the  $i$ -th cluster  $w_{ij}(x_i)$ :

$$307 \quad c_i^{(r)} = \frac{\sum_{j=1}^n w_{ij}^m x_j}{\sum_{j=1}^n w_{ij}^m} \quad (3), \quad w_{ij} = \frac{1}{\sum_{k=1}^c \left( \frac{\|x_i - c_i\|}{\|x_i - c_k\|} \right)^{\frac{2}{m-1}}} \quad (4), \quad \bar{x} = \frac{\sum_{i=1}^c \sum_{j=1}^n w_{ij}^m x_j}{n} \quad (5)$$

308 where  $x$  is a finite collection of  $n$  elements that will be partitioned into a collection of  $c$  fuzzy clusters,  $c_i$  is the centre of

带格式的: 缩进: 首行缩进: 0 厘米

each cluster,  $m$  is the hyper-parameter that controls the level of cluster fuzziness, and  $w_{ij}$  is the degree to which element  $x_i$  belongs to  $c_j$ , and  $\bar{x}$  is the centre vector of the collection. In Eq. (3),  $c_j^{(t)}$  represents the cluster centre in iteration  $t$ . If the minimum improvement in the objective function between two consecutive iterations satisfies the following equation, the algorithm terminates in iteration  $t$  (Eq. (6)):

$$\|c_i^{(t)} - c_i^{(t+1)}\| < \varepsilon \quad (6)$$

3) Minimize the objective function  $F_c$  to achieve data partitioning.

$$F_c = \sum_{j=1}^c \sum_{i=1}^n w_{ij}^m \|x_j - c_i\|^2 \quad (7)$$

The results of the FCM are the degree of membership of each pixel to the cluster centre as represented by numerical values. The pixels in each cluster have similar terrain features and precipitation characteristics.

Second, as mentioned above, the aim of Rule 2 is to derive an adjustment method for the C2 pixels based on learning from Rule 1. With the establishment of a regression relationship between the gauge observations and the corresponding CHIRP grid cell values of the C1 pixels by the RFR method, the determination of the C2 pixels follows a complicated and considerable procedure. With the exception of the C1 pixels, the remaining pixels in each cluster represent potential C2 pixels, which are called R pixels. The Pearson's correlation coefficient (PCC) and  $p$ -values between the satellite estimations (multi-year daily CHIRP grid cell values) at the R pixels and the C1 pixels are the criteria for the final determination of the C2 pixels. The PCC is defined as follows:

$$PCC_{x,y} = \frac{\sum_{i=1}^n (x_i - \bar{x})(y_i - \bar{y})}{\sqrt{\sum_{i=1}^n (x_i - \bar{x})^2} \sqrt{\sum_{i=1}^n (y_i - \bar{y})^2}} \quad (8)$$

where  $n$  is the number of samples,  $x_i$  and  $y_i$  are individual samples (CHIRP grid cell values at the C1 and C2 pixels, respectively),  $\bar{x}$  is the arithmetic mean of  $x$  calculated by  $\bar{x} = \frac{1}{n} \sum_{i=1}^n x_i$ , and  $\bar{y}$  is the arithmetic mean of  $y$  calculated by

$$\bar{y} = \frac{1}{n} \sum_{i=1}^n y_i.$$

The value range of the PCC ranges from -1 and +1. If there are no repeated data values, a perfect PCC of +1 or -1 occurs when each of the variables is a perfect monotonic function of the other. However, if the value is close to zero, there is zero correlation. In addition, the correlation is not only determined by the value of the correlation coefficient but also from the correlation test's  $p$ -value. The critical values for the PCC and  $p$ -value are 0.5 and 0.05, respectively; thus, a PCC value higher than 0.5 and a  $p$ -value lower than 0.05 indicate that the data are significantly correlated (Zhang and Chen, 2016). Therefore, the final determination of the C2 pixels must meet the following criteria:

$$|PCC| \geq 0.5 \quad \text{and} \quad p < 0.05 \quad (9)$$

Each R pixel has  $m$  PCC and  $p$ -values (the number of C1 pixels in the cluster), and the subset of C2 pixels is identified by excluding the data that failed the correlation test and retaining both the data with a maximum PCC of at least 0.5 and a  $p$ -value lower than 0.05, and the corresponding index of C1 pixels. The selected C2 pixels can then be considered as statistically similar to the precipitation characteristics of the corresponding C1 pixels in their defined spatial scope.

After identifying the C2 pixels and their corresponding C1 pixels, the adjustment method for the C2 pixels is derived from the regression model for the C1 pixels:

带格式的: 缩进: 首行缩进: 0 厘米

$$C2_{as} = \frac{1}{n} \sum_{k=1}^n Tree_{kC1}(Y_{sC2}) \quad (10)$$

域代码已更改

$$C2_{as} = f_{RFR}(Y_s) \quad (10)$$

where  $C2_{as}$  is the adjusted satellite precipitation estimate and  $Y_s$  is the CHIRP grid cell value at the C2 pixels, and  $f_{RFR}$  is the  $f_{RFR}$  of corresponding C1 pixel where  $Tree_{kC1}$  is the decision tree derived from the RFR algorithm at the corresponding C1 pixel.  $Y_{sC2}$  is the CHIRP grid cell value at the C2 pixels, and  $C2_{as}$  is the adjusted satellite precipitation estimate calculated by the average of the values from the RFR decision trees.

域代码已更改

域代码已更改

域代码已更改

### 3.1.4 Rule 3 of the WHU-SGCC method

Recognizing that precipitation has a spatial distribution, the assumption that the C3 pixels are statistically similar to the precipitation characteristics of the C2 pixels is adopted to establish the adjustment method for the C3 pixels.

First, the determination of the C3 pixels in each spatial cluster is based on the selection of C2 pixels. The satellite-based estimation values at the remaining pixels other than with exception of the C1 and C2 pixels are used to calculate the PCC and  $p$ -value with the satellite-based estimation values at the C2 pixels in the same cluster. The results of each pixel's  $k$  PCC and  $p$ -value (the number of C2 pixels in the cluster) are evaluated based on the correlation test (Eq. (9)) that the pixels with have a maximum PCC is of at least 0.5 and the  $p$ -value is of no more than 0.05, and then the corresponding index of C2 pixels are is retained. The selected pixels are called C3 pixels, which are statistically similar to the precipitation characteristics of the corresponding C2 pixels in the defined spatial seopearea.

After identifying the C3 pixels, a method for merging the CHIRP grid cell values at the C3 pixels ( $Y_s$ ) and the target reference values of  $C2_{as}$  at the corresponding C2 pixels is applied to estimate the adjusted precipitation values at the C3 pixels. This method combines the  $Y_s$  and  $C2_{as}$  values into one variable, as shown in Eq. (11):

$$w_i = \frac{C2_{as_i} + \lambda}{Y_s + \lambda} \quad i=1, \dots, n \quad (11)$$

where  $\lambda$  is a positive constant set to 10 mm (Sokol, 2003),  $C2_{as}$  is the adjusted precipitation values at the C2 pixels,  $Y_s$  is extracted from the CHIRP grid cell values at the corresponding location of the C2 pixels, and  $n$  is the number of C2 pixels in each spatial cluster.

Each  $w$  of the C3 pixels is assigned the same value as the corresponding C2 pixel. Therefore, the values of the C3 pixels are derived from Eq. (12):

$$C3_{as} = \max(w \times (Y_s + \lambda) - \lambda, 0) \quad (12)$$

where  $C3_{as}$  is the adjusted target precipitation value at one C3 pixel, and  $Y_s$  is the corresponding CHIRP grid cell value. To avoid precipitation estimates below 0, Eq. (12) sets these negative values to 0.

### 3.1.5 Rule 4 of the WHU-SGCC method

The pixels other than Excluding the C1, C2, and C3 pixels, the number of remaining pixels, are called C4 pixels which pixels and they are adjusted by Inverse-inverse Distance-distance Weighted-weighting (IDW). IDW is based on the concept of the first law of geography from 1970, which-It was defined as everything is related to everything else, but near things are more related than distant things. Therefore, the attribute value of an unsampled point is the weighted average of the known values within the neighbourhood, and the distance weighting can be determined by means of IDW (Lu and Wong, 2008). In Rule 4,

377 IDW is used to interpolate the unknown spatial precipitation data from the adjusted precipitation values at the C2 and C3  
 378 pixels. The IDW formulas are given as Eq. (13) and Eq. (14).

$$379 \quad R_{as} = \sum_{i=1}^n w_i R_i \quad (13)$$

$$380 \quad w_i = \frac{d_i^{-\alpha}}{\sum_{i=1}^n d_i^{-\alpha}} \quad \text{with} \quad \sum_{i=1}^n w_i = 1 \quad (14)$$

381 where  $R_{as}$  is the unknown spatial precipitation data,  $R_i$  is the adjusted precipitation values at the C2 and C3 pixels,  $n$  is the  
 382 number of C2 and C3 pixels,  $d_i$  is the distance from each C2 or C3 pixel to the unknown grid cell, and  $\alpha$  is the power  
 383 which is generally specified as a geometric form for the weight. Several researches studies (Simanton and Osborn 1980; Tung  
 384 1983) have experimented with variations in the power,  $\alpha$ ; the small  $\alpha$  tends to estimate values with the averages of sampled  
 385 grids in the neighbourhood, while a large  $\alpha$  tends to give larger weights to the nearest points and increasingly down-weights  
 386 points farther away (Chen and Liu, 2012; Lu and Wong, 2008). The value of  $\alpha$  has an influence on the spatial distribution of  
 387 the information from precipitation observations. For this reason,  $\alpha$  value is conducted-varied in the range of 0.1 to three (0.1,  
 388 0.3, 0.5, 1.0, 1.5, 2.0, 2.5 and 3.0) in this study.

389 It is noted that the unknown spatial precipitation data including include C1 and C4 pixels, because the C1 pixels values  
 390 were not adjusted in Rule 1.

391 In the end, after applying these four rules, we obtained complete daily adjusted regional precipitation maps for the four  
 392 seasons for the summer (JJA) over the Jinsha River basin.

### 393 3.2 Accuracy assessment

394 The performance of the WHU-SGCC adjusted precipitation estimates was evaluated by eight mathematic metrics: the  
 395 Pearson's correlation coefficient (PCC), root mean square error (RMSE), mean absolute error (MAE), relative bias (BIAS),  
 396 the Nash-Sutcliffe efficiency coefficient (NSE), probability of detection (POD), false alarm ratio (FAR) and critical success  
 397 index (CSI). The results of accuracy assessment are the average values validated by the leave-one-out cross method. Each  
 398 validated pixel will probably be a C2, C3 or C4 pixel in the process of the WHU-SGCC algorithm. The PCC, RMSE, MAE  
 399 and BIAS were used to evaluate how well the WHU-SGCC method adjusted the satellite estimation bias, while POD, FAR  
 400 and CSI were used to evaluate the performance of precipitation forecasting (Su et al., 2011). The PCC measures the strength  
 401 of the correlation relationship between the satellite estimations and observations. The RMSE is an absolute measurement used  
 402 to compare the difference between the satellite estimations and observations, and the MAE represents the average magnitude  
 403 of error estimations, considering both systematic and random errors. The NSE (Nash and Sutcliffe, 1970) determines the  
 404 relative magnitude of the variance of the residuals compared to the variance of the observations, bounded by minus infinity to  
 405 and 1; A negative value indicates a poor precipitation estimate, and a value of 1 indicates an optimal estimate is equal to  
 406 1. The BIAS measures the mean tendency of the estimated precipitation to be larger (positive values) or smaller (negative  
 407 values) than the observed precipitation and has with an optimal value of 0. The POD, also known as the hit rate, represents  
 408 the probability of rainfall detection, and the FAR is defined as the ratio of the false alarm of rainfall to the total number of  
 409 rainfall events. All of the accuracy assessment metrics are shown in Table 32.

410 **Table 23** Accuracy assessment metrics.

Accuracy assessment Index	Unit	Formula	Range	Optimal value
Pearson's Correlation Coefficient (PCC)	NA	$PCC = \frac{\sum_{i=1}^n (Y_{oi} - \bar{Y}_o)(C_i - \bar{C})}{\sqrt{\sum_{i=1}^n (Y_{oi} - \bar{Y}_o)^2} \cdot \sqrt{\sum_{i=1}^n (C_i - \bar{C})^2}}$	[-1,1]	1

Root Mean Square Error (RMSE)	mm	$RMSE = \sqrt{\frac{1}{n} \sum_{i=1}^n (C_i - Y_{oi})^2}$	$[0, +\infty)$	0
Mean Absolute Error (MAE)	mm	$MAE = \frac{1}{n} \sum_{i=1}^n  C_i - Y_{oi} $	$[0, +\infty)$	0
Relative Bias (BIAS)	NA	$BIAS = \frac{\sum_{i=1}^n (C_i - Y_{oi})}{\sum_{i=1}^n Y_{oi}}$	$(-\infty, +\infty)$	0
Nash-Sutcliffe Efficiency Coefficient (NSE)	NA	$NSE = 1 - \frac{\sum_{i=1}^n (C_i - Y_{oi})^2}{\sum_{i=1}^n (C_i - \bar{Y}_o)^2}$	$(-\infty, 1]$	1
Probability of Detection (POD)	NA	$POD = H/(H+M)$	$[0, 1]$	1
False Alarm Ratio (FAR)	NA	$FAR = F/(H+F)$	$[0, 1]$	0
Critical Success Index (CSI)	NA	$CSI = H/(H+M+F)$	$[0, 1]$	1

Note:  $Y_{oi}$  is the observation data; and  $C_i$  is the adjusted value using the WHU-SGCC method for the test sample pixel;  $\bar{Y}_o$  is the arithmetic mean of  $Y_o$  and is given by  $\bar{Y}_o = \frac{1}{n} \sum_{i=1}^n Y_{oi}$ ;  $\bar{C}$  is the arithmetic mean of  $C$  and is given by  $\bar{C} = \frac{1}{n} \sum_{i=1}^n C_i$ ;  $H$  represents the number of both observed and estimated precipitation events (successfully forecasted); and  $F$  is the number of false alarms when the observed precipitation was below the threshold and estimated precipitation was above threshold (false alarms; and).  $M$  is the number of events in which the estimated precipitation was below the threshold and observed precipitation was above the threshold (missed forecasts). The POD and FAR values are dimensionless numbers ranging from 0 to 1. The precipitation threshold (event/no event) was set to 0.1 mm/day.

#### 4 Results and Discussion

A total of 18,482 daily pixels were adjusted by blending the satellite estimations (CHIRP) and observations (rain gauge stations) using the WHU-SGCC approach over the Jinsha River Basin during the JJA from 1990 to 2014. The number percentage of pixels adjusted by each rule in the WHU-SGCC method is shown in Table 43. The number of C1 pixels was the number of training gauge stations, which accounted for 0.16% of the total pixels (18,482) inside the basin. Due to the leave-one-out cross validation step, the different training samples will have the different numbers of C2, C3 and C4 pixels respectively inside the Jinsha River Basin. The percentage of C2 and C3 pixels are highest in fall, followed by summer, spring and winter. In the spring, the average percentage of C2 pixels was approximately 21%, the average percentage of C3 pixels was approximately 17%, and the percentage of C4 pixels was approximately 61%. In the summer, the percentage of C2 pixels was ranging from 15.59% to 18.36%, the percentage of C3 pixels was ranging from 21.72% to 24.40%, and the percentage of C4 pixels was approximately 60%. In the full, the average percentage of C2 pixels was approximately 31%, the average percentage of C3 pixels was approximately 22%, and the average percentage of C4 pixels was approximately 47%. In the winter, the average percentage of C2 pixels was approximately 16%, the average percentage of C3 pixels was approximately 19%, and the average percentage of C4 pixels was approximately 65%. Besides, the pixel type of the validation gauge station is shown in Table D1. Each validation gauge station could be identified as either C2, C3 or C4 pixels to evaluate the performances of all the rules in the WHU-SGCC method. The number of C4 pixels was approximately 10822 with the percentage around 60%, the number of C3 pixels was approximately 4331 with the percentage ranging from 21.72% to 24.40%, and the number of C2 pixels was approximately 3300 with the percentage ranging from 15.59% to 18.36%.

Table 3 The percentage of each class pixels adjusted by each rule using the WHU-SGCC method within the Jinsha River Basin.

Validation	C2 Pixels (%)	C3 Pixels (%)	C4 Pixels (%)
------------	---------------	---------------	---------------

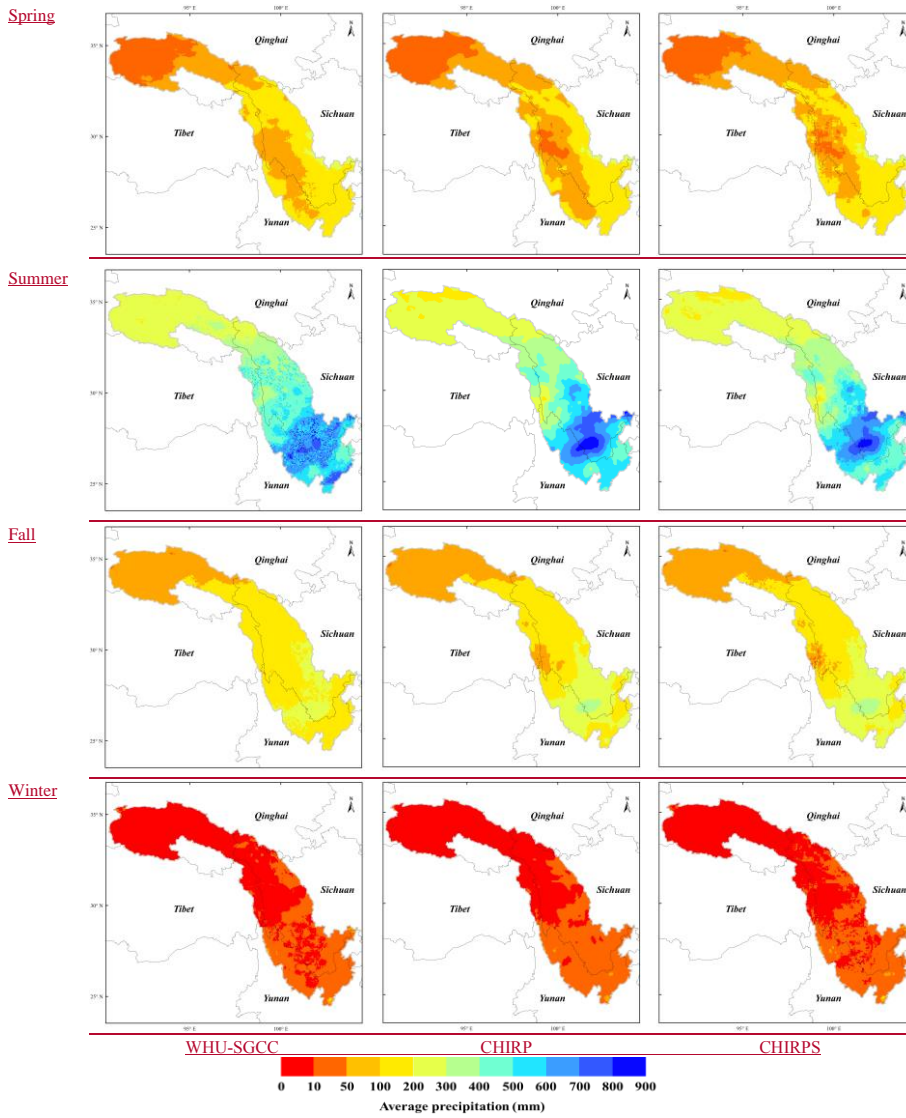
gauge station	Spring	Summer	Fall	Winter	Spring	Summer	Fall	Winter	Spring	Summer	Fall	Winter
\$2908	20.80%	16.59%	29.15%	15.52%	17.76%	22.85%	20.82%	18.16%	61.29%	60.40%	49.87%	66.16%
\$6004	20.89%	15.59%	29.40%	15.65%	16.29%	22.24%	20.64%	18.83%	62.66%	62.01%	49.81%	65.36%
\$6021	21.38%	17.91%	32.46%	15.65%	17.55%	24.40%	21.85%	19.91%	60.91%	57.53%	45.53%	64.28%
\$6029	21.77%	18.06%	32.60%	16.03%	17.31%	24.06%	21.61%	19.64%	60.76%	57.72%	45.63%	64.18%
\$6034	21.09%	17.86%	31.22%	14.86%	17.78%	23.95%	23.07%	20.19%	60.97%	58.03%	45.55%	64.79%
\$6038	20.48%	17.36%	30.72%	15.56%	16.12%	21.72%	23.74%	17.63%	63.23%	60.76%	45.39%	66.65%
\$6144	21.42%	18.11%	31.97%	16.00%	16.46%	24.03%	21.78%	19.38%	61.96%	57.70%	46.09%	64.46%
\$6146	21.33%	17.22%	31.77%	15.70%	17.12%	24.24%	21.42%	18.34%	61.39%	58.38%	46.65%	65.81%
\$6152	21.32%	17.17%	31.27%	15.57%	17.56%	22.59%	22.32%	18.94%	60.96%	60.08%	46.26%	65.34%
\$6167	21.46%	18.19%	32.36%	15.84%	16.90%	23.51%	21.72%	19.03%	61.48%	58.14%	45.76%	64.98%
\$6247	21.66%	18.32%	31.44%	16.10%	17.16%	23.89%	22.19%	19.55%	61.03%	57.63%	46.21%	64.20%
\$6251	21.09%	17.86%	31.28%	15.73%	17.39%	23.53%	22.88%	18.50%	61.36%	58.46%	45.68%	65.62%
\$6257	21.17%	17.93%	30.99%	15.95%	16.15%	21.88%	23.55%	19.13%	62.53%	60.04%	45.30%	64.77%
\$6357	21.62%	18.14%	31.59%	15.64%	17.12%	23.75%	22.54%	19.52%	61.10%	57.95%	45.71%	64.68%
\$6374	21.52%	18.08%	31.92%	14.32%	17.38%	23.23%	21.90%	19.20%	60.95%	58.53%	46.02%	66.32%
\$6459	21.30%	18.10%	32.14%	15.64%	16.92%	23.45%	21.16%	19.17%	61.62%	58.29%	46.54%	65.03%
\$6462	21.67%	18.29%	32.68%	15.92%	17.28%	23.68%	21.55%	19.14%	60.90%	57.87%	45.61%	64.78%
\$6475	21.49%	18.10%	32.49%	15.98%	16.36%	23.50%	22.08%	19.53%	62.00%	58.24%	45.28%	64.33%
\$6479	20.42%	17.88%	31.34%	15.69%	16.35%	22.79%	19.36%	18.74%	63.07%	59.17%	49.14%	65.41%
\$6485	21.44%	18.36%	32.78%	15.64%	17.43%	23.91%	21.82%	19.85%	60.97%	57.57%	45.24%	64.35%
\$6543	21.52%	18.25%	32.51%	15.87%	16.97%	23.72%	21.78%	18.90%	61.35%	57.87%	45.56%	65.06%
\$6565	21.21%	17.54%	30.93%	15.52%	17.81%	24.08%	23.55%	19.96%	60.83%	58.23%	45.36%	64.37%
\$6571	21.62%	17.89%	31.31%	14.94%	17.03%	23.07%	20.83%	18.94%	61.19%	58.89%	47.70%	65.97%
\$6586	21.73%	18.33%	21.73%	15.49%	17.35%	23.99%	17.35%	19.59%	60.76%	57.53%	60.76%	64.77%
\$6651	20.90%	18.07%	32.46%	15.38%	17.78%	23.98%	22.13%	19.95%	61.16%	57.79%	45.25%	64.51%
\$6664	20.94%	18.22%	32.43%	15.50%	16.64%	23.06%	21.00%	18.70%	62.26%	58.56%	46.42%	65.64%
\$6666	21.06%	17.98%	31.59%	15.39%	18.03%	23.97%	22.41%	19.64%	60.76%	57.89%	45.84%	64.82%
\$6671	20.71%	18.16%	32.55%	15.67%	16.53%	23.63%	21.89%	20.03%	62.61%	58.06%	45.41%	64.14%
\$6684	21.36%	18.04%	32.65%	15.46%	17.72%	23.15%	21.95%	19.28%	60.76%	58.65%	45.24%	65.10%
\$6778	21.63%	18.11%	32.25%	15.91%	17.31%	23.14%	22.11%	19.52%	60.90%	58.59%	45.48%	64.41%

**Table 4** The number of each class pixels adjusted by each rule using the WHU-SGCC method inside the Jinsha River Basin.

Validation-gauge station	C1 Pixels (%)	C2 Pixels (%)	C3 Pixels (%)	C4 Pixels (%)
S2908	29 (0.16%)	3066 (16.59%)	4224 (22.85%)	11163 (60.40%)
S6004	29 (0.16%)	2882 (15.59%)	4111 (22.24%)	11460 (62.01%)
S6021	29 (0.16%)	3311 (17.91%)	4510 (24.40%)	10632 (57.53%)
S6029	29 (0.16%)	3338 (18.06%)	4447 (24.06%)	10668 (57.72%)
S6034	29 (0.16%)	3300 (17.86%)	4427 (23.95%)	10726 (58.03%)
S6038	29 (0.16%)	3209 (17.36%)	4014 (21.72%)	11230 (60.76%)
S6144	29 (0.16%)	3347 (18.11%)	4442 (24.03%)	10664 (57.70%)
S6146	29 (0.16%)	3183 (17.22%)	4480 (24.24%)	10790 (58.38%)
S6152	29 (0.16%)	3173 (17.17%)	4176 (22.59%)	11104 (60.08%)
S6167	29 (0.16%)	3362 (18.19%)	4346 (23.51%)	10745 (58.14%)
S6247	29 (0.16%)	3385 (18.32%)	4416 (23.89%)	10652 (57.63%)
S6251	29 (0.16%)	3301 (17.86%)	4348 (23.53%)	10804 (58.46%)
S6257	29 (0.16%)	3313 (17.93%)	4043 (21.88%)	11097 (60.04%)
S6357	29 (0.16%)	3352 (18.14%)	4390 (23.75%)	10711 (57.95%)
S6374	29 (0.16%)	3341 (18.08%)	4294 (23.23%)	10818 (58.53%)
S6459	29 (0.16%)	3345 (18.10%)	4334 (23.45%)	10774 (58.29%)
S6462	29 (0.16%)	3380 (18.29%)	4377 (23.68%)	10696 (57.87%)
S6475	29 (0.16%)	3345 (18.10%)	4344 (23.50%)	10764 (58.24%)
S6479	29 (0.16%)	3305 (17.88%)	4212 (22.79%)	10936 (59.17%)
S6485	29 (0.16%)	3393 (18.36%)	4419 (23.91%)	10641 (57.57%)
S6543	29 (0.16%)	3373 (18.25%)	4384 (23.72%)	10696 (57.87%)
S6565	29 (0.16%)	3241 (17.54%)	4450 (24.08%)	10762 (58.23%)
S6571	29 (0.16%)	3306 (17.89%)	4263 (23.07%)	10884 (58.89%)
S6586	29 (0.16%)	3387 (18.33%)	4434 (23.99%)	10632 (57.53%)
S6651	29 (0.16%)	3340 (18.07%)	4432 (23.98%)	10681 (57.79%)
S6664	29 (0.16%)	3368 (18.22%)	4262 (23.06%)	10823 (58.56%)
S6666	29 (0.16%)	3323 (17.98%)	4431 (23.97%)	10699 (57.89%)
S6671	29 (0.16%)	3356 (18.16%)	4367 (23.63%)	10730 (58.06%)
S6684	29 (0.16%)	3335 (18.04%)	4278 (23.15%)	10840 (58.65%)
S6778	29 (0.16%)	3347 (18.11%)	4277 (23.14%)	10829 (58.59%)

#### 4.1 Model performance based on overall accuracy evaluations

The multi-year (1990-2014) average seasonal precipitation over the Jinsha River Basin interpolated from WHU-SGCC, CHIRP and CHIRPS is shown in Fig. 4. There exist some differences in the spatial pattern of precipitation estimates. Overall, the WHU-SGCC method exhibits the similar spatial distribution of precipitation to the CHIRP and CHIRPS, while the WHU-SGCC method attenuated the intense rain in the central area. The statistical accuracy evaluations are needed to further analyze the performance of the WHU-SGCC method.



448 **Figure 4** The multi-year (1990-2014) average seasonal precipitation over the Jinsha River Basin interpolated from WHU-SGCC, CHIRP  
 449 and CHIRPS.  
 450

451 To test the performance of the WHU-SGCC method for precipitation estimates, the ~~statistical analyses of~~ PCC, RMSE,  
 452 BAE, BIAS, NSE, POD, FAR, and CSI were calculated and are presented in Table 5-4. (The results were derived from the 22  
 453 clusters for the FCM in Rule 2, as shown in Appendix BE, and  $\alpha = 0.1$  for the IDW in Rule 4 after the comparison of the  
 454 RMSEs). After the correction, the PCC in the WHU-SGCC method shows an improvement relative to the CHIRP and CHIRPS  
 455 estimates. The spring and fall have better correlations than the summer and winter. In addition, the NSE of the WHU-SGCC  
 456 provides substantial improvements over CHIRP and CHIRPS, especially in the spring and fall which were better than the  
 457 summer and winter. The RMSE and MAE are the largest in the summer, followed by the fall, spring, and winter; however, the

performances of the BIAS in the summer and fall are better than those in the spring and winter, which might be influenced by the greater precipitation in the summer and fall than in the spring and winter. The assessments of the POD and CSI are lowest, and the FAR is largest in the winter due to the overestimation of no rain events estimated by the satellite-based data set.

Compared with the estimates of CHIRP and CHIRPS, the PCCs of the WHU-SGCC method are improved to more than 0.5 in the spring and fall and to approximately to 0.5 in the winter. In addition, the RMSE and MAE of the WHU-SGCC were all lower than those of CHIRP and CHIRPS. The absolute values of the BIAS of the WHU-SGCC are substantially improved in the spring, followed by the summer, winter and fall. Although the absolute value of the BIAS of the WHU-SGCC in fall are not significantly better than those of CHIRP and CHIRPS, all of the values are approximately 0. The NSEs of the WHU-SGCC reached 0.2836, 0.2944 and 0.1853 in the spring, fall and winter, respectively, which are substantially better than the negative or zero values of CHIRP and CHIRPS. In the summer, the NSE of the WHU-SGCC is still negative, but it is improved to be nearly zero, which indicates that the adjusted results are similar to the average level of the rain gauge observations. It is worth noting that in the spring, summer and fall, the POD values of the WHU-SGCC are in the range of 0.95 to 1, better than CHIRP and CHIRPS, and the FAR values of the WHU-SGCC are no more than 0.3, lower than CHIRP and CHIRPS; these results represent the better ability of the WHU-SGCC method to predict precipitation events. The rainfall detection ability is the worst in the winter compared to the other seasons. This can be explained by the seasonal distribution of precipitation in the Jinsha River Basin, in which the most rainfall occurs in the summer, followed by the fall, spring and winter. In addition, the spatial distribution of C2 and C3 pixels also significantly impact the overall accuracy in different seasons that the most uniform in the fall, while the sparsest in the winter. The worst errors of forecasting performance in the summer may be attributed to the highest precipitation. The limited precipitation event detection in the winter could also be explained by the lowest precipitation (Xu et al., 2019).

Compared with the satellite images of CHIRP and CHIRPS, the results of the WHU-SGCC method provide the greatest improvements for regional daily precipitation estimates over the Jinsha River Basin during the JJA from 1990 to 2014. After bias adjustment of the WHU-SGCC, PCC was improved by 3.34% and 31.81% compared to CHIRP and CHIRPS, respectively. Meanwhile, the RMSE and MAE of the WHU-SGCC was decreased by 6.91% and 6.59% compared to CHIRP, and by 22.71% and 22.15% compared to CHIRPS. Although, the absolute value of BIAS of WHU-SGCC was no significant improvement than CHIRP and slightly higher than CHIRPS, all of the values were approximately to 0. This results of BIAS indicates that all the three kinds of data were much the same on the performance of relative bias. Nevertheless, the NSE of the WHU-SGCC reached -0.0137, an increase of 93.33% and 98.32% compared to CHIRP and CHIRPS, respectively. The NSE of WHU-SGCC was still negative, but it was improved to be zero that indicates the adjusted results are close to the average level of the rain gauge observations, while the NSEs of CHIRP and CHIRPS were much worse. It is noted that the POD of WHU-SGCC was approximate to 1, better than CHIRP and CHIRPS, and the FAR of WHU-SGCC was 0.11, lower than CHIRP and CHIRPS, which represents the better ability on precipitation event predictions of the WHU-SGCC.

**Table 5-4** Overall accuracy assessments during for the four seasons JJA from 1990 to 2014.

Statistic	Spring			Summer			Fall			Winter		
	WHU-SGCC	CHIRP	CHIRPS									
PCC	0.5376	0.3644	0.2132	0.2536	0.2454	0.1924	0.5508	0.3889	0.2661	0.4722	0.2490	0.1716
RMSE	2.9526	3.4332	5.1926	8.7608	9.4108	11.3354	4.7981	4.9038	7.7506	0.8120	0.9042	1.0569
MAE	1.3380	1.5426	1.9948	5.4564	5.8415	7.0088	2.0973	2.2943	2.9925	0.2093	0.7398	0.6905
BIAS	-0.1148	-0.2490	-0.1783	-0.0167	-0.0443	-0.0134	-0.0566	-0.0563	-0.0231	-0.1775	-0.2083	-0.3093
NSE	0.2836	0.0745	-1.0817	-0.0139	-0.2083	-0.8293	0.2944	0.0168	-1.4692	0.1853	0.0161	-0.3098
POD	0.9605	0.8572	0.2918	0.9932	0.9578	0.4351	0.9612	0.9047	0.2326	0.6988	0.5786	0.2076
FAR	0.2416	0.4515	0.3888	0.1146	0.2323	0.1601	0.2386	0.4301	0.2638	0.5242	0.7082	0.6381
CSI	0.6928	0.5001	0.2335	0.8799	0.7405	0.401	0.7089	0.5303	0.2144	0.3668	0.2210	0.1352

491

492

**Table 5** Overall accuracy assessment during the JJA from 1990 to 2014.

Statistic	WHU-SGCC	CHIRP	CHIRPS
PCC	0.2536	0.2454	0.1924
RMSE	8.7608	9.4108	11.3354
MAE	5.4564	5.8415	7.0088
BIAS	-0.0167	-0.0443	-0.0134
NSE	-0.0139	-0.2083	-0.8293
POD	0.9932	0.9578	0.4351
FAR	0.1146	0.2323	0.1601
CSI	0.8799	0.7405	0.4010

493

494

495

496

497

498

499

500

501

502

503

504

505

506

507

508

509

510

511

512

513

514

515

516

517

518

519

520

521

522

523

524

525

The spatial distributions of the statistical comparisons between the observations and the WHU-SGCC precipitation estimations are shown in Fig. 45 and Fig. 6. Overall, the variation in the PCC as seen in Fig. 4 (a) shows that low correlations are observed in areas with lower elevation, particularly in the southern southeast Jinsha River Basin, where there is higher precipitation and a greater density of rain gauges. The PCC is highest in the fall, followed by the spring and winter, and finally by summer. This result is in contrast to the result in (Rivera et al., 2018), because of the few days for heavy rains in this study area. The higher correlations are located in the north-central area along the Tongtian River, Jinsha River and upstream part of the Yalong River, which has complex terrain and few rain gauges. The RMSE is lowest in the winter than in the spring, fall and summer, which can be attributed to the lower precipitation in the winter and the greatest in the summer. The spatial distribution of the RMSE shows that, the smaller errors are scattered in the northwest area of the river basin, with values lower than 5 mm, while the highest errors are located along the border between the lower reaches of the Jinsha Jiang River and the river basin. This is related to the climate regimes of the Jinsha River Basin, which includes more rainfall in the south and southeast areas than in the north, and northwest.

The results show that the WHU-SGCC method improves the correlation relative to CHIRP and CHIRPS, especially in central and southeast river basin during the spring, fall and winter, with most of the PCC values falling between 0.4 and 0.8 (Fig. 5). As shown by the RMSE (Fig. 6), the WHU-SGCC can also correct the precipitation errors in the central and southeast river basin, especially along the downstream part of the Yalong River. In addition, the WHU-SGCC slightly improved the RMSE around the convergence of the rivers, where it is less than 5 mm in the spring and fall, and most of RMSE values are less than 1 mm in the winter. In spite of the correction, the RMSE values in the summer are still substantial.

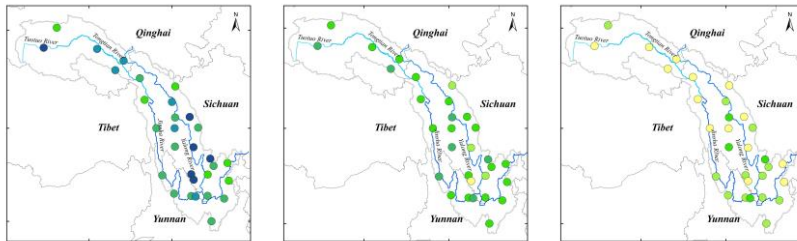
All of the spatial distribution statistics indicate that the statistical relationships established during the process of the WHU-SGCC method are susceptible to the mode values of the rain gauge stations data, especially in the summer. Although the average summer precipitation in the southern Jinsha River Basin was more than 600 mm (Fig. 2), days of light rain still represent a large percentage, which causes large biases and limits the performance over the south, while there are sufficient data with similar precipitation features for the WHU-SGCC in the north. Nevertheless, the WHU-SGCC approach is still effective at adjusting the satellite biases by blending the data with the observations, particularly in the complicated mountainous regions, where higher PCCs correspond to lower RMSEs.

The higher correlations noted over the north-central area of the river basin are in a drier region with complex terrain and sparse rain gauges. With respect to the spatial distribution of RMSE, Fig. 4 (b) indicates that smaller errors were scattered in the northwest area of the river basin, with values lower than 5 mm, while the highest errors, which were over 10 mm, are located over the border between the lower reaches of the Jinsha Jiang River and the river basin. All the values of MAE were below 10 mm and the spatial behaviour was similar to that of the RMSE. Fig. 4 (c) shows that the lower MAE values were located over the mountainous region southwest of Qinghai and west of Sichuan, with values below 6 mm. The spatial distribution of the BIAS (Fig. 4 (d)) indicates that the WHU-SGCC has good agreement with the observations, with the most

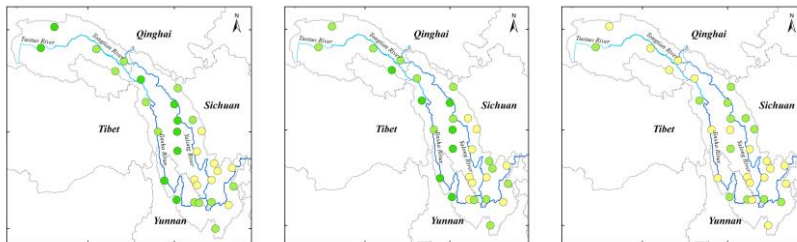
域代码已更改

526 values ranging from -0.1-0.1. All the spatial distribution statistics indicate that the statistical relationships established during  
 527 the process of the WHU-SGCC method is susceptible to the mode values of the rain gauge stations data. Although the average  
 528 annual precipitation in the southern Jinsha River Basin was more than 600 mm (Fig.2), the days of light rain were still in the  
 529 great percentage that caused the large biases and limited the performance over the south area, while there were sufficient data  
 530 with similar precipitation features for WHU-SGCC over the north area. Nevertheless, the WHU-SGCC approach is still  
 531 effective in adjusting the satellite biases by blending with the observations, particularly in the complicated mountainous region  
 532 where there were higher PCC corresponding to lower values of RMSE, MAE and BIAS.—  
 533  
 534

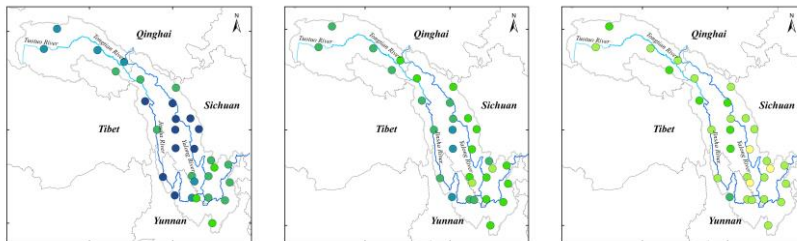
Spring



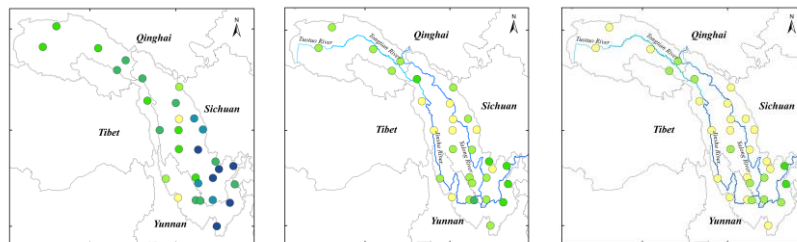
Summer



Fall



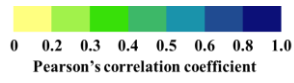
Winter



WHU-SGCC

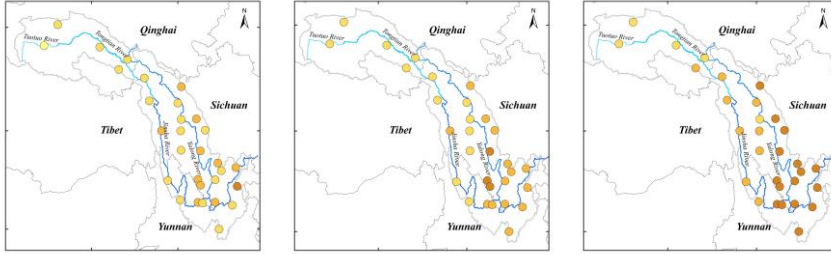
CHIRP

CHIRPS

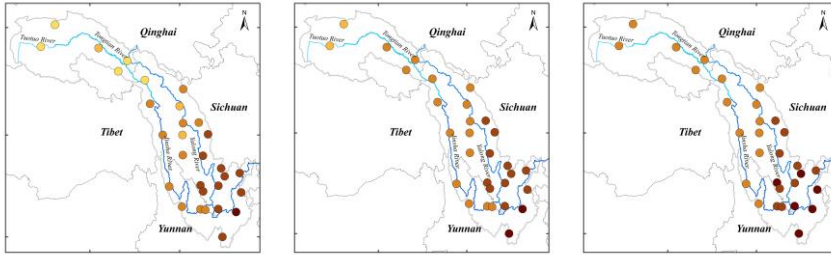


535  
536 **Figure 5** Spatial distribution of the Pearson's correlation coefficient of the overall agreement between observations and the WHU-SGCC,  
537 CHIRP and CHIRPS estimations in the four seasons from 1990 to 2014.

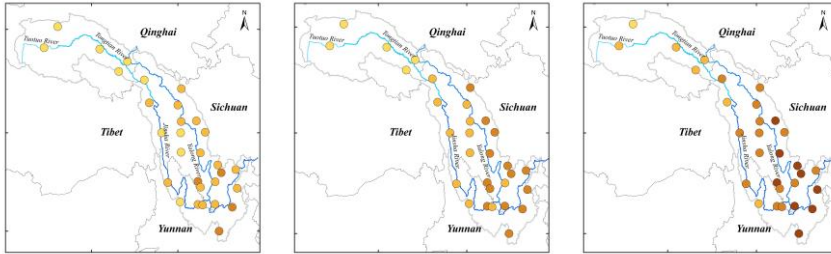
538  
539 Spring



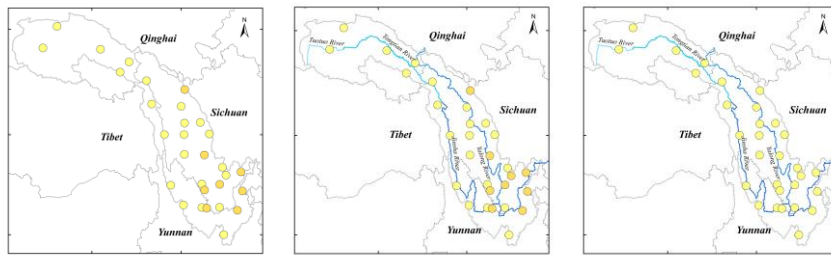
Summer



Fall



Winter



WHU-SGCC

CHIRP

CHIRPS

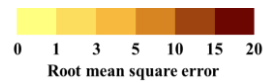


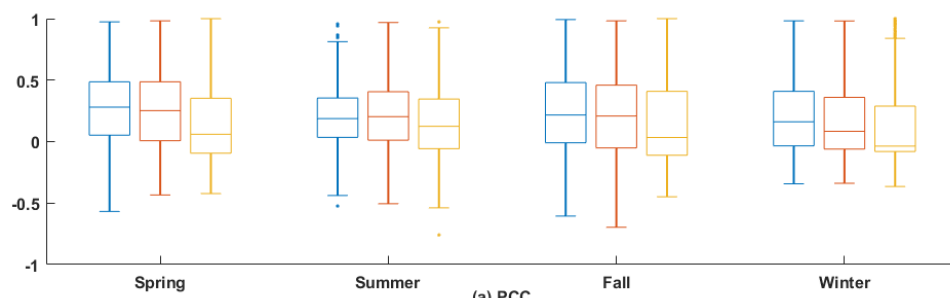
**Figure 6** Spatial distribution of the root mean square errors of the overall agreement between observations and the WHU-SGCC, CHIRP and CHIRPS estimations in the four seasons from 1990 to 2014.

**Figure 4** Spatial distribution of the statistical analyses of the overall agreement between observations and the WHU-SGCC estimations on leave-one-out cross validation during the JJA from 1990 to 2014: a) Pearson's correlation coefficient, b) root mean square error c) mean absolute error, and d) relative bias.

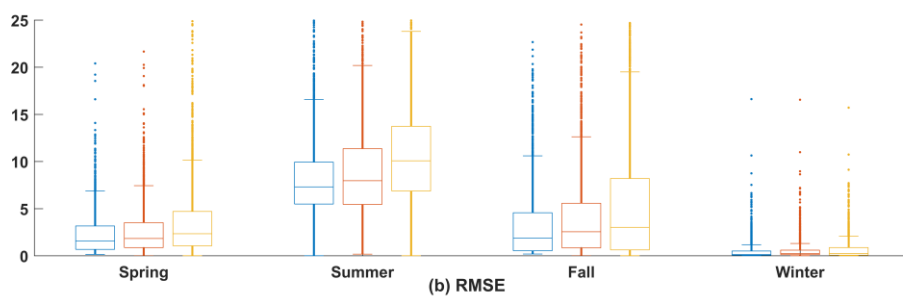
#### 4.2 Model performance based on daily accuracy evaluations

After the overall accuracy evaluations for JJA were conducted, further evaluations of the daily accuracy in the four seasons were investigated, and the results were shown in Fig. 57. The evaluation of the daily accuracy indicates that the PCCs of the WHU-SGCC were slightly better than those of CHIRP and CHIRPS in the spring, fall and winter but were not as good in the summer and winter. The WHU-SGCC had lower RMSEs and MAEs than CHIRP and CHIRPS, especially compared to CHIRPS. The daily RMSE and MAE in the summer are the highest, although the WHU-SGCC still corrects the errors. CHIRP and CHIRPS were roughly the same, while WHU-SGCC has the reduction of errors and biases compared to CHIRP and CHIRPS, especially the greater decreases when compared to CHIRPS. Figure 5-7 indicates that there was a slight no-significant increase in the PCC, with average improvements of 0.02-0.04 and 0.04-0.14, respectively; however, the PCC is a relative metric about of the magnitude of the association between paired variables, and a relative consistency may not mean indicate absolute proximity. Thus, the absolute measure indicated by the RMSE may be more reasonable. In this study, the RMSE and MAE derived from the WHU-SGCC were reduced by approximately 15% and 30-34% on average compared to CHIRP and CHIRPS, respectively. As for BIAS, WHU-SGCC method can correct the CHIRP precipitation bias in the spring, fall and winter, but the results are not as good compared with CHIRPS. The larger BIAS values and higher PCCs in the spring and fall may be attributed to the seasonal variations, when the CHIRP is highly consistent with the observations but subject to large biases. After the correction, a substantial decrease in BIAS occurs in the winter, and there is no significant reduction in the summer; all of the median and average adjusted values are approximately 0. The slight reduction was reflected in the BIAS, with an 8% to 45% reduction compared to CHIRP and CHIRPS, while all the values were concentrated between -0.5 and 0.5. All the precipitation estimations derived from WHU-SGCC, CHIRP, and CHIRPS represented well agreement with the observations in relative bias. The WHU-SGCC method shown provides an obvious improvement in the NSE relative to CHIRP and CHIRPS, while though the median and average values were still less than 0, which may be due to the inherent uncertainty in the CHIRP. Moreover, in terms of the POD, FAR and CSI, except for the results in winter, the WHU-SGCC method seems appears to be more promising in better at detecting precipitation than CHIRP and CHIRPS; the results of POD and CSI are closest to 1, although FAR is worse than CHIRPS on some days although it performs poorly on FAR relative to CHIRPS in some days. However, the POD and CSI of WHU-SGCC were closest to 1. However, the overall result of FAR is the best in the WHU-SGCC. The POD and FAR results are the worst in the winter, and the CSI is slightly higher, which may be attributed to the overestimation of no-rain events and the inherent uncertainty in the CHIRP.

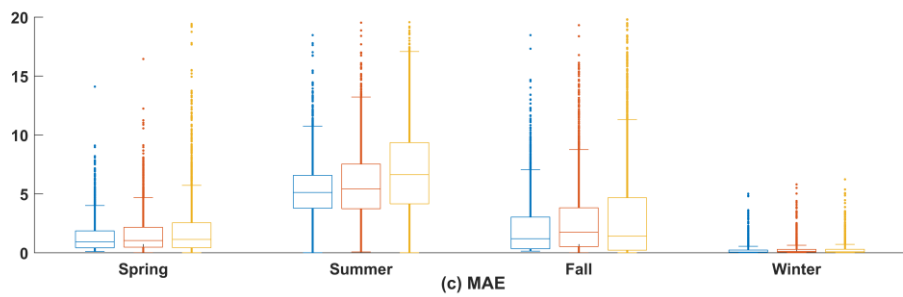
Overall, the WHU-SGCC approach can be regarded as an effective tool for adjustments of daily precipitation adjustments estimates, and improves estimate performance.



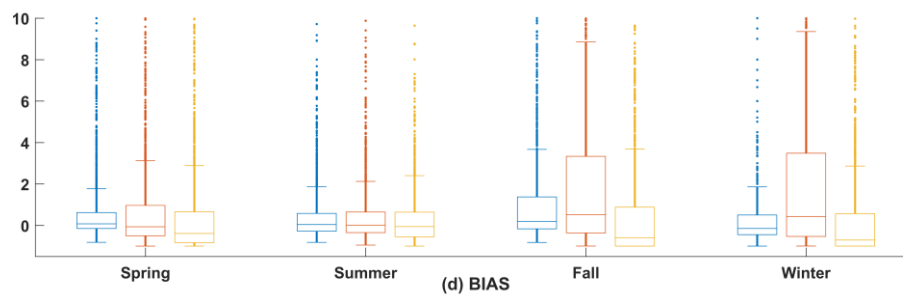
575



576

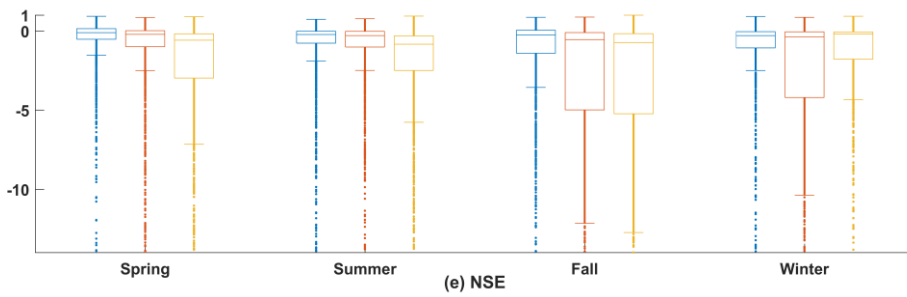


577

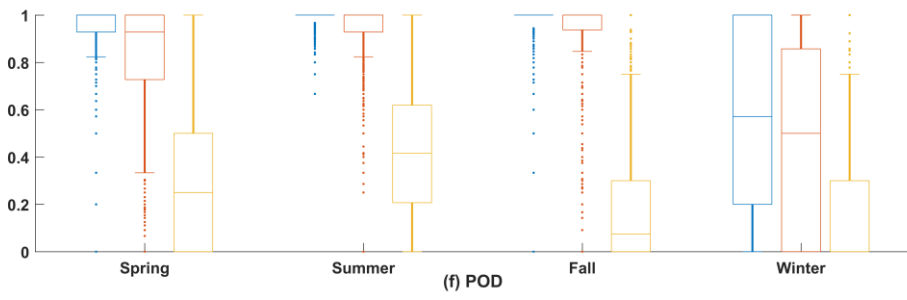


578

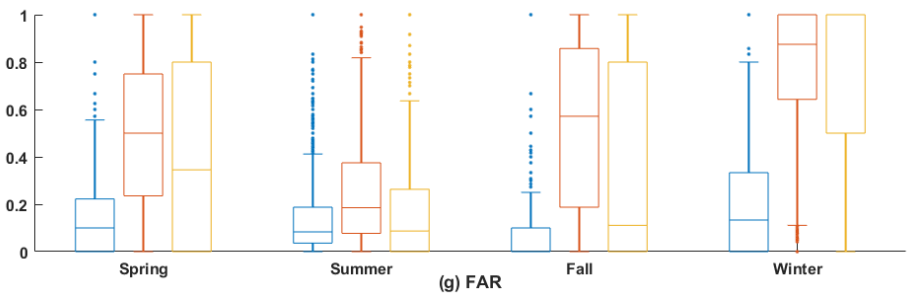
579



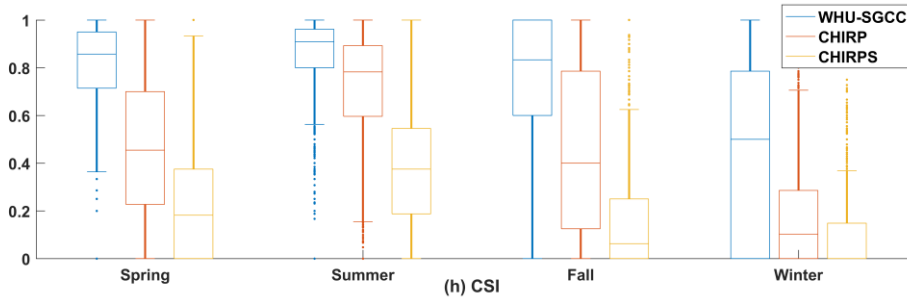
580



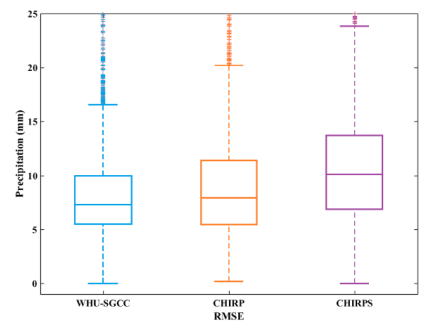
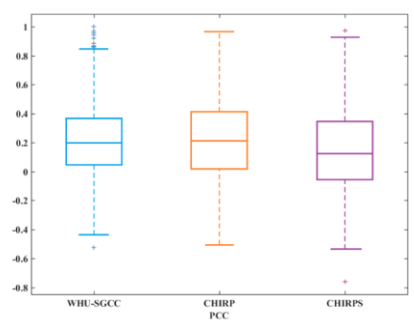
581



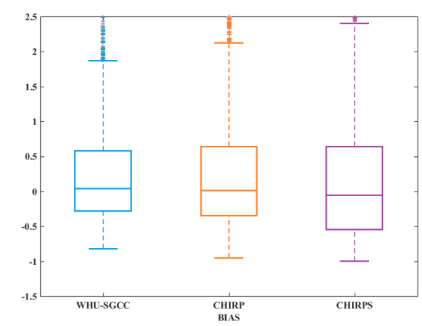
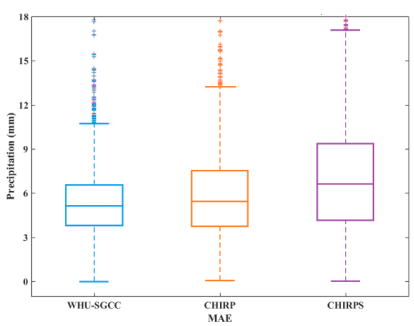
582



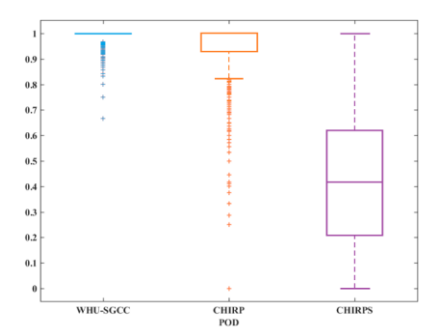
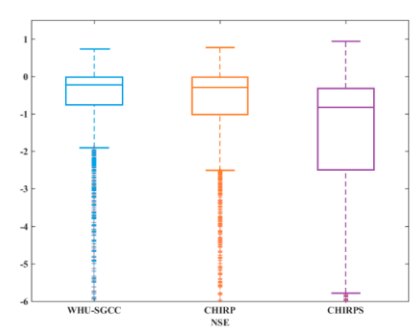
583  
584



585  
586



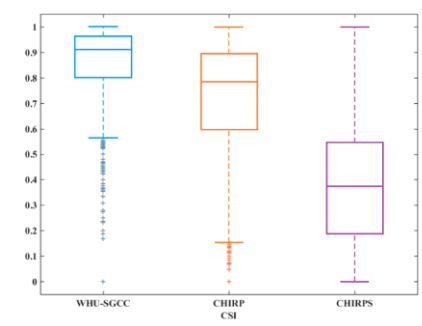
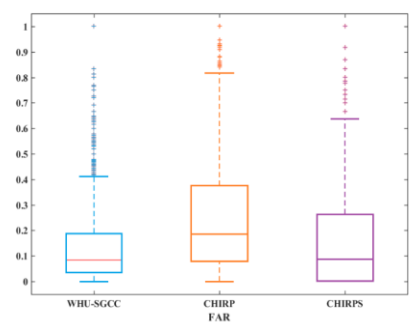
587  
588



(e)

(f)

589



(g) (h)  
 Figure 5-7: Statistical analysis of the agreement between the daily observations and the WHU-SGCC, CHIRP and CHIRPS estimates with the leave-one-out cross validation: a) Pearson's correlation coefficient, b) root mean square error, c) mean absolute error, d) relative bias, e) Nash-Sutcliffe efficiency coefficient, f) probability of detection, g) false alarm ratio, and h) critical success index.

#### 4.3 Model performance on rain events predictions

To measure the WHU-SGCC performance on different predicting rain events predictions, the daily precipitation thresholds of 0.1, 10, 25, and 50 mm were considered, and the results was are shown in Table 6-5 and Table 76. The days average percentage of each class of rain events at the validation gauge station during the four seasons JJA from 1990 to 2014 were are shown in Table 5. The major rain events inside within the Jinsha River Basin were no rain (<0.1 mm) and light rain (0.1-10 mm), which accounted for more than 80% for 54.76% of the total days (the average percentage of rain event days in of is the total days at each gauge station), while the number of days with daily precipitation greater than over the 50 mm was least the smallest (no more than 1% of the total days) and fewer than 5% of the days had daily precipitation in the range of 25 mm to 50 mm only accounting for 0.72%. In the spring, fall and summer, significantly more no-rain days occurred than rainy days, and approximately 5% of the days had daily precipitation of 10-50 mm. The seasonal distribution of rainfall was concentrated in the summer, and 54.76%, 14.01% and 3.62% of the days had daily precipitation of 0.1-10, 10-25, and 25-50 mm, respectively. And the percentage of the daily precipitation of <0.1, 10-25, and 25-50 mm were 26.89%, 14.01% and 3.62% respectively. The results indicated that the average daily precipitation was less than 10 mm, though in the summer seasons throughout the during the multi-years of the study.

As well as, the spatial distribution of precipitation was also uneven, with an increase from north to south.

Table 5 The average percentage of each class of rain events at the validation gauge station during the four seasons from 1990 to 2014 within the Jinsha River Basin.

Season	Rain event (mm)				
	<0.1	[0.1,10)	[10,25)	[25,50)	>=50
Spring	57.87%	38.43%	3.29%	0.39%	0.02%
Summer	26.89%	54.76%	14.01%	3.62%	0.72%
Fall	57.32%	36.62%	4.99%	0.93%	0.14%
Winter	85.78%	13.99%	0.21%	0.01%	0.00%

Table 6 The days of each class of rain events at the validation gauge station during the JJA from 1990 to 2014 inside the Jinsha River.

Validation gauge station	Rain event (mm)					Total days
	<0.1	[0.1,10)	[10,25)	[25,50)	>=50	
52908	637	1186	134	9	0	1966
56004	628	1243	128	3	0	2002
56021	535	1305	166	9	0	2015
56029	556	1328	190	5	0	2079
56034	558	1351	185	17	0	2111
56038	459	1329	222	16	0	2026
56144	562	1153	321	25	0	2061
56146	467	1278	267	19	0	2031
56152	466	1255	307	35	1	2064
56167	565	1234	278	20	0	2097
56247	591	1089	246	34	0	1960
56251	466	1247	320	30	0	2063

56257	336	1212	429	59	0	2036
56357	313	1247	373	63	1	1997
56374	393	1191	351	47	0	1982
56459	487	1080	377	102	13	2059
56462	185	1315	430	86	2	2018
56475	544	983	352	148	20	2047
56479	667	931	298	156	28	2080
56485	588	905	232	100	37	1862
56543	332	1200	289	41	1	1863
56565	526	1020	349	120	13	2028
56571	674	819	301	159	49	2002
56586	730	950	223	79	9	1991
56651	402	1056	391	137	31	2017
56664	727	797	306	166	56	2052
56666	858	791	226	128	44	2047
56671	616	886	289	148	70	2009
56684	768	899	246	114	19	2046
56778	682	930	274	119	43	2048

In terms of performance with respect to different daily rain events, the WHU-SGCC approach had the lowest errors than CHIRP and CHIRPS, as indicated by the RMSE, MAE and BIAS for events with total rainfall lower than 25 mm, but the performance of WHU-SGCC for total rainfall higher than 25 mm is not promising for events with total rainfall greater than 25 mm in the summer (Fig. 8), not improve compared to CHIRP and CHIRPS. This negative performance for total rainfall higher than 25 mm in the summer might be attributed to the overestimation of rainfall by CHIRP and CHIRPS. For the seasonal distribution of precipitation (Table 5) This negative performance on the total rainfall higher than 25 mm was probably caused by (Table 6). The average daily precipitation within the basin was less than 10 mm inside the basin over the study period, during the multi-year summer seasons, which provided results in numerous large amount of rain gauge stations data with the values lower than 10 mm, which had that caused a significantly impact on the establishment of statistical relationships establishment for the WHU-SGCC. The estimates of extreme rain events might also be attenuated during the process of WHU-SGCC adjustment. In hence

Besides, the POD and CSI results of CHIRPS are the worst, while the results of the WHU-SGCC are the highest, which indicate its superiority for the detection of precipitation events. As for the results of the WHU-SGCC, the assessments of POD and CSI are the best in the summer, followed by the fall, spring, and winter, which are related to the seasonal rainfall pattern of more rain in the summer and less in the winter.

Therefore, the approach of WHU-SGCC approach is applicable for the detection of rainfall events over in the Jinsha River Basin, while in the summer is better with the rainfall less than or approximately equal to the average daily precipitation. Due to the homogenization of the WHU-SGCC method, its performance for short intense and extreme rain events was poorer than those of CHIRP and CHIRPS, which should be improved in a future study.

less than 10 mm, or even than 25mm. Due to the 4.34% of summer days with the daily precipitation over the 25 mm, the performance of WHU-SGCC on these rain events was poorer than the results of CHIRP and CHIRPS.

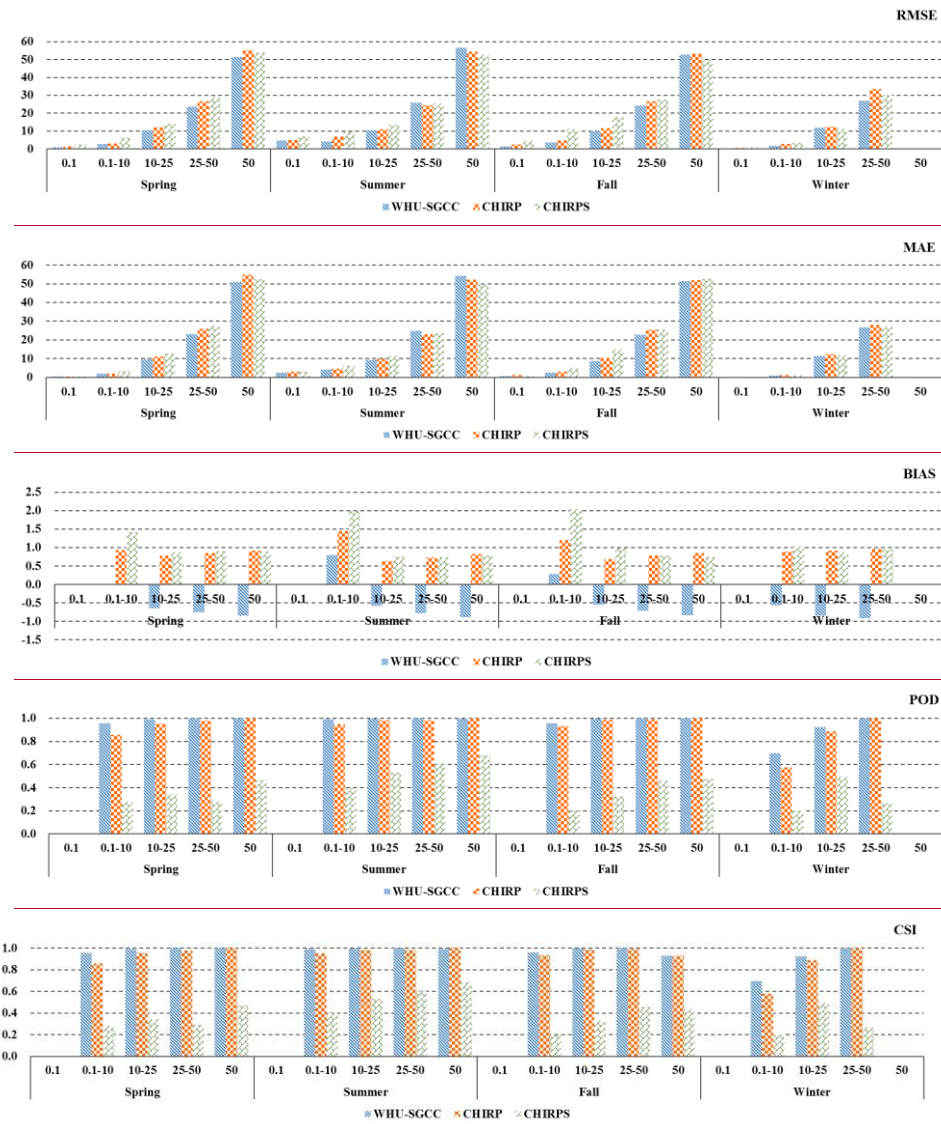


Figure 8 Accuracy assessment of liquid precipitation events from 1990 to 2014.

Table 7 Accuracy assessment on liquid precipitation events during the JJA from 1990 to 2014.

Rain Event	RMSE			MAE			BIAS		
	WHU-SGCC	CHIRP	CHIRPS	WHU-SGCC	CHIRP	CHIRPS	WHU-SGCC	CHIRP	CHIRPS
<0.1	4.7253	5.0802	7.1643	2.5927	2.9562	2.9145	/	/	/
(0.1,10)	4.1661	6.8684	9.6022	3.9885	4.5534	6.2462	0.8021	1.4435	1.9842
(10,25)	10.4281	11.0848	13.4427	9.2722	9.6866	11.5909	-0.5762	0.6342	0.7559
(25,50)	25.7494	24.5600	25.4975	24.8386	23.0967	23.4927	-0.7784	0.7250	0.7388
50	56.6072	54.5037	52.7875	54.4168	52.1557	49.4318	-0.8861	0.8297	0.7852

## 5 Data availability

All the resulting dataset derived from the WHU-SGCC approach is available on PANGAEA, with the following DOI: <https://doi.pangaea.de/10.1594/PANGAEA.900620> (Shen et al., 2019). The high-resolution (0.05°) daily precipitation estimation data over the Jinsha River Basin ~~in the summer~~ from 1990 to 2014 can be downloaded in TIFF format.

## 6 Conclusions

This study provides a novel approach ~~in~~ the WHU-SGCC method, for merging daily satellite-based precipitation estimates with observations. A case study of ~~the~~ Jinsha River Basin was conducted to verify the effectiveness of the WHU-SGCC approach during ~~all the four seasons~~ ~~JA~~ from 1990 to 2014, and the adjusted precipitation estimates were compared to CHIRP and CHIRPS. The WHU-SGCC method aims to reduce the ~~systematic and random errors and uncertainties~~ in CHIRP data over ~~a regions that has with~~ complicated mountainous terrain and sparse rain gauges. To the best of the authors' knowledge, this study is the first to use daily CHIRP and CHIRPS data in this area.

According to our findings, the following conclusions can be drawn: (1) The WHU-SGCC method is effective for the adjustment of precipitation biases from points ~~to surfaces~~. ~~The precipitation adjusted by the WHU-SGCC method can achieve greater accuracy compared with CHIRP and CHIRPS, with average improvements of Pearson's correlation coefficient (PCC) of 0.01-0.23 and 0.06-0.32, respectively. The PCCs were improved to more than 0.5 in the spring and fall and to approximately 0.5 in the winter, and they were the worst in the summer, which may be attributed to the greater precipitation in the summer and lower precipitation in the winter. In addition, the NSE of the WHU-SGCC provides substantial improvements over CHIRP and CHIRPS, which reached 0.2836, 0.2944 and 0.1853 in the spring, fall and winter, respectively. In the summer, the NSE of the WHU-SGCC is still negative, but it is improved to be nearly zero, which indicates that the adjusted results are similar to the average level of the rain gauge observations. The precipitation estimated by the WHU-SGCC method can achieve greater accuracy, which was evaluated with PCC, RMSE, MAE, BIAS, NSE, POD, FAR and CSI. Particularly, the NSE statistic was improved by 93.33% and 98.32% compared to CHIRP and CHIRPS, respectively, and ~~a~~ All of the measured errors were reduced except for the BIAS, which showed with no significant improvement in the summer; but was approximately ~~to~~ 0. Overall, The results show that compared to CHIRPS, the WHU-SGCC approach can achieve substantial improvements ~~good performance in error correction of CHIRP and CHIRPS precipitation estimate accuracy.~~ (2) Moreover, ~~the~~ spatial distribution of ~~the~~ precipitation estimate derived from the WHU-SGCC method is related to the ~~topographic complexity of the topography~~. These ~~random errors over the lower elevations-elevation regions and the large size of light precipitation events with short durations rainstorms in the region~~ resulted in a limited improvement in accuracy, with PCC values less than 0.3. However, higher PCCs and lower errors were observed over the north-central ~~area-part~~ of the river basin, which is a drier region with complex terrain and sparse rain gauges. ~~All~~ The spatial distribution statistics indicate that the WHU-SGCC method is promising for ~~the~~ adjustment of satellite biases by blending with the observations over ~~regions of the complex terrain region~~. (3) The leave-one-out cross validation of WHU-SGCC on daily rain events confirmed that the model ~~was is~~ effective in the detection of precipitation events ~~that are less than or approximately equal to 25 mm due to the less the~~ average annual precipitation ~~inside in~~ the Jinsha River Basin. ~~According to the comparison,~~ The WHU-SGCC approach achieves ~~error~~ reductions of the RMSE, MAE and BIAS metrics, ~~while~~ on rain events less than 25 mm ~~in the summer~~. Specifically, ~~the~~ WHU-SGCC has the best ability to reduce precipitation errors for daily accuracy evaluations, with average reductions of 15% and 34% compared to CHIRP and CHIRPS, respectively. ~~compared with CHIRP, the RMSE value was reduced by approximately by 5.92% 39.44%, the MAE value by 4.28% 12.41%, and the absolute BIAS value by 9.15% 44.43%; compared with CHIRPS, the RMSE and MAE values were reduced by 11.04% 56.61%, and the absolute BIAS value by 23.77% 59.58%. In spite of the corrections, the uncertainties in the precipitation forecasts in the summer are still large, which may due to the homogenization attenuating the simulation of extreme rain events.~~~~

In conclusion, the WHU-SGCC approach can help adjust the biases of daily satellite-based precipitation estimates over the Jinsha River Basin, which contains the complicated mountainous terrains with sparse rain gauges, particularly on the daily precipitation events less than 25 mm in the summer. This approach is a promising tool to monitor monsoon-daily precipitation over the Jinsha River Basin, considering the spatial correlation and historical precipitation characteristics between raster pixels located in regions with similar topographic features. Future development of the WHU-SGCC approach will focus on the following three aspects: (1) the improvement of the adjusted precipitation quality to better monitor extreme rainfall events by blending multiple data sources for different rain events and applying in all seasons; (2) the introduction of more climatic factors and multi-model ensembles to achieve a more accurate spatial distributions of precipitation; and (3) investigations of the performance over the other areas and on the for particular hydrological cases to validate the applicability of WHU-SGCC approach.

#### Appendix A: Geographical characteristics of rain stations

The station identification numbers and relevant geographical characteristics are shown in Table A1.

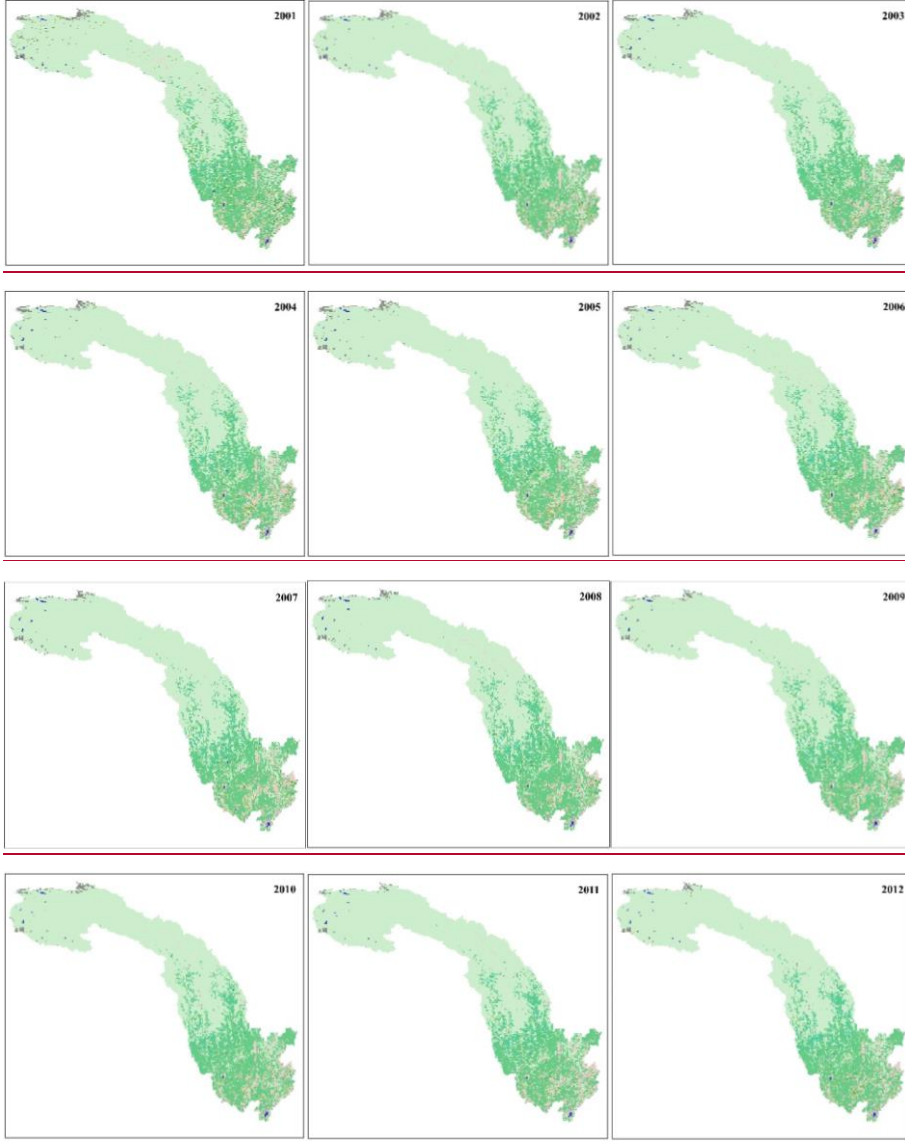
Table A1-2 Geographical characteristics of the rain stations.

Station number	Province	Lat (°N)	Lon (°E)	Elevation (m)
52908	Qinghai	35.13	93.05	4823
56004	Qinghai	34.13	92.26	4744
56021	Qinghai	34.07	95.48	5049
56029	Qinghai	33.00	96.58	4510
56034	Qinghai	33.48	97.08	4503
56144	Tibet	31.48	98.35	4743
56038	Sichuan	32.59	98.06	4285
56146	Sichuan	31.37	100.00	4703
56152	Sichuan	32.17	100.20	4401
56167	Sichuan	30.59	101.07	3374
56247	Sichuan	30.00	99.06	2948
56251	Sichuan	30.56	100.19	4284
56257	Sichuan	30.00	100.16	3971
56357	Sichuan	29.03	100.18	4280
56374	Sichuan	30.03	101.58	3902
56459	Sichuan	27.56	101.16	3002
56462	Sichuan	29.00	101.30	4019
56475	Sichuan	28.39	102.31	1850
56479	Sichuan	28.00	102.51	2470
56485	Sichuan	28.16	103.35	2060
56565	Sichuan	27.26	101.31	2578
56571	Sichuan	27.54	102.16	1503
56666	Sichuan	26.35	101.43	1567
56671	Sichuan	26.39	102.15	1125
56543	Yunnan	27.50	99.42	3216
56586	Yunnan	27.21	103.43	2349
56651	Yunnan	26.51	100.13	2449
56664	Yunnan	26.38	101.16	1540
56684	Yunnan	26.24	103.15	2184
56778	Yunnan	25.00	102.39	1975

#### Appendix B: Multi-year land cover type

The multi-year land cover types in the Jinsha River Basin from 2001 to 2013 are shown in Fig. B1. All of the land cover type maps were derived from the MODIS/Terra+Aqua Land Cover Type Yearly L3 Global 500 m SIN Grid V051 data set, which is available online at [https://search.earthdata.nasa.gov/search/granules?p=C200106111-LPDAAC\\_ECS&q=MCD12&ok=MCD12](https://search.earthdata.nasa.gov/search/granules?p=C200106111-LPDAAC_ECS&q=MCD12&ok=MCD12) (last access: 23 July 2019). Fig. B1 shows that the land use had no obvious changes over the study period. In addition, the upstream area of the Jinsha River is an untraversed region that has not been affected

707 significantly by human activities. Thus, the land use in the study area has hardly changed.



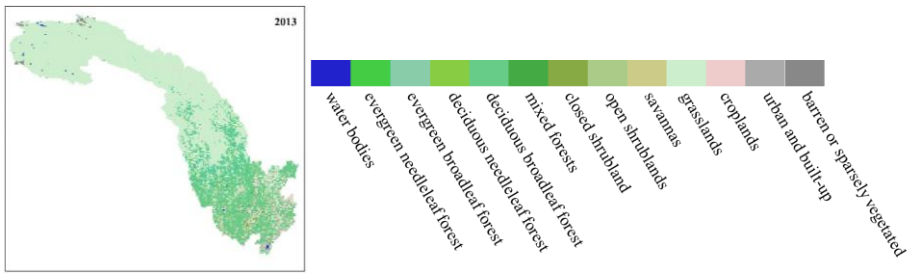
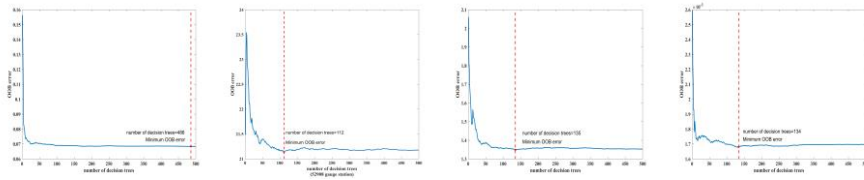


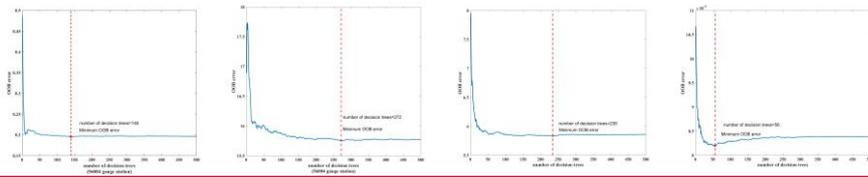
**Figure B1** Land cover types over the Jinsha River Basin from 2001 to 2013.

**Appendix AC: The selection of decision trees for random forest regression**

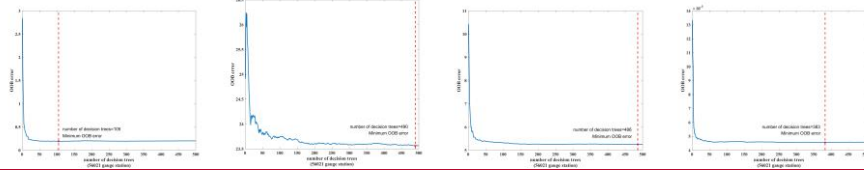
52908



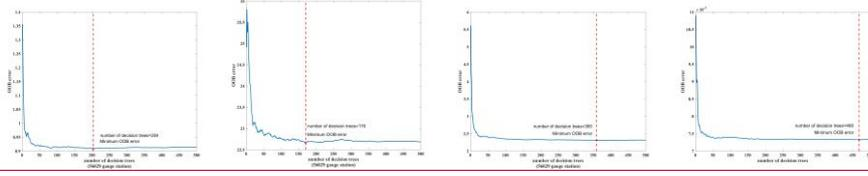
56004



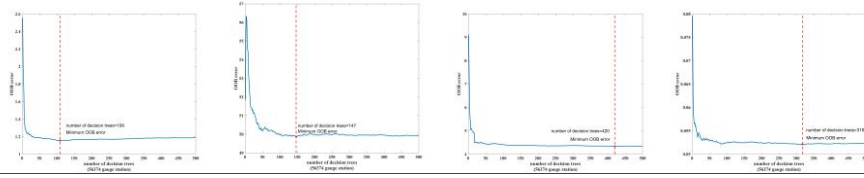
56021



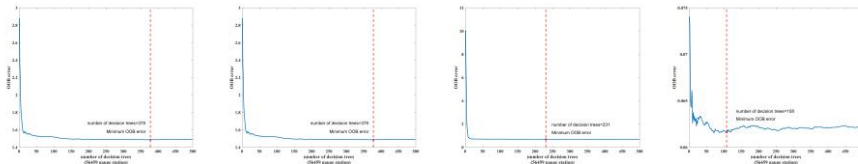
56029



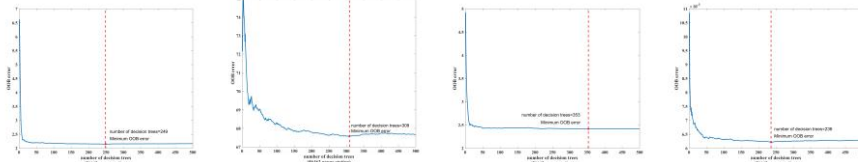
56374



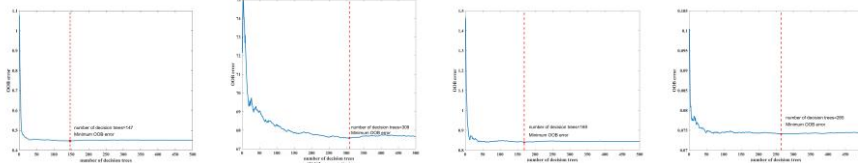
56459



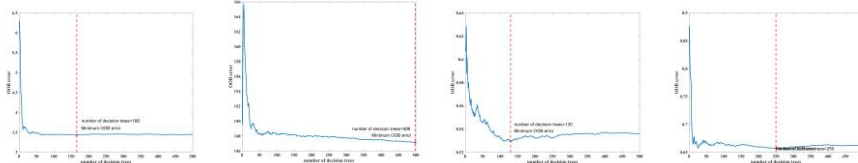
56462



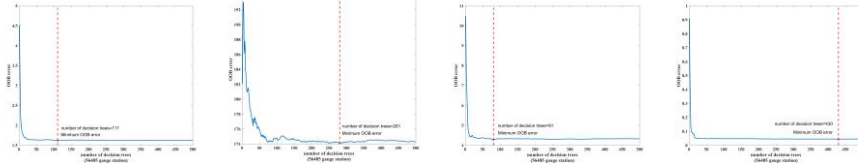
56475



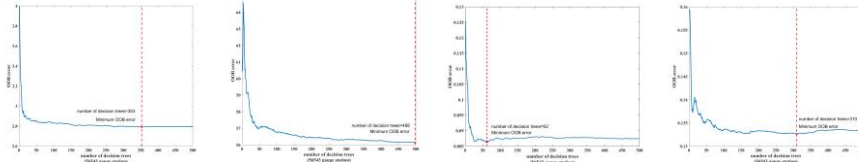
56479



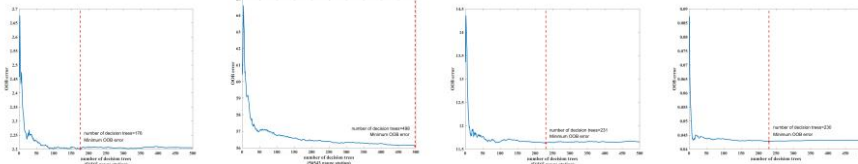
56485



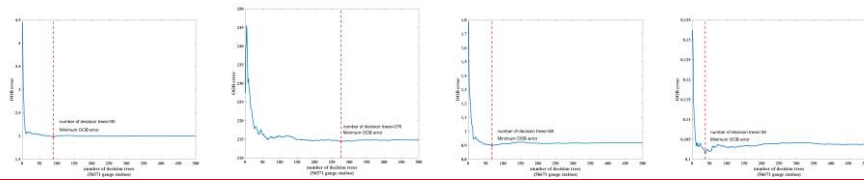
56543



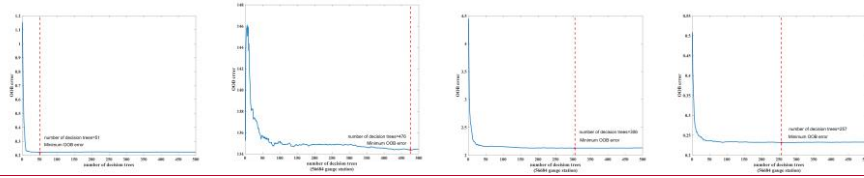
56565



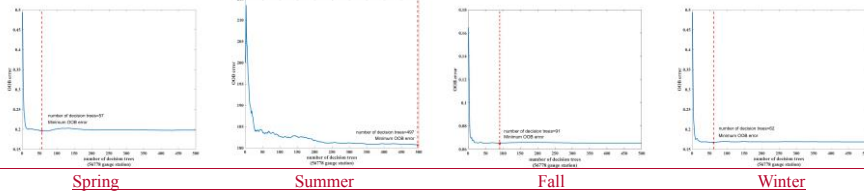
56571



56684



56778

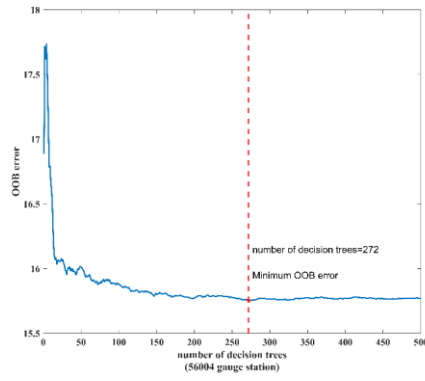
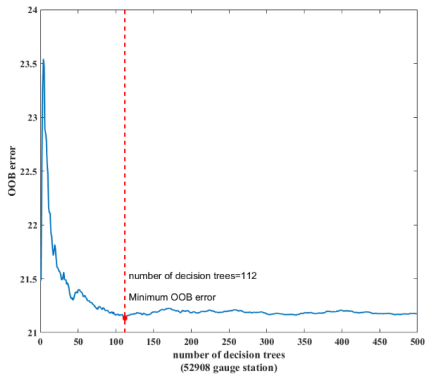


Spring

Summer

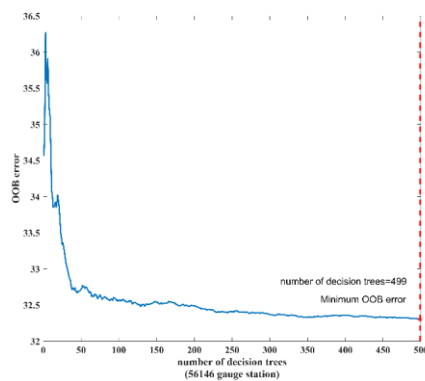
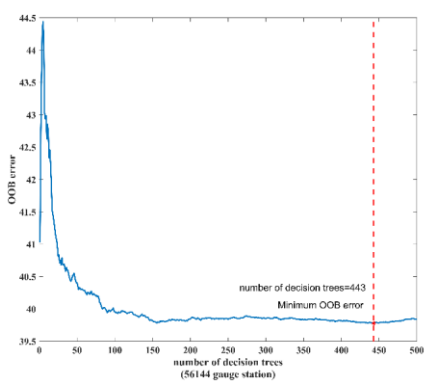
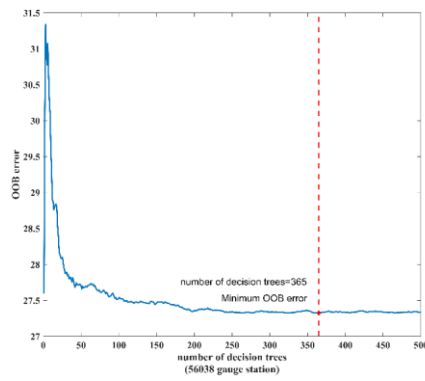
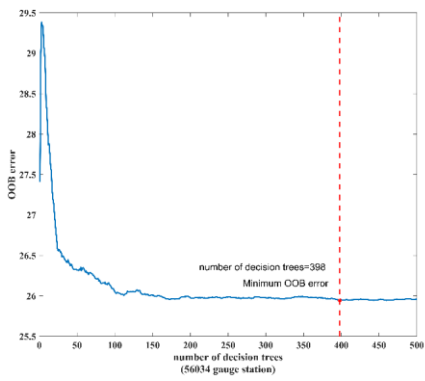
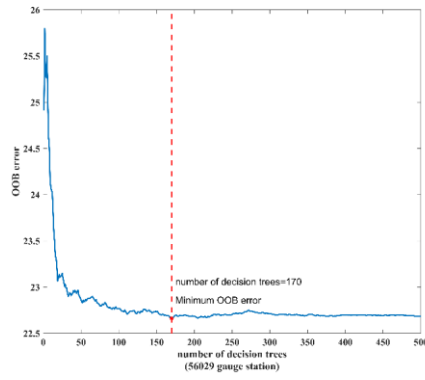
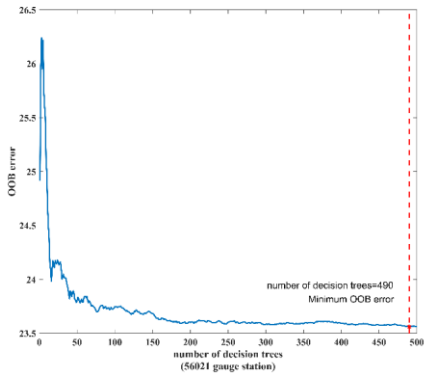
Fall

Winter



716  
717

718

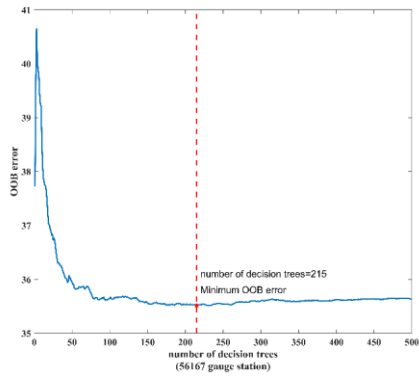
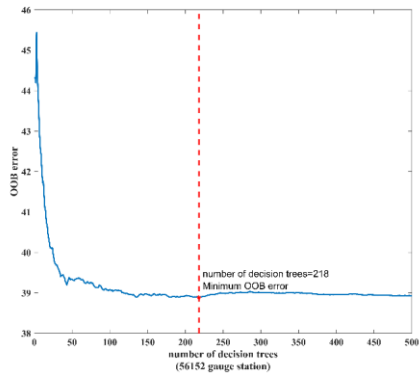


719

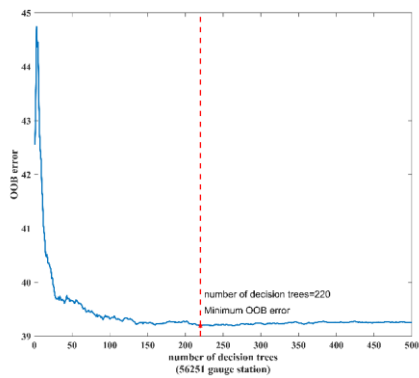
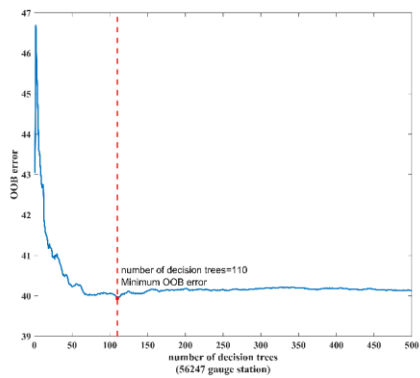
720

721

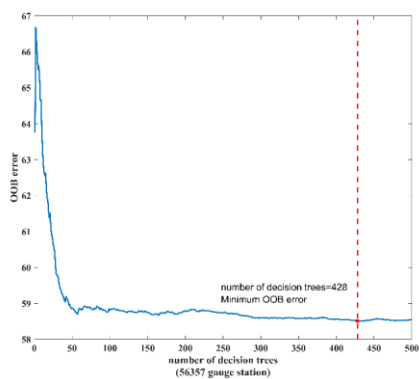
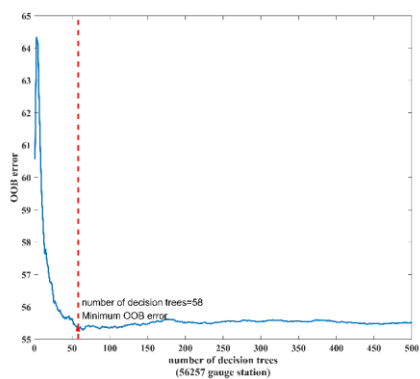
722

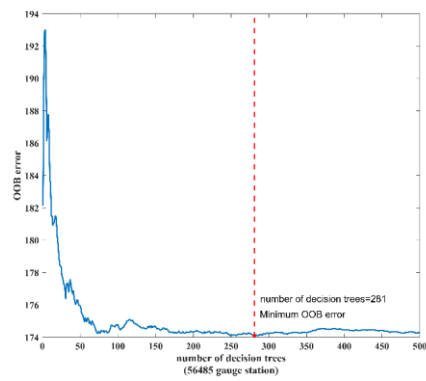
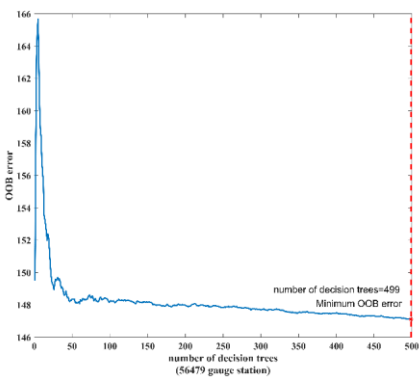
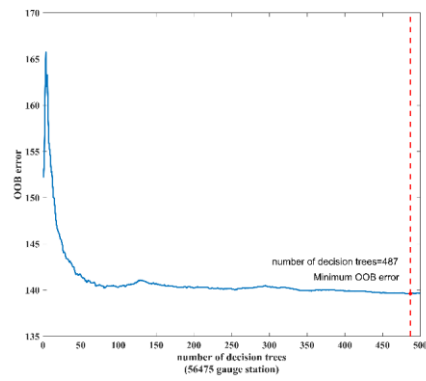
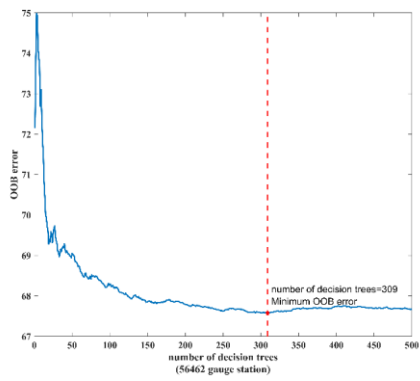
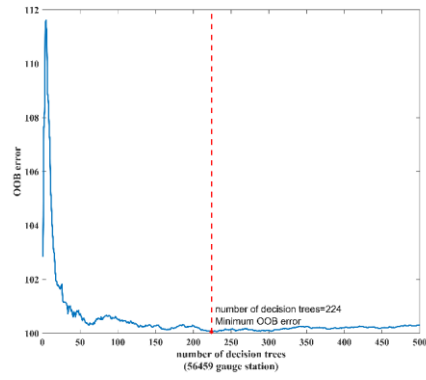
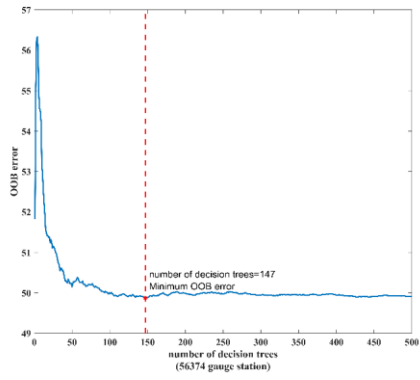


723



724



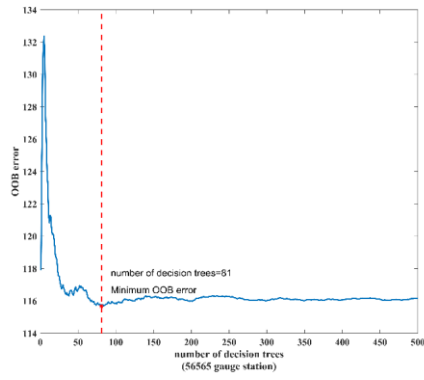
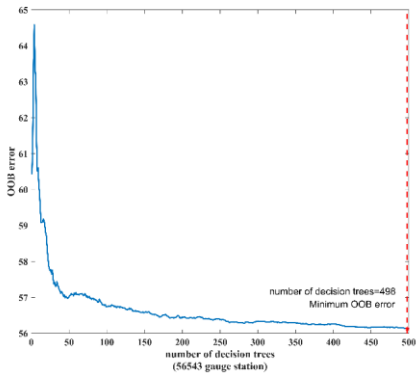


725

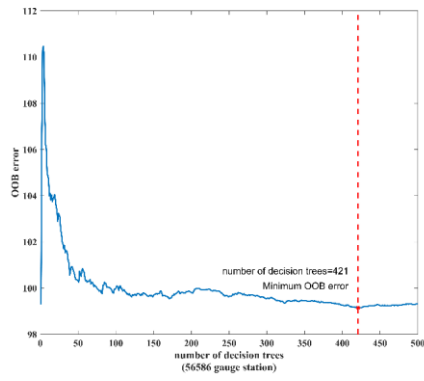
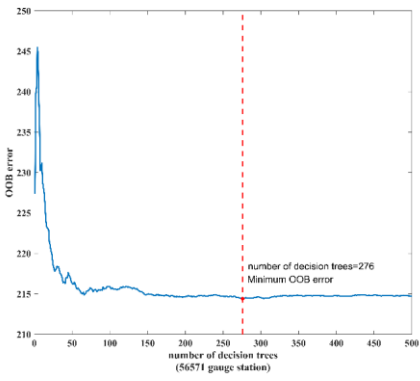
726

727

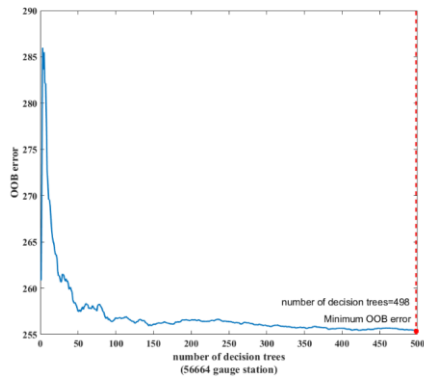
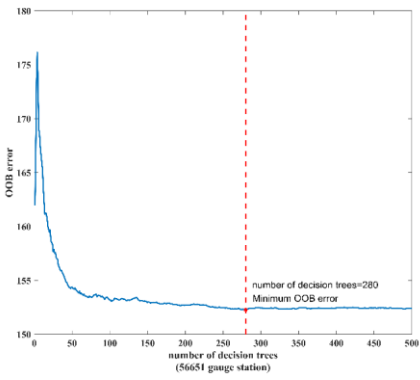
728



729



730



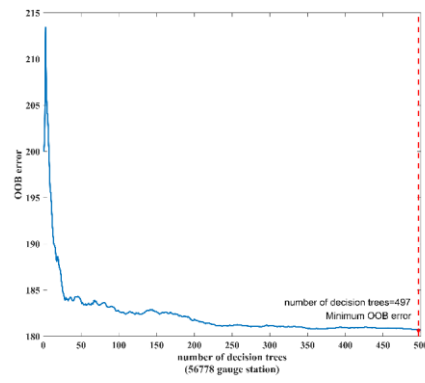
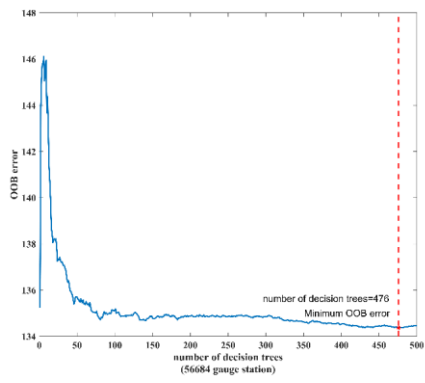
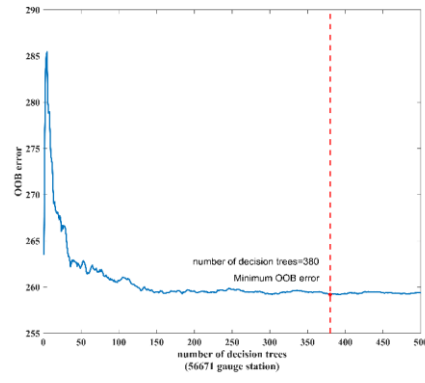
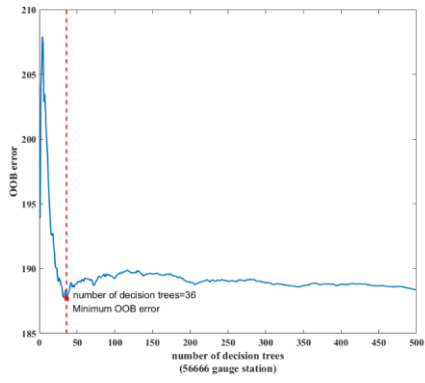


Figure A1-C1 The changes in the out-of-bag (OOB) error with increasing the number of decision trees increase by means of random forest regression at each gauge station.

752  
753  
754  
755  
756  
757  
758  
759  
760  
761

**Appendix D: Spatial distribution of C1, C2 and C3 pixels**

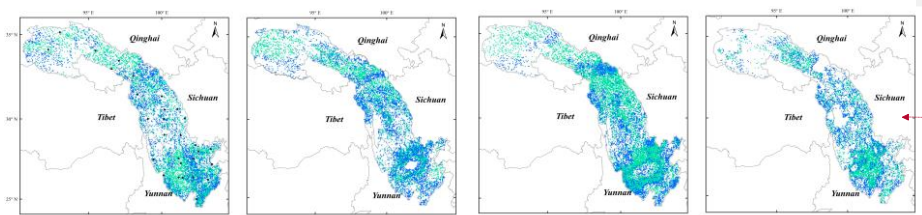
763

**Table D1 Pixel type of the validation gauge station.**

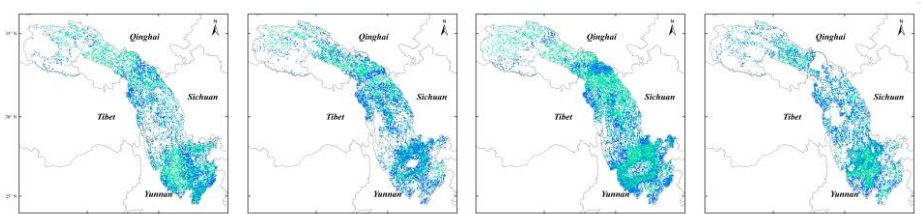
<u>Validation gauge station</u>	<u>Pixel type</u>	<u>Spring</u>	<u>Summer</u>	<u>Fall</u>	<u>Winter</u>
<u>52908</u>	<u>C4</u>	<u>C4</u>	<u>C4</u>	<u>C4</u>	<u>C4</u>
<u>56004</u>	<u>C4</u>	<u>C4</u>	<u>C4</u>	<u>C4</u>	<u>C4</u>
<u>56021</u>	<u>C2</u>	<u>C2</u>	<u>C2</u>	<u>C2</u>	<u>C3</u>
<u>56029</u>	<u>C2</u>	<u>C3</u>	<u>C2</u>	<u>C3</u>	<u>C3</u>
<u>56034</u>	<u>C2</u>	<u>C3</u>	<u>C2</u>	<u>C3</u>	<u>C3</u>
<u>56038</u>	<u>C4</u>	<u>C4</u>	<u>C4</u>	<u>C4</u>	<u>C4</u>
<u>56144</u>	<u>C4</u>	<u>C4</u>	<u>C4</u>	<u>C4</u>	<u>C4</u>
<u>56146</u>	<u>C4</u>	<u>C4</u>	<u>C4</u>	<u>C4</u>	<u>C4</u>
<u>56152</u>	<u>C2</u>	<u>C3</u>	<u>C3</u>	<u>C4</u>	<u>C4</u>
<u>56167</u>	<u>C4</u>	<u>C2</u>	<u>C2</u>	<u>C4</u>	<u>C4</u>
<u>56247</u>	<u>C4</u>	<u>C4</u>	<u>C4</u>	<u>C4</u>	<u>C4</u>
<u>56251</u>	<u>C2</u>	<u>C2</u>	<u>C3</u>	<u>C3</u>	<u>C3</u>
<u>56257</u>	<u>C4</u>	<u>C4</u>	<u>C4</u>	<u>C4</u>	<u>C4</u>
<u>56357</u>	<u>C4</u>	<u>C4</u>	<u>C4</u>	<u>C4</u>	<u>C4</u>
<u>56374</u>	<u>C4</u>	<u>C4</u>	<u>C3</u>	<u>C4</u>	<u>C4</u>
<u>56459</u>	<u>C4</u>	<u>C4</u>	<u>C4</u>	<u>C4</u>	<u>C4</u>
<u>56462</u>	<u>C4</u>	<u>C4</u>	<u>C4</u>	<u>C4</u>	<u>C4</u>
<u>56475</u>	<u>C4</u>	<u>C3</u>	<u>C3</u>	<u>C3</u>	<u>C3</u>
<u>56479</u>	<u>C4</u>	<u>C4</u>	<u>C4</u>	<u>C4</u>	<u>C4</u>
<u>56485</u>	<u>C3</u>	<u>C2</u>	<u>C2</u>	<u>C3</u>	<u>C3</u>
<u>56543</u>	<u>C3</u>	<u>C3</u>	<u>C4</u>	<u>C4</u>	<u>C4</u>
<u>56565</u>	<u>C2</u>	<u>C2</u>	<u>C3</u>	<u>C3</u>	<u>C3</u>
<u>56571</u>	<u>C2</u>	<u>C4</u>	<u>C4</u>	<u>C4</u>	<u>C4</u>
<u>56586</u>	<u>C2</u>	<u>C3</u>	<u>C2</u>	<u>C3</u>	<u>C3</u>
<u>56651</u>	<u>C3</u>	<u>C2</u>	<u>C2</u>	<u>C3</u>	<u>C3</u>
<u>56664</u>	<u>C4</u>	<u>C4</u>	<u>C4</u>	<u>C4</u>	<u>C4</u>
<u>56666</u>	<u>C3</u>	<u>C3</u>	<u>C3</u>	<u>C3</u>	<u>C3</u>
<u>56671</u>	<u>C3</u>	<u>C2</u>	<u>C2</u>	<u>C3</u>	<u>C3</u>
<u>56684</u>	<u>C2</u>	<u>C2</u>	<u>C2</u>	<u>C4</u>	<u>C4</u>
<u>56778</u>	<u>C4</u>	<u>C3</u>	<u>C3</u>	<u>C4</u>	<u>C4</u>

764  
765  
766

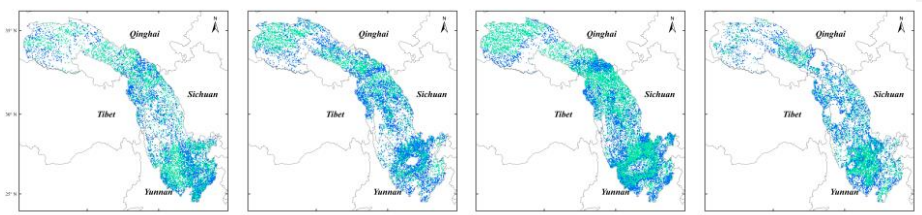
52908



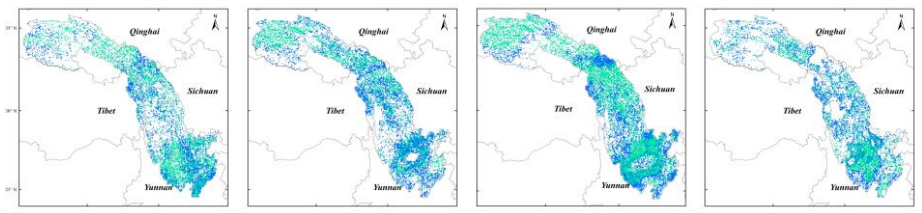
56004



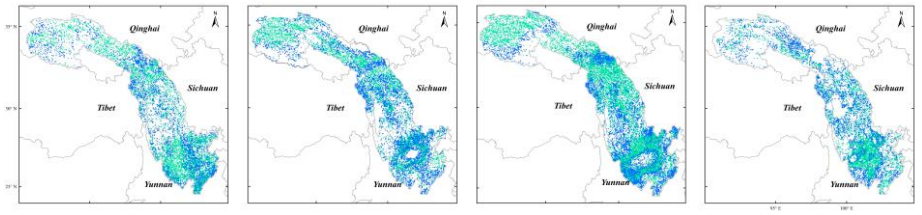
56021



56029

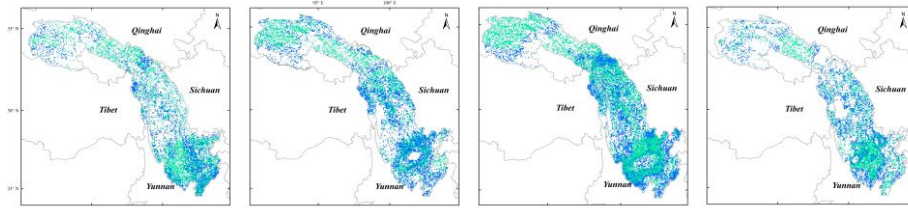


56034

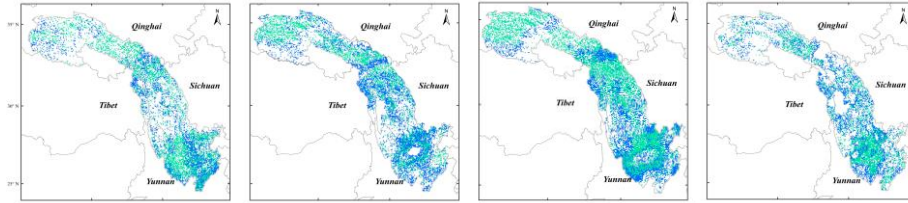


带格式表格

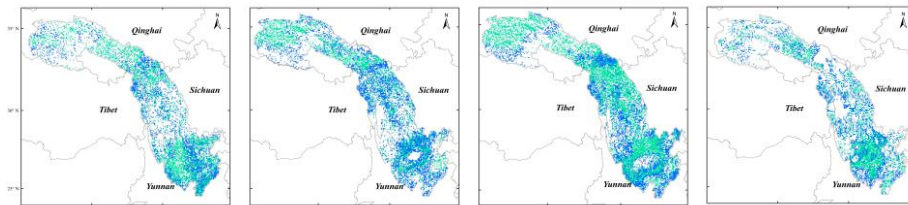
56038



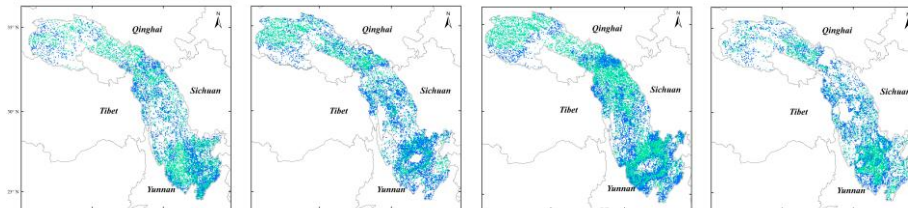
56144



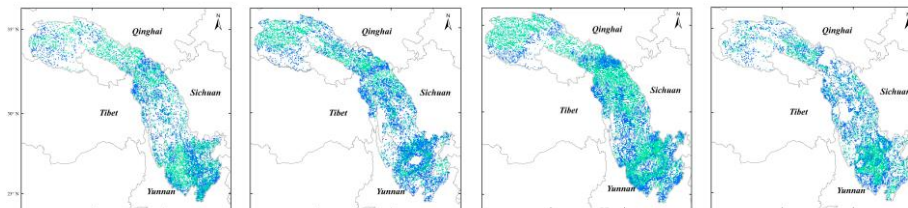
56146



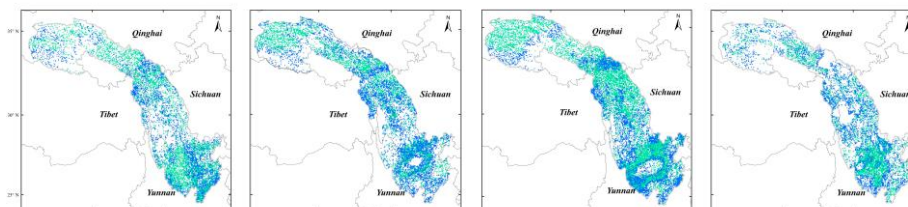
56152



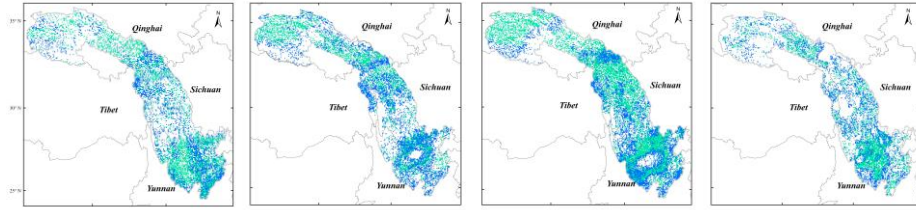
56167



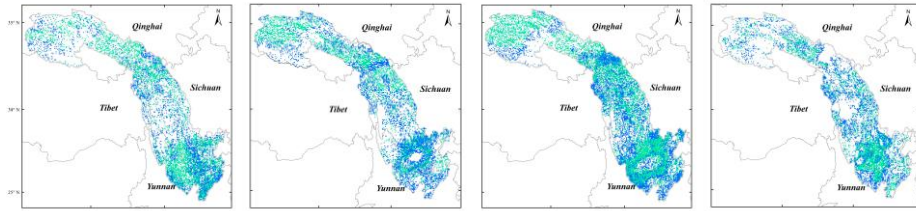
56247



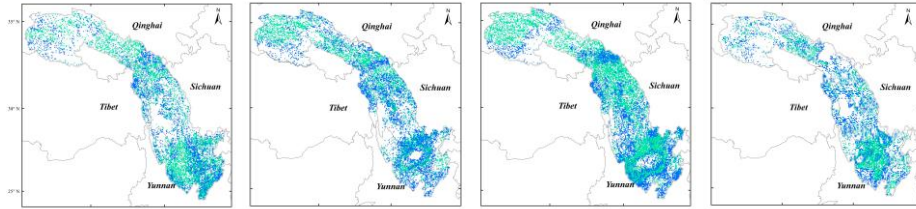
[56251](#)



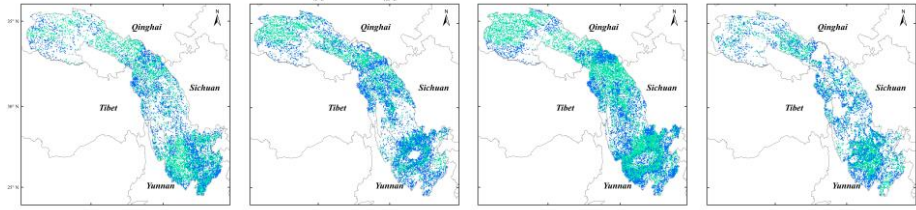
[56257](#)



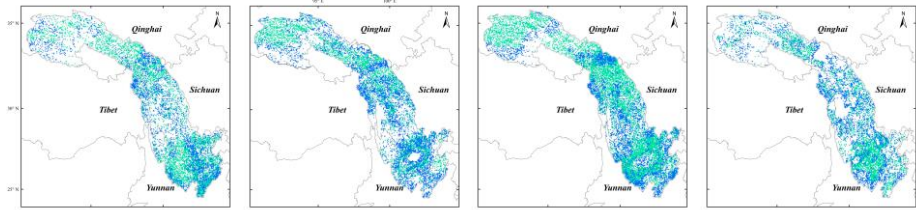
[56357](#)



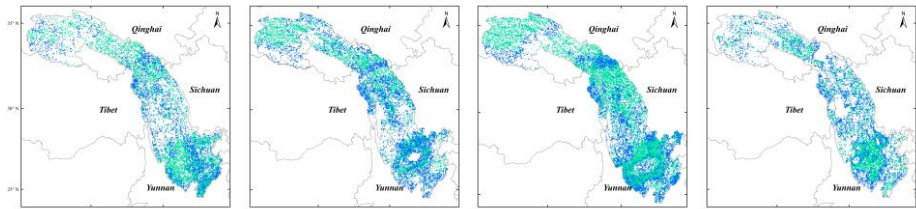
[56374](#)



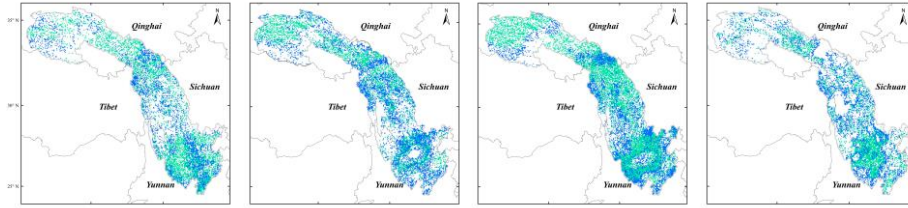
[56459](#)



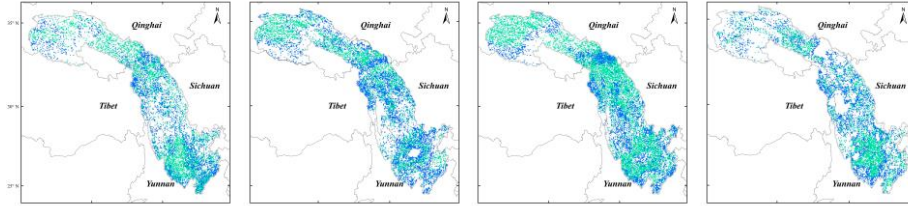
[56462](#)



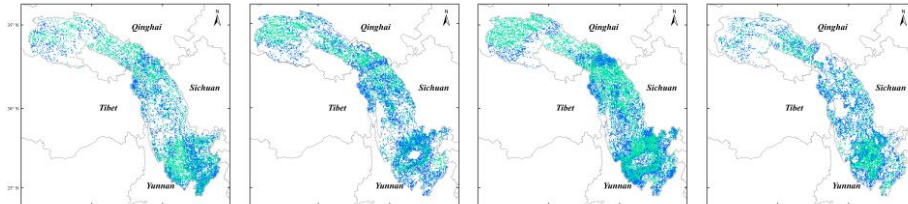
S6475



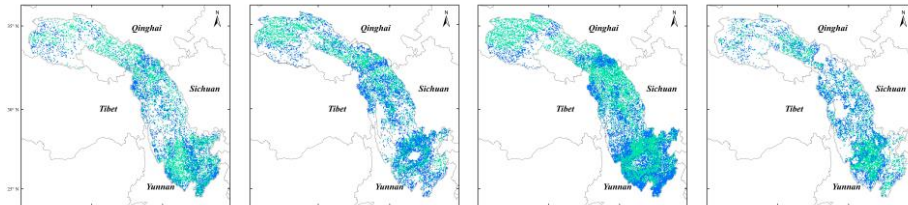
S6479



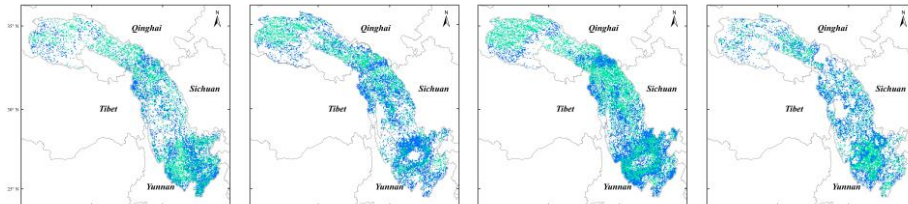
S6485



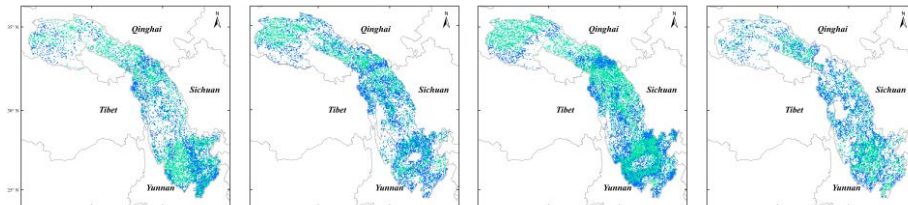
S6543



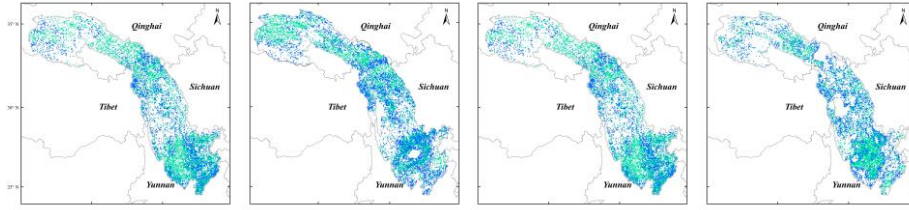
S6565



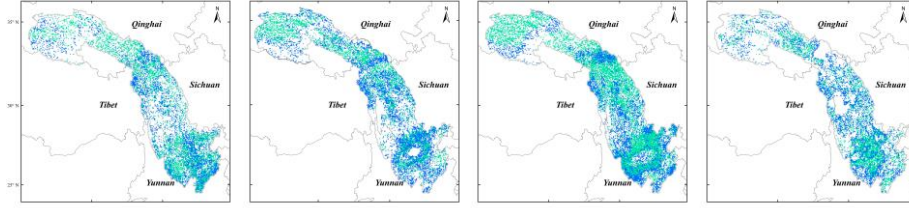
S6571



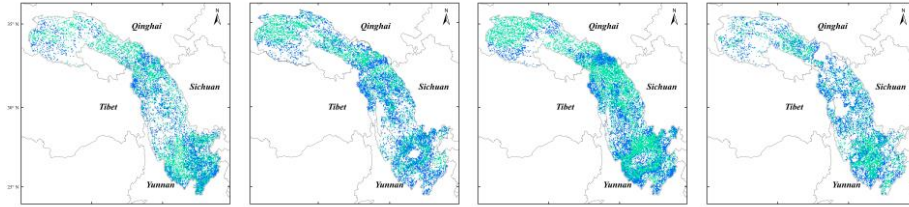
56586



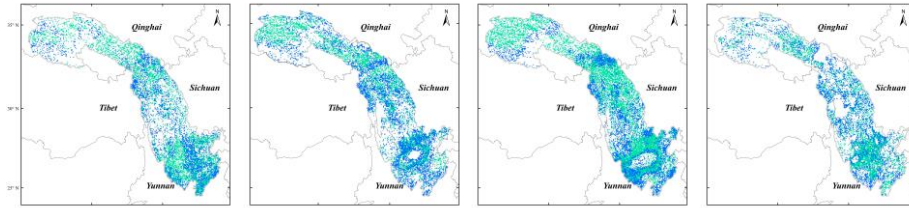
56651



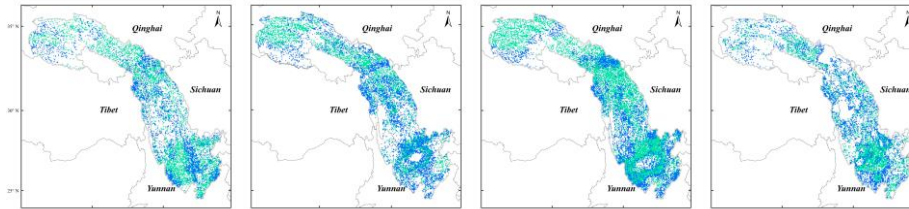
56664



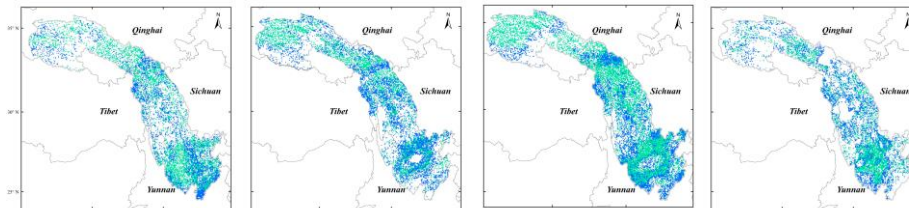
56666



56671



56684



56778

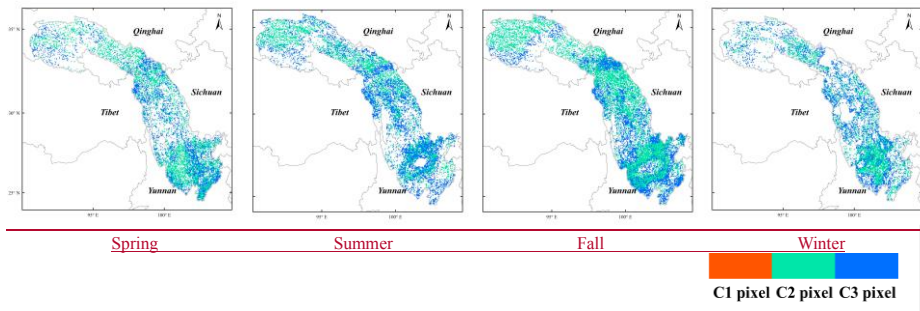


Figure D1 Spatial distribution of each class of pixels adjusted by each rule using the WHU-SGCC method in the Jinsha River Basin.

Appendix BE: Spatial Clustering from the FCM method

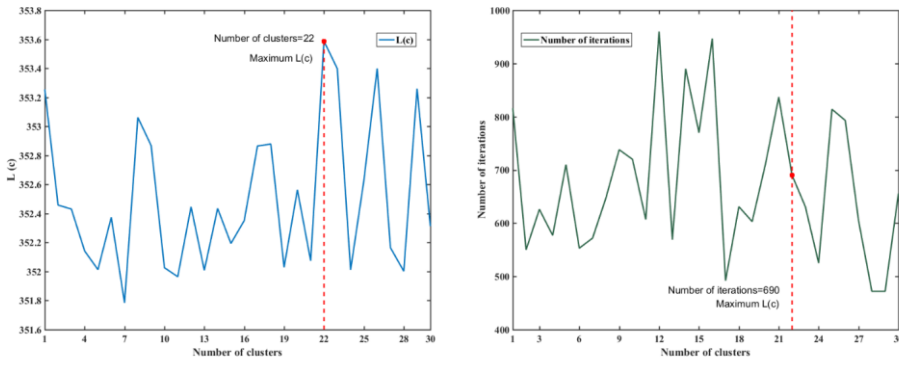
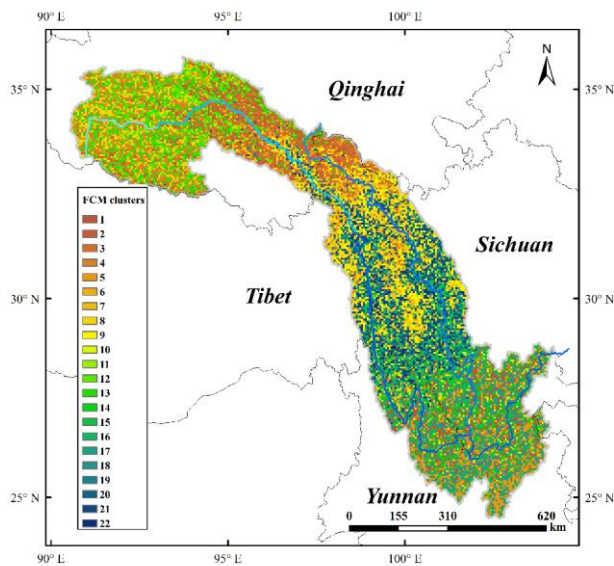


Figure B1-E1 The optimum number of clusters determined by the maximum  $L(c)$  with the iterative process.



773 **Figure B2-E2** Spatial clustering as defined by the FCM method for in the Jinsha River Basin.

774 This appendix demonstrates shows how to set the number of clusters in the FCM method.

775 To adjust the pixels other than those offer the gauged stations, the pixels that are statistically similar to the C1 pixels were  
 776 selected. According to Rule 2, the C2 pixels were identified in a spatial seope area defined by the FCM method. In the following  
 777 experiments of Rule 2, we set the parameters  $m=2, \epsilon=0.00001$ , and the maximum number of iterations was set 1000 (an  
 778 enough a sufficiently large value with the consideringation of the algorithm efficiency). In order to To determine the optimal  
 779 numbers of clusters, the value of  $c$  value was conducted varied in the range from 1 to 30 with an incremental interval value  
 780 of 1 in this study. During the running of FCM approach, the The  $L(c)$  values during the running of the FCM are were shown  
 781 in Fig EB1. The optimum number of clusters was 22, with and the number of iterations was 690 less than the maximum number  
 782 of iterations.

783 Therefore, the number of clusters was set to 22, and the number of iterations was still set to 1000 for fully operations by  
 784 means of the FCM. The spatial clusterings results with consideringation of the terrain factors was are shown in Fig. EB2.  
 785 Overall In general, the spatial results of the FCM have many of the same characteristics as spatial the areas defined by the  
 786 terrain changes variations, especially with respect to the slope and runoff directions, which may influence the regional rainfall  
 787 to some extent.

## 789 7 Acknowledgments

790 This work was supported by the National Natural Science Foundation of China program (no. 41771422), the Nature Science  
 791 Foundation of Hubei Province (no. 2017CFB616), the fundamental research funds for the central universities (no.  
 792 2042017kf0211), and the LIESMARS Special Research Funding.

793 The authors would like to thank data support: the Climate Hazards Group at the University of California, Santa Barbara, for  
 794 providing CHIRP and CHIRPS datasets (<http://chg.ucsb.edu/data/>), and the National Climate Center (NCC) of the China  
 795 Meteorological Administration (CMA) for providing the daily rain gauged observations and gridded precipitation observations  
 796 (<http://data.cma.cn/>). The authors also thank the PANGAEA Data Publisher for Earth & Environmental Science platform for

797 providing the storage to disseminate the data generated in this experiment.

798 The authors are grateful for the editor and anonymous reviewers for their useful suggestions that clearly improved this paper.

## 799 References

- 800 [Adler, R. F., Huffman, G. J., Chang, A., Ferraro, R., Xie, P. P., Janowiak, J., Rudolf, B., Schneider, U., Curtis, S., Bolvin, D.,](#)  
801 [Gruber, A., Susskind, J., Arkin, P., and Nelkin, E.: The version-2 global precipitation climatology project \(GPCP\) monthly](#)  
802 [precipitation analysis \(1979-present\), J. Hydrometeorol., 4, 1147-1167, doi:10.1175/1525-](#)  
803 [7541\(2003\)004<1147:tvgep>2.0.co;2, 2003.](#)
- 804 [AghaKouchak, A., Behrangi, A., Sorooshian, S., Hsu, K., and Amitai, E.: Evaluation of satellite-retrieved extreme precipitation](#)  
805 [rates across the central United States, J. Geophys. Res.-Atmos., 116, 11, doi:10.1029/2010jd014741, 2011.](#)
- 806 [Agutu, N. O., Awange, J. L., Zerihun, A., Ndehedehe, C. E., Kuhn, M., and Fukuda, Y.: Assessing multi-satellite remote sensing,](#)  
807 [reanalysis, and land surface models' products in characterizing agricultural drought in East Africa, Remote Sens. Environ.,](#)  
808 [194, 287-302, doi:10.1016/j.rse.2017.03.041, 2017.](#)
- 809 [Ali, H., and Mishra, V.: Contrasting response of rainfall extremes to increase in surface air and dewpoint temperatures at urban](#)  
810 [locations in India, Sci Rep, 7, 1228, doi:10.1038/s41598-017-01306-1, 2017.](#)
- 811 [Anders, A. M., Roe, G. H., Hallet, B., Montgomery, D. R., Finnegan, N. J., and Putkonen, J.: Spatial patterns of precipitation](#)  
812 [and topography in the Himalaya, Tectonics, Climate, and Landscape Evolution, 398, 39-53, doi:10.1130/2006.2398\(03\),](#)  
813 [2006.](#)
- 814 [Aonashi, K., Awaka, J., Hirose, M., Kozu, T., Kubota, T., Liu, G., Shige, S., Kida, S., Seto, S., Takahashi, N., and Takayabu,](#)  
815 [Y. N.: GSMaP Passive Microwave Precipitation Retrieval Algorithm : Algorithm Description and Validation, Journal of](#)  
816 [the Meteorological Society of Japan, 87A, 119-136, 10.2151/jmsj.87A.119, 2009.](#)
- 817 [Ashouri, H., Hsu, K.-L., Sorooshian, S., Braithwaite, D. K., Knapp, K. R., Cecil, L. D., Nelson, B. R., and Prat, O. P.:](#)  
818 [PERSIANN-CDR: Daily Precipitation Climate Data Record from Multisatellite Observations for Hydrological and](#)  
819 [Climate Studies, Bulletin of the American Meteorological Society, 96, 69-83, doi:10.1175/bams-d-13-00068.1, 2015.](#)
- 820 [Bai, L., Shi, C. X., Li, L. H., Yang, Y. F., and Wu, J.: Accuracy of CHIRPS Satellite-Rainfall Products over Mainland China,](#)  
821 [Remote Sens., 10, 28, doi:10.3390/rs10030362, 2018.](#)
- 822 [Beck, H. E., Vergopolan, N., Pan, M., Levizzani, V., van Dijk, A. I. J. M., Weedon, G. P., Brocca, L., Pappenberger, F., Huffman,](#)  
823 [G. J., and Wood, E. F.: Global-scale evaluation of 22 precipitation datasets using gauge observations and hydrological](#)  
824 [modeling, Hydrology and Earth System Sciences, 21, 6201-6217, 10.5194/hess-21-6201-2017, 2017.](#)
- 825 [Beck, H. E., Wood, E. F., Pan, M., Fisher, C. K., Miralles, D. G., van Dijk, A. I. J. M., McVicar, T. R., and Adler, R. F.: MSWEP](#)  
826 [V2 Global 3-Hourly 0.1 degrees Precipitation: Methodology and Quantitative Assessment, Bulletin of the American](#)  
827 [Meteorological Society, 100, 473-502, 10.1175/bams-d-17-0138.1, 2019.](#)
- 828 [Behrangi, A., Andreadis, K., Fisher, J. B., Turk, F. J., Granger, S., Painter, T., and Das, N.: Satellite-Based Precipitation](#)  
829 [Estimation and Its Application for Streamflow Prediction over Mountainous Western US Basins, J. Appl. Meteorol.](#)  
830 [Climatol., 53, 2823-2842, doi:10.1175/jamc-d-14-0056.1, 2014.](#)
- 831 [Behrangi, A., Hsu, K. L., Imam, B., Sorooshian, S., Huffman, G. J., and Kuligowski, R. J.: PERSIANN-MSA: A Precipitation](#)  
832 [Estimation Method from Satellite-Based Multispectral Analysis, J. Hydrometeorol., 10, 1414-1429,](#)  
833 [10.1175/2009jhm1139.1, 2009.](#)
- 834 [Berndt, C., Rabiei, E., and Haberlandt, U.: Geostatistical merging of rain gauge and radar data for high temporal resolutions](#)  
835 [and various station density scenarios, Journal of Hydrology, 508, 88-101, doi:10.1016/j.jhydrol.2013.10.028, 2014.](#)
- 836 [Cattani, E., Merino, A., Guijarro, J. A., and Levizzani, V.: East Africa Rainfall Trends and Variability 1983-2015 Using Three](#)  
837 [Long-Term Satellite Products, Remote Sens., 10, 26, doi:10.3390/rs10060931, 2018.](#)

838 Chen, F. W., and Liu, C. W.: Estimation of the spatial rainfall distribution using inverse distance weighting (IDW) in the middle  
839 of Taiwan, *Paddy Water Environ.*, 10, 209-222, 10.1007/s10333-012-0319-1, 2012.

840 Chen, J., Brissette, F. P., Chaumont, D., and Braun, M.: Finding appropriate bias correction methods in downscaling  
841 precipitation for hydrologic impact studies over North America, *Water Resources Research*, 49, 4187-4205,  
842 doi:10.1002/wrcr.20331, 2013.

843 Derin, Y., Anagnostou, E., Berne, A., Borga, M., Boudevillain, B., Buytaert, W., Chang, C.-H., Delrieu, G., Hong, Y., Hsu, Y.  
844 C., Lavado-Casimiro, W., Manz, B., Moges, S., Nikolopoulos, E. I., Sahl, D., Salerno, F., Rodriguez-Sanchez, J.-P.,  
845 Vergara, H. J., and Yilmaz, K. K.: Multiregional Satellite Precipitation Products Evaluation over Complex Terrain, *J.*  
846 *Hydrometeorol.*, 17, 1817-1836, 10.1175/jhm-d-15-0197.1, 2016.

847 Duan, Z., Liu, J. Z., Tuo, Y., Chiogna, G., and Disse, M.: Evaluation of eight high spatial resolution gridded precipitation  
848 products in Adige Basin (Italy) at multiple temporal and spatial scales, *Sci. Total Environ.*, 573, 1536-1553,  
849 doi:10.1016/j.scitotenv.2016.08.213, 2016.

850 Dunn, J. C.: A fuzzy relative of the ISODATA Process and Its Use in Detecting Compact Well-Separated Clusters, *Journal of*  
851 *Cybernetics*, 3, 32-57, 1973.

852 Durre, I., Menne, M. J., Gleason, B. E., Houston, T. G., and Vose, R. S.: Comprehensive Automated Quality Assurance of  
853 Daily Surface Observations, *J. Appl. Meteorol. Climatol.*, 49, 1615-1633, doi:10.1175/2010jame2375.1, 2010.

854 Funk, C., Peterson, P., Landsfeld, M., Pedreros, D., Verdin, J., Shukla, S., Husak, G., Rowland, J., Harrison, L., Hoell, A., and  
855 Michaelsen, J.: The climate hazards infrared precipitation with stations-a new environmental record for monitoring  
856 extremes, *Sci. Data*, 2, 21, doi:10.1038/sdata.2015.66, 2015 a.

857 Funk, C., Verdin, A., Michaelsen, J., Peterson, P., Pedreros, D., and Husak, G.: A global satellite-assisted precipitation  
858 climatology, *Earth Syst. Sci. Data*, 7, 275-287, 10.5194/essd-7-275-2015, 2015 b.

859 Funk, C., Peterson, P., Landsfeld, M., Pedreros, D., Verdin, J., Rowland, J., Bo, E., Husak, G. J., Michaelsen, J. C., and Verdin,  
860 A. P.: A Quasi-Global Precipitation Time Series for Drought Monitoring Data Series 832, *Usgs Professional Paper, Data*  
861 *Series*, 2014.

862 Genuer, R., Poggi, J. M., Tuleau-Malot, C., and Villa-Vialaneix, N.: Random Forests for Big Data, *Big Data Res.*, 9, 28-46,  
863 doi:10.1016/j.bdr.2017.07.003, 2017.

864 [Hou, A. Y., Kakar, R. K., Neeck, S., Azarbarzin, A. A., Kummerow, C. D., Kojima, M., Oki, R., Nakamura, K., and Iguchi, T.:  
865 The Global Precipitation Measurement Mission, \*Bulletin of the American Meteorological Society\*, 95, 701-722,  
866 \[10.1175/bams-d-13-00164.1, 2014.\]\(#\)](#)

867 [Huffman, G. J., Adler, R. F., Arkin, P., Chang, A., Ferraro, R., Gruber, A., Janowiak, J., McNab, A., Rudolf, B., and Schneider,  
868 U.: The Global Precipitation Climatology Project \(GPCP\) Combined Precipitation Dataset, \*Bulletin of the American\*  
869 \*Meteorological Society\*, 78, 5-20, doi:10.1175/1520-0477\(1997\)078<0005:tgpepg>2.0.co;2, 1997.](#)

870 [Huffman, G. J., Adler, R. F., Bolvin, D. T., Gu, G., Nelkin, E. J., Bowman, K. P., Hong, Y., Stocker, E. F., and Wolff, D. B.:  
871 The TRMM multisatellite precipitation analysis \(TMPA\): Quasi-global, multiyear, combined-sensor precipitation  
872 estimates at fine scales, \*J. Hydrometeorol.\*, 8, 38-55, 10.1175/jhm560.1, 2007.](#)

873 [Huffman, G. J., Adler, R. F., Bolvin, D. T., and Nelkin, E. J.: The TRMM Multi-Satellite Precipitation Analysis \(TMPA\), in:  
874 Satellite Rainfall Applications for Surface Hydrology, edited by: Gebremichael, M., and Hossain, F., Springer Netherlands,  
875 Dordrecht, 3-22, 2010.](#)

876 [Huffman, G. J., D. T. Bolvin, D. Braithwaite, K. Hsu, R. Joyce, P. Xie.: NASA Global Precipitation Measurement Integrated  
877 Multi-satellite Retrievals for GPM \(IMERG\), \*NASA Algorithm theoretical basis document \(ATBD\) version 5.2.\*, 35 pp.  
878 \[https://pmm.nasa.gov/sites/default/files/document\\\_files/IMERG\\\_ATBD\\\_V5.2.pdf\]\(https://pmm.nasa.gov/sites/default/files/document\_files/IMERG\_ATBD\_V5.2.pdf\), 2018.](#)

879 Johnson, R. W.: *An Introduction to the Bootstrap*, Chapman & Hall/CRC Press, 49-54 pp., 1998.

880 [Joyce, R. J., Janowiak, J. E., Arkin, P. A., and Xie, P. P.: CMORPH: A method that produces global precipitation estimates](#)

881 [from passive microwave and infrared data at high spatial and temporal resolution, \*J. Hydrometeorol.\*, 5, 487-503,](#)  
882 [10.1175/1525-7541\(2004\)005<0487:camtpg>2.0.co;2, 2004.](#)

883 [Joyce, R. J., and Xie, P.: Kalman Filter-Based CMORPH, \*J. Hydrometeorol.\*, 12, 1547-1563, 10.1175/jhm-d-11-022.1, 2011.](#)

884 Katsanos, D., Retalis, A., and Michaelides, S.: Validation of a high-resolution precipitation database (CHIRPS) over Cyprus  
885 for a 30-year period, *Atmospheric Research*, 169, 459-464, doi:10.1016/j.atmosres.2015.05.015, 2016a.

886 Katsanos, D., Retalis, A., Tymvios, F., and Michaelides, S.: Analysis of precipitation extremes based on satellite (CHIRPS)  
887 and in situ dataset over Cyprus, *Natural Hazards*, 83, 53-63, doi:10.1007/s11069-016-2335-8, 2016b.

888 Kummerow, C., Barnes, W., Kozu, T., Shiue, J., and Simpson, J.: The Tropical Rainfall Measuring Mission (TRMM) sensor  
889 package, *J. Atmos. Ocean. Technol.*, 15, 809-817, doi:10.1175/1520-0426(1998)015<0809:ttrmmt>2.0.co;2, 1998.

890 Long, D., and Singh, V. P.: Assessing the impact of end-member selection on the accuracy of satellite-based spatial variability  
891 models for actual evapotranspiration estimation, *Water Resources Research*, 49, 2601-2618, doi:10.1002/wrcr.20208,  
892 2013.

893 Lu, G. Y., and Wong, D. W.: An adaptive inverse-distance weighting spatial interpolation technique, *Comput. Geosci.*, 34,  
894 1044-1055, 10.1016/j.cageo.2007.07.010, 2008.

895 Maggioni, V., and Massari, C.: on the performance of satellite precipitation products in riverine flood modeling: A review,  
896 *Journal of Hydrology*, 558, 214-224, 10.1016/j.jhydrol.2018.01.039, 2018.

897 [Maggioni, V., Meyers, P. C., and Robinson, M. D.: A Review of Merged High-Resolution Satellite Precipitation Product](#)  
898 [Accuracy during the Tropical Rainfall Measuring Mission \(TRMM\) Era, \*J. Hydrometeorol.\*, 17, 1101-1117, 10.1175/jhm-](#)  
899 [d-15-0190.1, 2016.](#)

900 Mahmoud, M. T., Al-Zahrani, M. A., and Sharif, H. O.: Assessment of global precipitation measurement satellite products over  
901 Saudi Arabia, *Journal of Hydrology*, 559, 1-12, 10.1016/j.jhydrol.2018.02.015, 2018.

902 ~~Mahmoud, M. T., Hamouda, M. A., and Mohamed, M. M.: Spatiotemporal evaluation of the GPM satellite precipitation~~  
903 ~~products over the United Arab Emirates, *Atmospheric Research*, 219, 200-212, 10.1016/j.atmosres.2018.12.029, 2019.~~

904 Martens, B., Cabus, P., De Jongh, I., and Verhoest, N. E. C.: Merging weather radar observations with ground-based  
905 measurements of rainfall using an adaptive multiquadric surface fitting algorithm, *Journal of Hydrology*, 500, 84-96,  
906 doi:10.1016/j.jhydrol.2013.07.011, 2013.

907 Nash, J. E., Sutcliffe, J. V.: River flow forecasting through conceptual models, Part I - A discussion of principles, *Journal of*  
908 *Hydrology*, 10, 282-290, doi.org/10.1016/0022-1694(70)90255-6, 1970.

909 Nogueira, S. M. C., Moreira, M. A., and Volpato, M. M. L.: Evaluating Precipitation Estimates from Eta, TRMM and CHIRPS  
910 Data in the South-Southeast Region of Minas Gerais State-Brazil, *Remote Sens.*, 10, 16, doi:10.3390/rs10020313, 2018.

911 Ning, S., Wang, J., Jin, J., and Ishidaira, H.: Assessment of the Latest GPM-Era High-Resolution Satellite Precipitation  
912 Products by Comparison with Observation Gauge Data over the Chinese Mainland, *Water*, 8, 481-497,  
913 doi:10.3390/w8110481, 2016.

914 Paredes-Trejo, F. J., Barbosa, H. A., and Kumar, T. V. L.: Validating CHIRPS-based satellite precipitation estimates in  
915 Northeast Brazil, *J. Arid. Environ.*, 139, 26-40, doi:10.1016/j.jaridenv.2016.12.009, 2017.

916 [Prakash, S.: Performance assessment of CHIRPS, MSWEP, SM2RAIN-CCI, and TMPA precipitation products across India,](#)  
917 [Journal of Hydrology, 571, 50-59, 10.1016/j.jhydrol.2019.01.036, 2019.](#)

918 Pessoa, F. C. L., Blanco, C. J. C., and Gomes, E. P.: Delineation of homogeneous regions for streamflow via fuzzy c-means in  
919 the Amazon, *Water Pract. Technol.*, 13, 210-218, doi:10.2166/wpt.2018.035, 2018.

920 ~~Rivera, J. A., Marianetti, G., and Hinrichs, S.: Validation of CHIRPS precipitation dataset along the Central Andes of Argentina,~~  
921 ~~Atmospheric Research, 213, 437-449, doi:10.1016/j.atmosres.2018.06.023, 2018.~~

922 Roy, T., Gupta, H. V., Serrat-Capdevila, A., and Valdes, J. B.: Using satellite-based evapotranspiration estimates to improve  
923 the structure of a simple conceptual rainfall&ndash;runoff model, *Hydrology and Earth System Sciences*, 21, 879-896,

doi:10.5194/hess-21-879-2017, 2017.

Skofronick-Jackson, G., Petersen, W. A., Berg, W., Kidd, C., Stocker, E. F., Kirschbaum, D. B., Kakar, R., Braun, S. A., Huffman, G. J., Iguchi, T., Kirstetter, P. E., Kummerow, C., Meneghini, R., Oki, R., Olson, W. S., Takayabu, Y. N., Furukawa, K., and Wilheit, T.: The Global Precipitation Measurement (GPM) Mission for Science and Society, *Bulletin of the American Meteorological Society*, 98, 1679-1695, 10.1175/bams-d-15-00306.1, 2017.

Schmit, T. J., Gunshor, M. M., Menzel, W. P., Gurka, J. J., Li, J., and Bachmeier, A. S.: Introducing the next generation Advanced Baseline Imager on goes-R, *Bulletin of the American Meteorological Society*, 86, 1079+, 10.1175/bams-86-8-1079, 2005.

Shen, G. Y., Chen, N. C., Wang, W., and Chen, Z. Q.: High-resolution daily precipitation estimation data from WHU-SGCC method: A novel approach for blending daily satellite (CHIRP) and precipitation observations over the Jinsha River Basin. PANGAEA, <https://doi.pangaea.de/10.1594/PANGAEA.900620>, 2019.

Simanton, J. R., and Osborn, H. B.: RECIPROCAL-DISTANCE ESTIMATE OF POINT RAINFALL, *Journal of the Hydraulics Division-Asce*, 106, 1242-1246, 1980.

Simpson, J., Adler, R. F., and North, G. R.: A PROPOSED TROPICAL RAINFALL MEASURING MISSION (TRMM) SATELLITE, *Bulletin of the American Meteorological Society*, 69, 278-295, doi:10.1175/1520-0477(1988)069<0278:aptrmm>2.0.co;2, 1988.

Sokol, Z.: The use of radar and gauge measurements to estimate areal precipitation for several Czech River basins, *Stud. Geophys. Geod.*, 47, 587-604, doi:10.1023/a:1024715702575, 2003.

Su, F. G., Gao, H. L., Huffman, G. J., and Lettenmaier, D. P.: Potential Utility of the Real-Time TMPA-RT Precipitation Estimates in Streamflow Prediction, *J. Hydrometeorol.*, 12, 444-455, doi:10.1175/2010jhm1353.1, 2011.

Thiemig, V., Rojas, R., Zambrano-Bigiarini, M., and De Roo, A.: Hydrological evaluation of satellite-based rainfall estimates over the Volta and Baro-Akobo Basin, *Journal of Hydrology*, 499, 324-338, doi:10.1016/j.jhydrol.2013.07.012, 2013.

Trejo, F. J. P., Barbosa, H. A., Penaloza-Murillo, M. A., Moreno, M. A., and Farias, A.: Intercomparison of improved satellite rainfall estimation with CHIRPS gridded product and rain gauge data over Venezuela, *Atmosfera*, 29, 323-342, doi:10.20937/atm.2016.29.04.04, 2016.

Tung, Y. K.: POINT RAINFALL ESTIMATION FOR A MOUNTAINOUS REGION, *J. Hydraul. Eng.-ASCE*, 109, 1386-1393, 10.1061/(asce)0733-9429(1983)109:10(1386), 1983.

Ushio, T., Sasashige, K., Kubota, T., Shige, S., Okamoto, K. i., Aonashi, K., Inoue, T., Takahashi, N., Iguchi, T., Kachi, M., Oki, R., Morimoto, T., and Kawasaki, Z.-I.: A Kalman Filter Approach to the Global Satellite Mapping of Precipitation (GSMaP) from Combined Passive Microwave and Infrared Radiometric Data, *Journal of the Meteorological Society of Japan*, 87A, 137-151, 10.2151/jmsj.87A.137, 2009.

Ushio, T., and Kachi, M.: Kalman filtering applications for global satellite mapping of precipitation (GSMaP), in: *Satellite rainfall applications for surface hydrology*, Springer, 105-123, 2010.

Verdin, A., Rajagopalan, B., Kleiber, W., and Funk, C.: A Bayesian kriging approach for blending satellite and ground precipitation observations, *Water Resources Research*, 51, 908-921, 2015.

Vila, D. A., de Goncalves, L. G. G., Toll, D. L., and Rozante, J. R.: Statistical Evaluation of Combined Daily Gauge Observations and Rainfall Satellite Estimates over Continental South America, *J. Hydrometeorol.*, 10, 533-543, doi:10.1175/2008jhm1048.1, 2009.

Wang, P. H.: PATTERN-RECOGNITION WITH FUZZY OBJECTIVE FUNCTION ALGORITHMS - BEZDEK, *JC, SIAM Rev.*, 25, 442-442, 1983.

Xie, P. P., and Arkin, P. A.: Analyses of global monthly precipitation using gauge observations, satellite estimates, and numerical model predictions, *Journal of Climate*, 9, 840-858, doi:10.1175/1520-0442(1996)009<0840:aogmpu>2.0.co;2; 1996.

967 [Xie, P., Joyce, R., Wu, S., Yoo, S.-H., Yarosh, Y., Sun, F., and Lin, R.: Reprocessed, Bias-Corrected CMORPH Global High-](#)  
968 [Resolution Precipitation Estimates from 1998, \*J. Hydrometeorol.\*, 18, 1617-1641, 10.1175/jhm-d-16-0168.1, 2017.](#)

969 [Xu, L., Chen, N., Zhang, X., Chen, Z., Hu, C., and Wang, C.: Improving the North American multi-model ensemble \(NMME\)](#)  
970 [precipitation forecasts at local areas using wavelet and machine learning, \*Clim. Dyn.\*, 53, 601-615, 10.1007/s00382-018-](#)  
971 [04605-z, 2019.](#)

972 Yang, T. T., Asanjan, A. A., Welles, E., Gao, X. G., Sorooshian, S., and Liu, X. M.: Developing reservoir monthly inflow  
973 forecasts using artificial intelligence and climate phenomenon information, *Water Resources Research*, 53, 2786-2812,  
974 doi:10.1002/2017wr020482, 2017.

975 Yang, Z., Hsu, K., Sorooshian, S., Xu, X., Braithwaite, D., and Verbist, K. M. J.: Bias adjustment of satellite-based precipitation  
976 estimation using gauge observations: A case study in Chile, *Journal of Geophysical Research: Atmospheres*, 121, 3790-  
977 3806, doi:10.1002/2015jd024540, 2016.

978 Yuan, Z., Xu, J. J., and Wang, Y. Q.: Projection of Future Extreme Precipitation and Flood Changes of the Jinsha River Basin  
979 in China Based on CMIP5 Climate Models, *Int. J. Environ. Res. Public Health*, 15, 17, 10.3390/ijerph15112491, 2018.

980 Zambrano-Bigiarini, M., Nauditt, A., Birkel, C., Verbist, K., and Ribbe, L.: Temporal and spatial evaluation of satellite-based  
981 rainfall estimates across the complex topographical and climatic gradients of Chile, *Hydrology and Earth System Sciences*,  
982 21, 1295-1320, doi:10.5194/hess-21-1295-2017, 2017.

983 Zhang, X., and Chen, N. C.: Reconstruction of GF-1 Soil Moisture Observation Based on Satellite and In Situ Sensor  
984 Collaboration Under Full Cloud Contamination, *Ieee Transactions on Geoscience and Remote Sensing*, 54, 5185-5202,  
985 10.1109/tgrs.2016.2558109, 2016.

986 Zhang, Y. R., Sun, A., Sun, H. W., Gui, D. W., Xue, J., Liao, W. H., Yan, D., Zhao, N., and Zeng, X. F.: Error adjustment of  
987 TMPA satellite precipitation estimates and assessment of their hydrological utility in the middle and upper Yangtze River  
988 Basin, China, *Atmospheric Research*, 216, 52-64, 10.1016/j.atmosres.2018.09.021, 2019.